6-2005

Stabilization of Curtain Coater at High Speeds

Peeyush Tripathi
Western Michigan University

STABILIZATION OF CURTAIN COATER AT HIGH SPEEDS

by

Peeyush Tripathi

A Dissertation
Submitted to the
Faculty of the Graduate Collage
In partial fulfillment of the
requirements for the
Degree of Doctor of Philosophy
Department of Paper Engineering, Chemical Engineering
and Imaging

Dr. Margaret Joyce, Advisor

Western Michigan University
Kalamazoo, Michigan
June 2005

INFORMATION TO USERS

The quality of this reproduction is dependent upon the quality of the copy submitted. Broken or indistinct print, colored or poor quality illustrations and photographs, print bleed-through, substandard margins, and improper alignment can adversely affect reproduction.

In the unlikely event that the author did not send a complete manuscript and there are missing pages, these will be noted. Also, if unauthorized copyright material had to be removed, a note will indicate the deletion.

ProQuest Information and Learning Company
300 North Zeeb Road
P.O. Box 1346
Ann Arbor, MI 48106-1346

Dedicated to my mother
Ms. Shushila Tripathi

TABLE OF CONTENTS

Table of Contents – Continued

...

Table of Contents – Continued

Table of Contents – Continued

LIST OF TABLES

#1 A STUDY FOR THE STATISTICAL OPTIMIZATION OF A CURTAIN COATER

2 UNDERSTANDING THE ROLE OF SURFACTANTS IN THE STABILIZATION OF A COATING CURTAIN

List of Tables – Continued

LIST OF FIGURES

#1 A STUDY FOR THE STATISTICAL OPTIMIZATION OF A CURTAIN COATER

A Study for the Statistical Optimization of a Curtain Coater

Peeyush Tripathi[a]
Dr. Margaret Joyce[a]
Dr. Do Ik Lee[a]
Dr. Paul D. Fleming[a]
Dr. Masahiro Sugihara[b]

[a]Center for Coating Development
Western Michigan University
[b]Mitsubishi Heavy Industries

ABSTRACT

High-speed curtain coating is an emerging technology trying to gain commercial acceptance by the paper industry as a non-impact coating process. Curtain coating could offer enormous economic and process advantages over conventional coating methods, due to its non-impact and excellent coverage at reduced coat weights. Due to its contour nature, it enables excellent coating coverage, resulting in equal coverage at lower coat weights than needed with contact metering coating methods, i.e., rod and blade. Due to non-impact and non-contact type of coating operation, curtain coating will operate with fewer sheet breaks or the strength requirements of the base sheet can greatly reduced. Being a contour coater, there is no film split patterning, and scratching. This results in the production of a defect-free coated surface. It is a versatile coating process, in that it enables a wide range of coating viscosities and coat weights to be applied with a single coater head.

In the current study, process and material parameters were varied through a Taguchi OA (first phase) and D-optimal (second phase) design of experiments (DOE), to stabilize a pilot curtain coater at high speeds. The statistical DOE, enabled us to recognize contribution of variables to the curtain stability and optimized them in a relatively few number of trials. The variables studied were curtain height, steam flow rate of a steam substitution system, measures of coating rheology, surfactant dosage, coat weight, web speed, base sheet roughness and base sheet sizing. Trials were conducted at Mitsubishi Heavy Industry's state of the art coating research center in Hiroshima, Japan.

The role of boundary layer air removal system was found to be critical to the stability of the curtain, especially at high speeds. Base sheet roughness, in combination with the parameters of the coating formulation, was found to be very important. Coating coverage improved with the smoothness of the base sheet and excellent coating coverage was possible at low coat weights.

Higher curtain height and shear thinning coating rheology was favored for obtaining curtain stability at high speeds. The sizing of the base sheet impacted coverage and curtain stability at high speeds due to its impact on the wettability of the base sheet by the liquid curtain. The role of surfactants, although good theoretical understanding exists, was inconclusive.

INTRODUCTION

High-speed curtain coating is an emerging technology seeking to gain commercial acceptance as a pre-metered and non-impact coating process (1-4). Curtain coating has the potential to provide significant economic and process advantages over conventional coating methods due to its ability to provide excellent coverage at low coat weights. Due to non-impact and non-contact type of coating operation, curtain coating will operate with fewer sheet breaks or the strength requirements of the base sheet can greatly reduced. Curtain coating can be considered as a wet lamination process, where lamination follows the contour of the base sheet, so there is no film split patterning; resulting in a defect-free coating surface. Curtain coating is a versatile coating process that enables the widest range of coatings and coat weights to be achieved with a single coating head (1-3).

High-speed curtain coating for pigmented coatings is still in its early stages of development (1-2). As a result, various phenomenological behaviors are still not very well understood. The stability of the curtain (1) and air entrapment at high speeds (1,2) are two of the major technical problems limiting the commercial acceptance of the curtain coater. To understand the causes for these limitations, an understanding of the basic operations of a curtain coater needs to be achieved.

An illustration of a curtain coater is depicted in Figure 1, which shows a side view of a slot die curtain coater. As seen from the illustration, the principle of a curtain coating operation is the flow of coating through a slot of a die, to produce a liquid curtain across the paper machine. Liquid exits the slot, forms a curtain and impinges on the moving paper. The moving web comes in contact with the curtain, pulling the curtain in the machine direction of the paper machine. Metering is accomplished by controlling the thickness of the coating curtain.

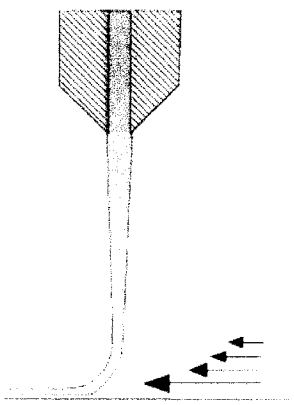

Figure 1. Curtain Coating

The curtain coating process can be divided into 3 distinct zones (Figure 2):

1. Curtain formation zone
2. Curtain zone
3. Impingement zone

The sheet formation zone begins as the coating exits the die. The internal design of the die and rheology of the coating are the most important issues governing the performance of the coater in this zone. Slot designs are sensitive to coating rheology and velocity. Therefore, they should be designed in such a way that enables a fully developed and stable flow profile to be achieved in the slot within a very short time. It is also important that no flow separation occurs within the slot.

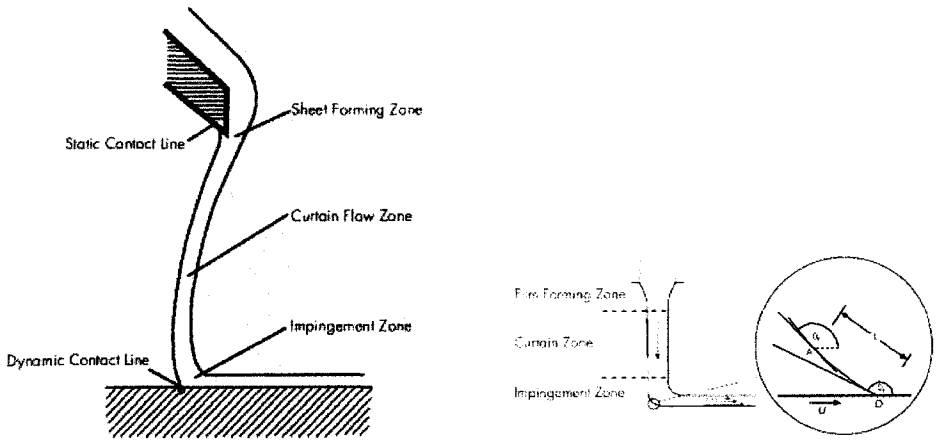

Figure 2. Three different zones in the curtain coating process.

The curtain zone begins with the development of a curtain as the fluid flows from the die. In this zone, the formation and stability of the curtain is the result of a complex relationship between inertial, viscous, surface, extensional, shearing, and gravitational forces (1,2). Thus, the rheology and surface characteristic of the coating plays an important role.

The point of contact between the free falling curtain and moving substrate and the adjoining space are termed the impingement zone. The complex interaction between the substrate and the curtain is a developing science. The presence of boundary layer air, associated with movement of the rough substrate, further adds to the complexity of these interactions.

Now that the basic operation of the curtain coater is understood, the operational parameters that control the stability of the curtain can be reviewed. An understanding of the physics of curtain formation has existed for decades. In 1961, Brown (5) proposed the following principle equations to describe the process, following the initial works of I.G. Wells (6). These principle equations are very useful in understanding the fundamental principles governing the influence of the interactions between inertial and surface tension forces on curtain stability.

By taking the x-axis as the direction of curtain fluid flow, the stress components could be defined as:

$$X_x = -p + 2\eta\partial u/\partial x, \quad (1a)$$

$$Y_y = -p + 2\eta\partial v/\partial y, \quad (1b)$$

$$Z_z = -p \qquad S(1c)$$

Now, if p is defined as, $p = -(1/3)(X_x + Y_y + Z_z)$ and W=0
u>>v (effect of surface tension assumed negligible) then

$$Y_y = \text{constant} = -p_0 \qquad (2)$$

If incompressible flow is assumed, $\partial u/\partial x = -\partial v/\partial y$ and hence

$$X_x = -p_0 + 4\eta\partial u/\partial x \qquad (3)$$

Now, $\rho ut = Q = \text{constant}$

Thus, the following equation of the motion (4) is obtained:

$$Q\partial u/\partial x = \partial/\partial x(tX_x) + t\rho g, \qquad (4)$$

From equations 3 and 4,

$$\partial u/\partial x = (4\eta/\rho)\partial/\partial x(1/u\ \partial u/\partial x) + g/u \qquad (5)$$

and substituting for, $u = (4\eta g/\rho)^{1/3} U$ and $x = (4\eta/\rho)^{2/3} g^{-1/3} X$, a rearrangement gives

$$\partial/\partial X\ (1/U\partial U/\partial X) + 1/U - \partial U/\partial X = 0 \qquad (6)$$

Kistlar (7) showed the dependence of curtain stability on Reynolds number, ratio of web speed, U, impingement velocity, V, and Weber number (Figures 3-5). From these figures, the operational window for coat weight, Reynolds number and U/V ratios were defined for their given system. Triantafillopoulos, et. al., (1) showed the same experimentally

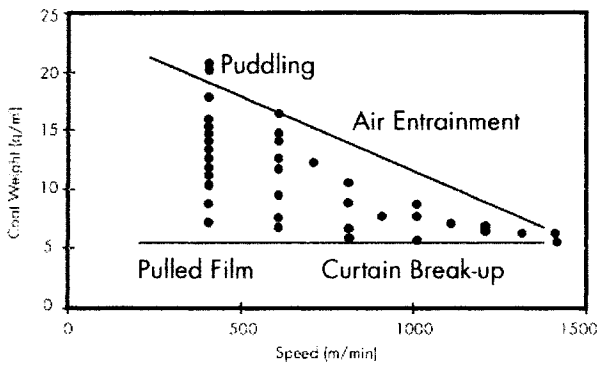

Figure 3. Influence of web speed (U) on coat weight development. At a constant speed, changing the flow rate varied the coat weight. The data were collected from pilot trials.

Triantafillopoulos, et. al., (1) compared the coating coverage achieved by a curtain coater with that of a metered size press (MSP). As evident from Table 1, the curtain coater provided far better coverage over the MSP even at low coating solids. The improved coating coverage (or lower coat weight for equivalent print quality) may result in significant improvements in the economics of coating operations.

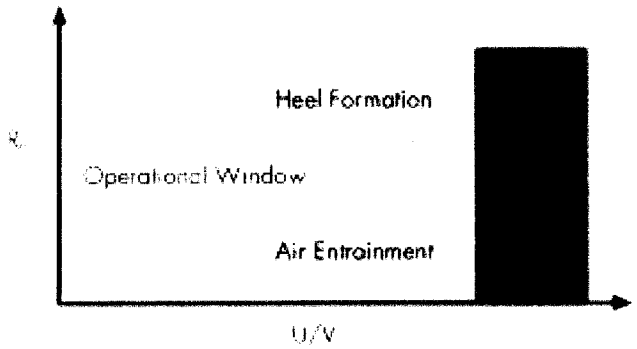

Figure 4. Proposed operating window for curtain coaters.

Table 1. Comparison of Coating Coverage with MSP and Curtain Coater [1]

Technology	Speed	Coat weight	Solids content	Coverage
CURTAIN	1200	5.8 g/m^2	54 %	85 %
MSP		5.0 g/m^2	63 %	60 %
		7.1 g/m^2	64 %	75 %
		8.5 g/m^2	64 %	87 %

Condition of Curtain Stability

The stability of a curtain has been shown to be related to the Weber number. The Weber number is a dimensionless flow parameter, which relates the inertial forces to the surface tensional forces of the free flowing curtain. In the past, it was believed that a Weber number >2 was required to obtain a stable curtain. However, a more in depth analysis of the physics of fluid flow suggests that the same criteria can be met at lower inertial forces, or a Weber number >1.5. From Figure 5, we see that the condition to form a liquid curtain is,

$$\rho V^2 H > 2\sigma \tag{7a}$$

or,

$$W_e > 2 \tag{7b}$$

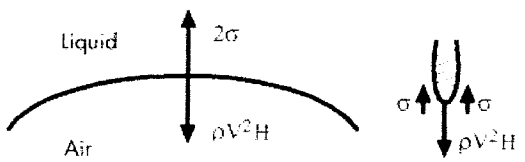

Figure 5. Inertial and surface tension forces in curtain formation.

Physical Conditions at the Impingement Zone

When trying to understand the operation of a curtain coater and dynamics of film formation, it is important to define the three physical conditions; the heel, strands, and

pulled film. A schematic of each physical condition is presented in Figure 7 and described below.

1. Heel-The heel is formed when the curtain is not completely moved in the direction of the web, but flows slightly in the opposite direction,
2. Strands- Strands occur due to insufficient flow, which causes a well formed curtain to break-up and contract into strands,
3. Pulled film-A pulled film happens when the coating fails to impact the substrate right below the slot and is pulled forward together with the web.

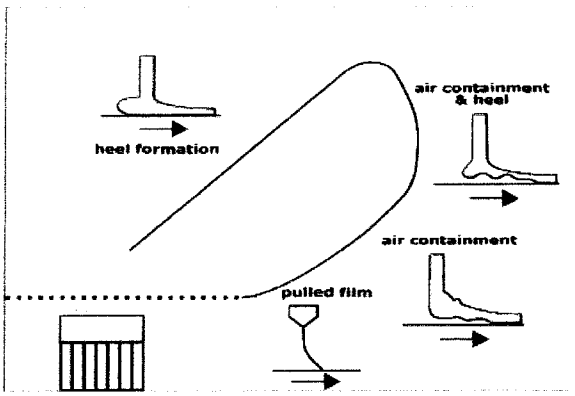

Figure 6. Operating Window for Curtain Coating.

Wilson, et al. (8), performed numerical simulations of the fluid flow in the heel (impingement zone). A summary of his observations is provided in Figure 7. These results match closely with work performed by Kistlar (7).

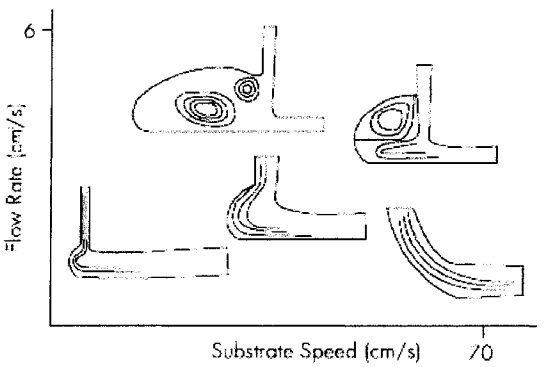

Figure 7. Shape of impingement zone with flow rate and web speed.

Clarke (9) worked on the development of re-circulating viscous eddies specifically for curtain coating operations. He described in detail, the rheological parameters important for the development of flow patterns within the heel. The results of his findings are summarized in Figure 8.

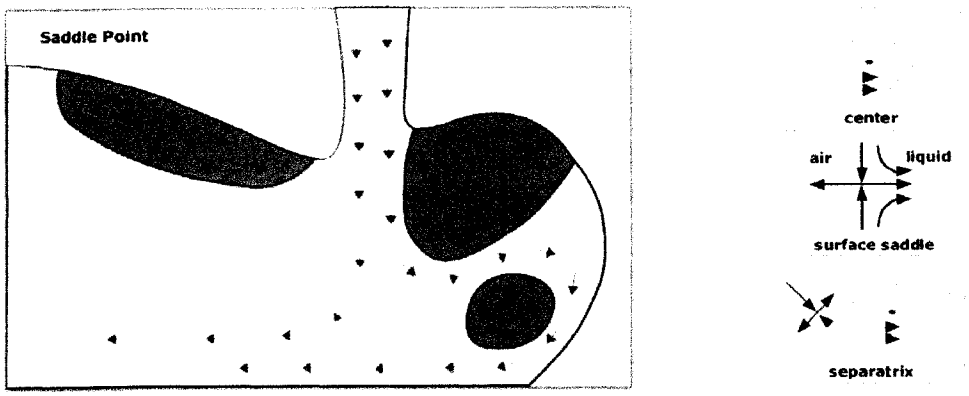

Figure 8. Three re-circulation zones in the heel.

Although much work has been done to understand the dynamics of the individual parameters of a curtain coating operation, no comprehensive work has been done to understand the influence of the process, substrate, and formulation parameters on curtain stability. Many parameters interact and produce a synergic effect on curtain operation. Developing a complete and comprehensive understanding of curtain parameters and their interaction is a prerequisite for stabilizing a curtain coater at high speeds.

OBJECTIVE

The objective of the proposed research was to stabilize a curtain coater at ultra high speeds and develop a fundamental understanding of the process. A comprehensive trial plan was devised to study the effect of various process, substrate, and coating parameters on curtain stability, runnability and coating quality (coverage).

EXPERIMENTAL DESIGN

The study was divided into two phases. In the first phase, a Taguchi OA design of experiment (DOE) was employed to quantify the effect of all 8 variables on curtain stability. The Taguchi OA was selected because it enables the quantification of the main effect of selected variables on the response variables in relatively few experiments. This step enabled us to determine the relative importance of process variable in the process. The results of Phase I was then used to select the 4 most important variables contributing to curtain coating stability and quality (coverage). These 4 variables were carried forward to Phase II. A partial-factorial DOE, D-optimal, was used in the phase II, A partial factorial design was selected to determine the extent of variable interaction and its effect on the process. Thus, it allowed for a more close examination of the contribution of the selected 4 factors.

The coating studies were performed on a pilot curtain coater at Mitsubishi Heavy Industries in Hiroshima, Japan. The coater was 850mm wide and equipped with a high-speed video camera to capture images of the curtain film during operation. The process variables considered were curtain height, steam flow rate of a steam substitution system, coating rheology, surfactant dosage, coat weight, web speed, base sheet roughness and basesheet sizing.

INTRODUCTION OF VARIABLES IN CURTAIN COATING

An explanation of the role of each of these variables on the curtain coating process will now be discussed to understand the importance.

Curtain Height

A curtain flow field is result of complex interactions between gravitational extensional and surface forces, which are influenced by such factors as coating rheology, web-curtain speed difference and curtain height. As the coating leaves the applicator nozzle, it falls under gravity until the point where it contacts the moving web. The curtain height influences the speed of the curtain as follows:

$$U^2 = U^2_o + 2gH \quad (8)$$

Here, U_o is the velocity of the curtain as it leaves the applicator lip and H, is the height of the curtain from the applicator lip. The Reynolds number is generally low in the die so the velocities in the die are very low (of the order of 0.20m/s). Thus, U_o can be neglected for all practical purposes and curtain speed can be considered free falling. A stable curtain, W_e>2, can be achieved by changing the velocity of the curtain by adjusting the curtain height. The effect of curtain height on curtain stability, at a given surface tension, is a dominant factor. Viscous effects, as it exits the slot, affect the velocity of liquid. A correction suggested to account for these effects is given below for the above equation as:

$$2gH = 2g(H - 0.5(\mu/\rho)^{2/3}) \quad (9)$$

The effect of curtain height is indirectly related to the lip opening. As the lip opening changes, the outlet velocity changes, for the same flow rate. Nevertheless, due to the low Reynolds number flow within the die, the contribution of the initial exit velocity of the curtain to the velocity at any given height is still dominated by gravitational forces. In preliminary studies conducted by Mitsubishi, the optimum height for the Mitsubishi curtain coater is in the range of 100 to 400 mm. Based on these findings, the curtain height was maintained in the 150 to 250 mm range for the current study.

Coating Rheology

The rheological parameters important to the runnability of a curtain coater vary within the 3 zones of the curtain coater described earlier (flow distribution through the die, curtain forming zone and impingement zone). Since the flow field is extensional, extensional rheology parameters are applicable. The coatings applied were typical clay-carbonate-latex web offset formulations. Carboxymethylated cellulose, CMC, was used as the rheology modifier to alter the shear thinning properties of the coating. The viscosity was kept in a narrow range (400-700 cps, Brookfield, # 4 Spindle, 100 rpm) and rheology changed from Newtonian to shear thinning by altering the amount of CMC applied.

Surface Tension and Surface Age (Surfactant Dosage)

To form a stable curtain at low flow rates, surface tension must be reduced to maintain a proper Weber number (W_e>2). Surfactants are used to reduce the surface tension of a coating. Low surface tensions favor a stable curtain at low flow rates. A large number of

surfactants are commercially available that differ substantially in efficiency and effectiveness, so the choice of surfactant is critical. As a curtain falls under gravity, the surface area of the curtain increases. The surface tension of a curtain will increase, depending on the initial surface excess of surfactant. Also, in a dynamic process surface age becomes important. The surface age of the process is the time the curtain takes from slot exit to impingement on to the substrate. The curtain height dictates the surface age. As shown in Figure 9, the surface tension of a curtain will change with curtain height due to the change in surface. The height of the curtain dictates the time available for surface aging. Change in surface tension with surface age may be the most important property of the surfactant. To reduce the surface tension of the coating, an anionic surfactant, Niaproof 4, was used. Niaproof was used because it is a highly soluble anionic surfactant known to industry to be effective in lowering the surface tension of aqueous coatings.

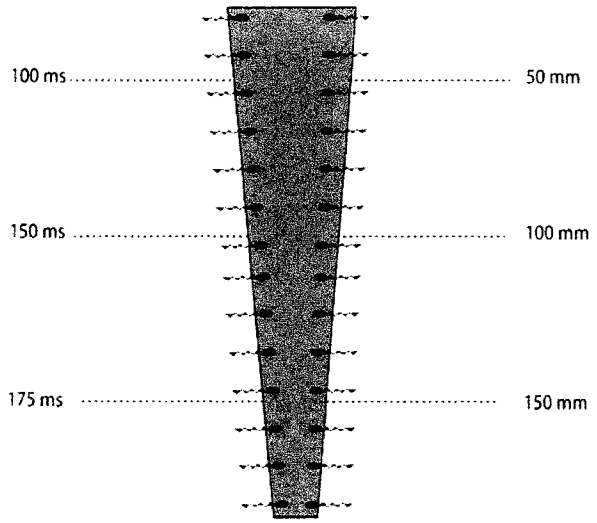

Figure 9. Surface tension and surface age.

Flow Rate (Coat weight)

The flow rate, along with web speed, determines the achievable coat weight. Curtain stability is also related to coat weight through the inertia term in the Weber number. Since curtain coaters are contour coaters, complete coverage is possible at much lower coat weights than with conventional contact surface coaters. Coat weights between 4-10 gsm are attainable and sufficient for coverage for most curtain coater applications. In the present study, coat weights of 12, 8 and 6 gms/m^2 were applied.

Web Speed

Web speed is important for the economic viability of any process. Higher web speeds translate into higher production and profitability. Web speed is also an important process variable in curtain coating, as it affects the process via many different mechanisms.

In curtain coating, web speed affects the onset of air entrapment, the amount of viscous drag, curtain stability, boundary layer air and effects of base sheet-coating interactions.

The most important effect of web speed on the process is the dependence of boundary layer air, (BLA), on the substrate speed. Web speed governs the thickness and ease of removal of BLA. As web speed increases, removal of the BLA becomes progressively difficult and manifests itself on the process as the onset of air-entrapment in the impingement zone. Viscous drag of the curtain is governed by the web-curtain speed difference, thus, along with coating rheology, it affects the shape of the impingement zone and curtain extension. In addition, as speed increases, the time scale for the wetting of the substrate by the coating becomes critical. Wetting is critical in the curtain as it affects the process in multiple ways. An acceptable coating viscosity operational range is also related to web speed. At low viscosities, a coating may splash in the impingement zone. Thus, web speed is an important process parameter and high-speed curtain coating puts additional constraints on the process.

Since high-speed curtain operation was the focus of the present study, 3 web speeds were used in the first phase of this study (800, 1400 and 1800 MPM).

Surface Sizing

The wetting properties of the paper affect the interaction between the curtain and the paper surface. The degree of interaction between the coating and the paper determines the amount of viscous drag on the curtain. The faster the coating wets the paper, the higher the viscous drag.

The type and amount of sizing agent present in the basepaper controls the wetting properties of the basepaper. Viscous drag influences the curvature of the curtain in the impingement zone. At higher machine speeds, there is a need to increase the wettability of the basesheet to account for the shorter contact time between the coating and basesheet at the point of impingement. To control the wettability of the papers, the papers were size press treated with an oxidized starch (Oji Inc., oxidized starch) prior to being curtain coated. The amount of starch applied was 1 gm/m^2 (C1S).

Base sheet Roughness

The roughness of the basesheet (Figure 10) influences the runnability of the curtain coater as it affects the efficiency of the BLA removal system and coating coverage. BLA is known to disrupt the stability of the curtain at high speeds and create coverage and surface defect issues in the dried coating layer. The effect of base sheet roughness and its mechanism on curtain coating is largely unknown. Roughness of the basesheet hastens the formation of the transition zone causing turbulent air flow to be achieved in a relatively short distance. The roughness scale of the moving substrate also affects the thickness of the boundary layer. The amplitude and frequency of the substrate roughness will affect coverage. The curtain simply follows the contour of the low amplitude roughness. However, for a high frequency and high amplitude roughness, the description of the film (curtain) becomes complex. High basesheet roughness may create craters, a unique problem in curtain coating.

In the present study, roughness was recognized to be of high importance and was assigned 3 levels of variance. Relatively high basesheet roughnesses of 7.7 PPS, 5.5 PPS and 3.5 PPS were used.

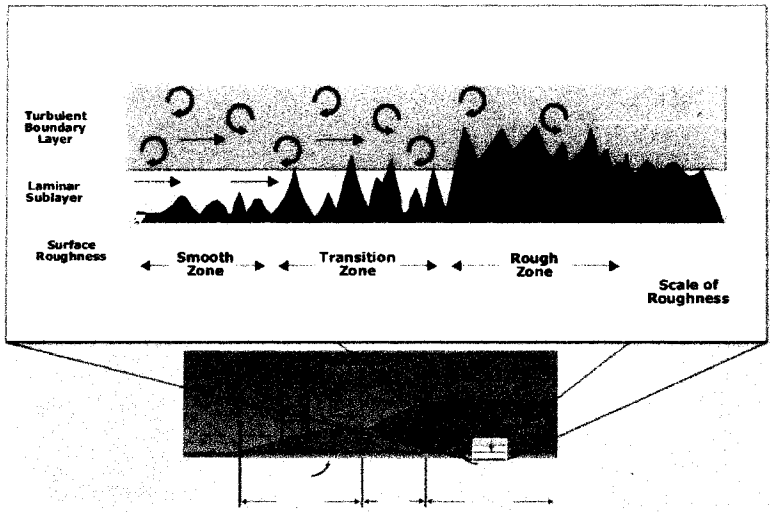

Figure 10. Scale of roughness and BLA thickness.

Boundary Layer Air Removal System

As a rough substrate moves at high speed, it drags air along, forming a boundary layer air; BLA. As this boundary layer hits the curtain it leads to air entrapment and curtain instability. Air entrapment at the impingement zone is on of the technical challenges in high-speed curtain coating. Even a minor entrapment leads to severe defects in coating quality. Efficient removal of boundary layer air is one of the pre-requisites for high-speed curtain coating. A BLA removal system was proposed (fig.11) to be used in curtain coating to delay the onset of air entrapment.

There are primarily two BLA removal systems currently proposed; in plate-vacuum system and steam substitution system. For in plate-vacuum systems, a polymeric plate in touch with the moving web followed by a vacuum box does the initial air removal. Mitsubishi Heavy Industries (MHI) was the pioneer to employ a novel steam substitution system (2), (SSS), to delay the onset of air entrapment at high curtain coating application speeds. The SSS (Figure 11) works by employing high velocity air through an ejector (air knife) onto the moving web to remove the bulk air being carried by the web towards the impingement zone. The incident angle of the air knife is optimized such that the total pressure on the downside of the web can be kept the lowest. After removal of the bulk air, steam is substituted for the air by mixing saturated steam with the remaining thin film of trapped air. The saturated steam, on mixing with the air, looses temperature and condenses, creating a mild vacuum in the impingement zone. The vacuum is controlled by the steam flow rate. The combined effect of heat and condensation of steam from the steam-air mixture attenuates any air current in the down side of SSS, resulting in a more stable curtain. Slight vacuum conditions and absence of convection currents also helps to stabilize the curtain.

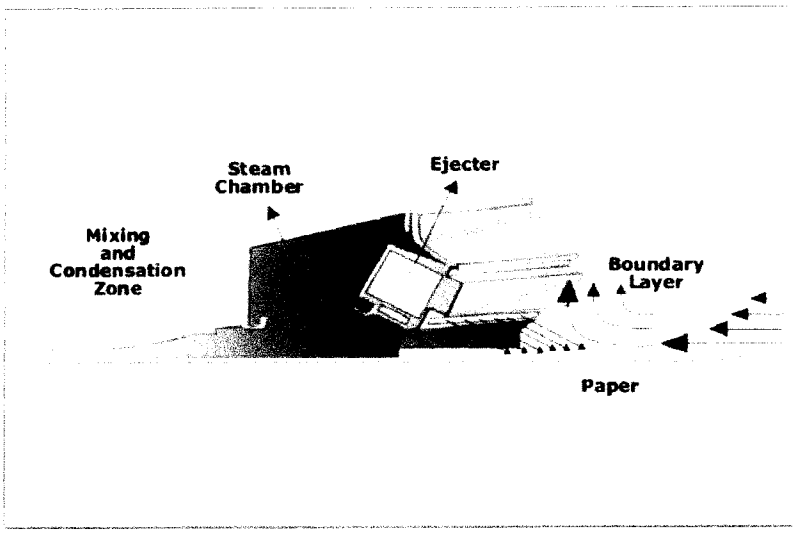

Figure 11. Steam Substitution System.

High temperature disturbs the BLA and immobile air in the micro roughness of the paper. As the air jet hits the moving web, a bifurcation of the jet takes place. A majority of the air jet goes away from the moving web but a fraction of the jet moves in the direction of the web even at the optimized air ejector angle. To minimize the effect of the partial air jet that moves with the web, the air pressure in the ejector must be adjusted according to the web speed and should be kept as low as possible. In this study, the level of steam in the SSS was changed by adjusting the steam flow rates per unit width of the coater and the air ejector pressure was changed with web speed according to an algorithm created by MHI.

CONSIDERATIONS OF CURTAIN STABILITY

A stable curtain is a prerequisite for a good curtain coating. Due to the absence of any definitions for curtain stability, curtain stability is difficult to describe and measure. Before attempting to measure, curtain instabilities needed first to be defined and a method to quantify them established. To accomplish this, videos of the curtain coater during operation were captured and analyzed by a group of observers to define the various curtain instabilities. Next, the videos were again observed and the severity of the instabilities was quantified on a scale of 1 to 5 with 1 indicating a very unstable curtain and 5 representing a stable curtain (Figures 12a-12d).

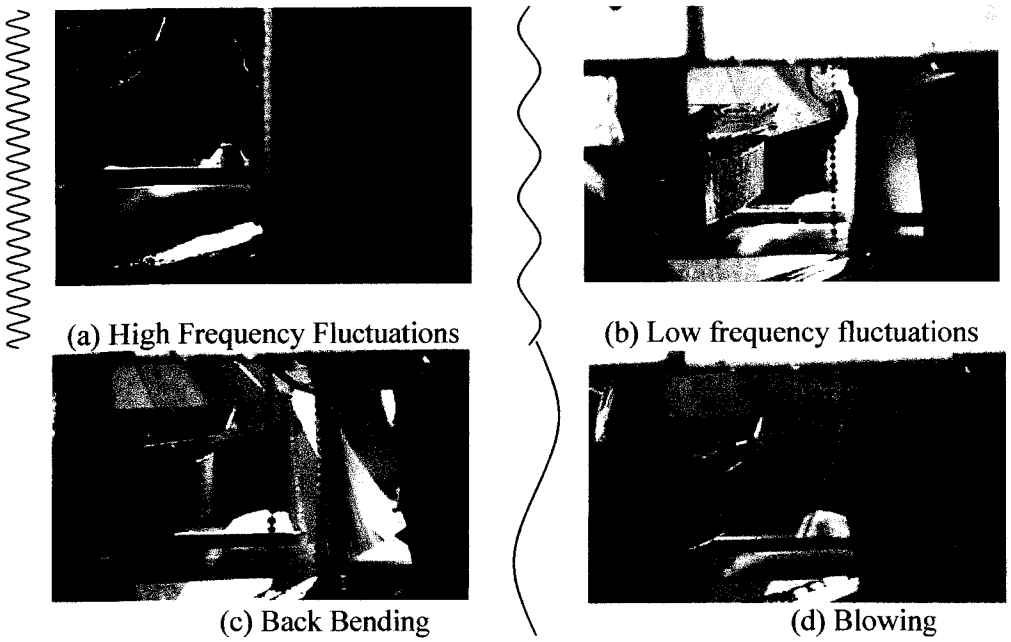

Figure 12. Curtain instabilities.

At high speeds, the curtain fluctuates in the cross direction of the paper machine. These fluctuations can be characterized by their sinusoidal frequency and amplitude. At stable operation, these fluctuations can have almost the same amplitude but very different frequencies. It was determined that the fluctuations originated from the uneven performance of the boundary layer air removal system in the cross direction of the machine. Upon further study of the problem, an uneven air ejector and steam profile in SSS was found. The problem was attributed to the way the SSS was machined. Upon remachining and adjustment of the profile, the problem was eliminated.

It was observed that at higher vacuum levels on the upside of the curtain, the curtain would bend backwards (c). The back bending seemed to have a positive effect on the overall stability of the curtain, as it delayed the onset of air-entrapment. In severe cases of unoptimized boundary layer air removal, blowing of the curtain occurred. Blowing was characterized by the violent down stream movement of the curtain as shown in Figure 12d.

Other types of curtain instabilities identified in this study were splashing and burps, which are both shown in Figure 13. Both effects were observed to be induced by viscosity and surface tension effects respectively. If the viscosity of the coating was low, splashing occurred. Operating at a low Weber number (low flow rate or high surface tension at a given flow rate) resulted in the presence of intermittent "burps" being introduced into the curtain. Both splashing and burps led to coating defects in the dried coating layer.

Based on these definitions, a stable curtain was defined as, one that is totally free of any of the effects mentioned above, and one that fell in the same plane as the curtain die or pulled forward (Figure 14).

Figure 13. Splashing.

Figure 14. Straight curtain.

DESIGN OF EXPERIMENT (DOE)

Having defined the criteria used to quantify the stability of the curtain, curtain coating trials were performed and videos were recorded. The studies were divided into two phases (See Appendix for full DOE). Each study was modeled using Stat-Ease, design of experiment modeling software. The first phase was designed to determine the 4 most dominant process variables, from 8, affecting the curtain stability. The second experimental phase was designed to optimize the performance of the curtain coater by further optimizing the 4 dominant variables identified in the first phase. In the second phase of the study, coating coverage was chosen as the response variable.

Prior to performing the curtain coater machine trials, rheological and surface tension studies were performed to set the levels of surfactant and rheology modifier, CMC, to be used in the coating formulations. The properties of the basesheet were adjusted by coating the paper with a 10% oxidized starch solution (Oji, Inc., Oxidized starch) with a metered size press (C1S). The paper was then calendered to adjust the roughness profiles and lower the permeability of the paper. Calendering was performed on an off-machine super calender at the Mitsubishi pilot plant facility.

The wetting properties of the basesheet were characterized by performing a 60 second Cobb test. The Parker Print roughness and permeability of the basepaper were also measured. The properties of the basesheets studied are given in Figure 15.

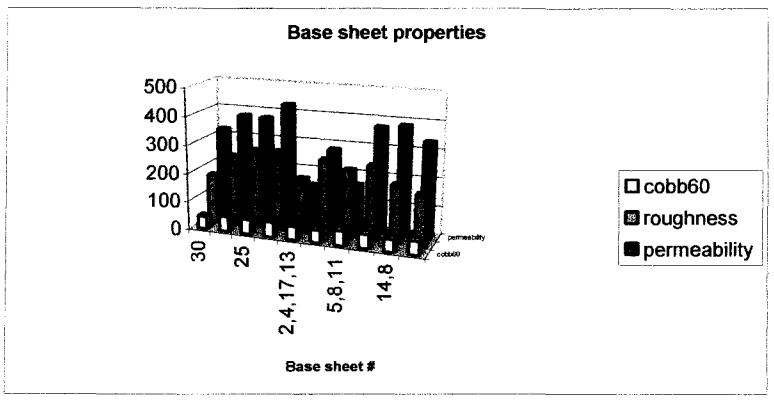

Figure 15. Differences in basesheet properties.

PRELIMINARY RHEOLOGICAL STUDY

A model offset coating formulation appropriate for a LWC heat set web offset commercial publication grade was prepared. The amount and type of each component used is listed in Table 2.

Table 2. Coating Formulation

	Coating Components	Commercial name	pph
Pigments	Clay	Ultra White 90	40
	GCC	Carbitol 90	60
Binders	S/B latex	JSR 2600	15
	CMC	Cellogen PR	0.55
Additives	Surfactant	Niaproof 4	As required
	Lubricant	Nopcote C-104	0.6
	Water retention	SPI resin 102A	0.5

A low molecular weight CMC was used as the rheology modifier and to improve the coating surface strength. The amount of CMC added to the coatings was varied by adding CMC solutions of different solids to the coating and adjusting the final coating solids with dilution water. The solids of the CMC solutions ranged from 0.1 % to 5.0%. The interactions between the different coating components; CMC, Clay and latex were characterized using several rheological test methods. To study the degree of interactions between the individual coating components, the rheology of the CMC alone, with clay, and with clay and latex were measured separately. The low shear viscosities of the coatings were measured using a Brookfield RVT viscometer. The high shear properties of the coatings were measured with a Hercules DVT viscometer. Dynamic rheological measurements were performed using a Haake dynamic stress rheometer using multiple geometries. At low levels of CMC addition, couette geometry was used. At higher levels of addition, a cone and plate geometry was used.

High shear studies were performed using a Hercules high shear DV10 rheometer, E bob. The results of the rheological tests are given below. Based on the findings of these tests, it was determined that the 0.3 to 0.60 % CMC levels should be used to give a broad range of shear thinning and thixotropic properties.

The changes in low shear viscosity of the clay solutions with CMC and latex additions are shown in Figure 16. The addition of CMC gradually increased the low shear viscosity of the clay and coating (clay and latex). The exponential increase in viscosity with clay addition levels above 2.0% is not observed for the coatings. This is probably due to the absorption of the CMC onto the clay surface decreasing the concentration of the CMC in the bulk solution.

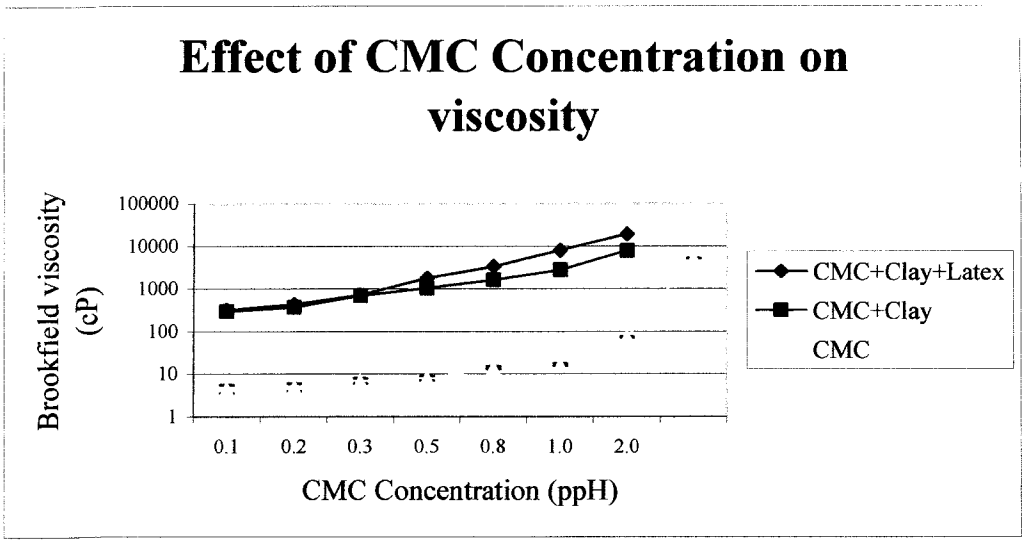

Figure 16. Change in low shear viscosity of coating with CMC addition.

The results of the high shear rheological studies show an increase in shear resistance and thixotropy with increasing levels of CMC addition (Figure 17). At the 0.1-0.2% level of CMC addition, the CMC and coatings are almost Newtonian (Figures 18 and 19). Comparison of Figures 17 and 18 suggests that the increase in shear resistance in the clay/CMC mixtures is most likely due to the hydration of the CMC with water, because both figures show a similar increase in thixotropy and shear resistance with CMC addition.

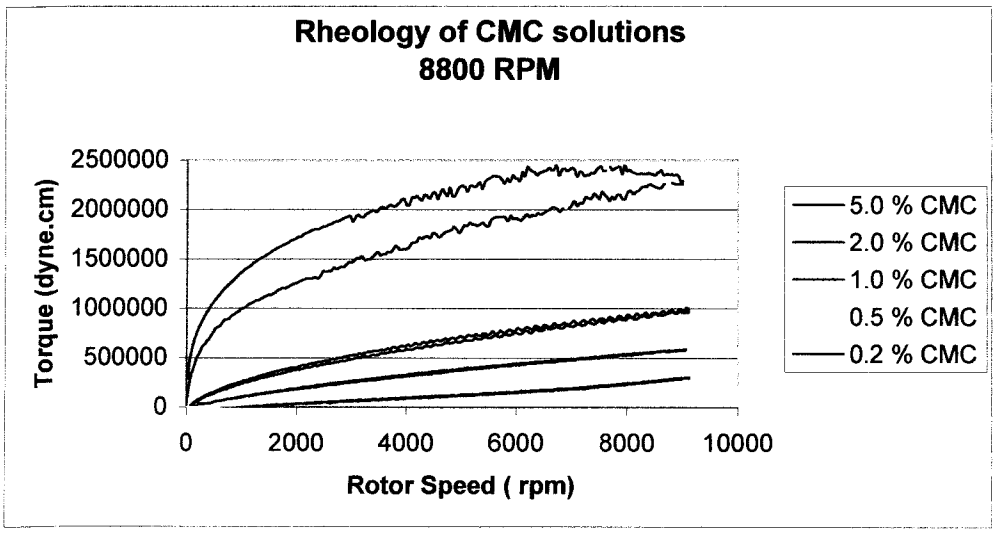

Figure 17. High shear rheogram of CMC solutions.

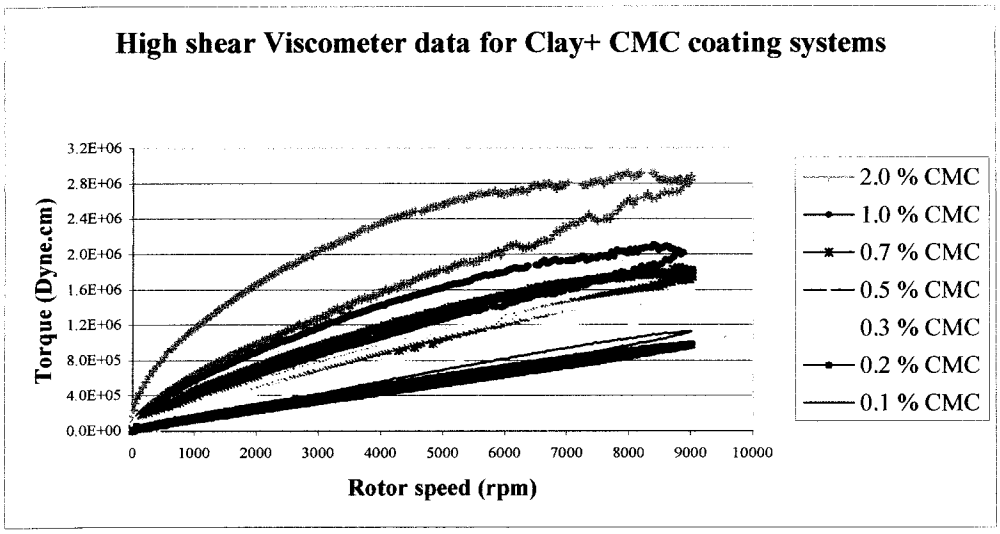

Figure 18. Influence of CMC on high shear clay rheology.

Comparison of Figures 19 and 20 show the changes in the viscoelastic properties of the coatings with CMC addition. The increase in elastic modulus and critical yield stress values with CMC addition indicates that the number and strength of interactions in the coating increase as the concentration of the CMC increases. The power law region is steeper for the viscous modulus than the elastic modulus. The results correlate well with the Hercules high shear rheograms, which show an increase in shear resistance with CMC addition. The strength of the clay/CMC interactions appears to be stronger than the clay/latex interactions. This is probably due to the partial absorption of the CMC onto the clay surfaces.

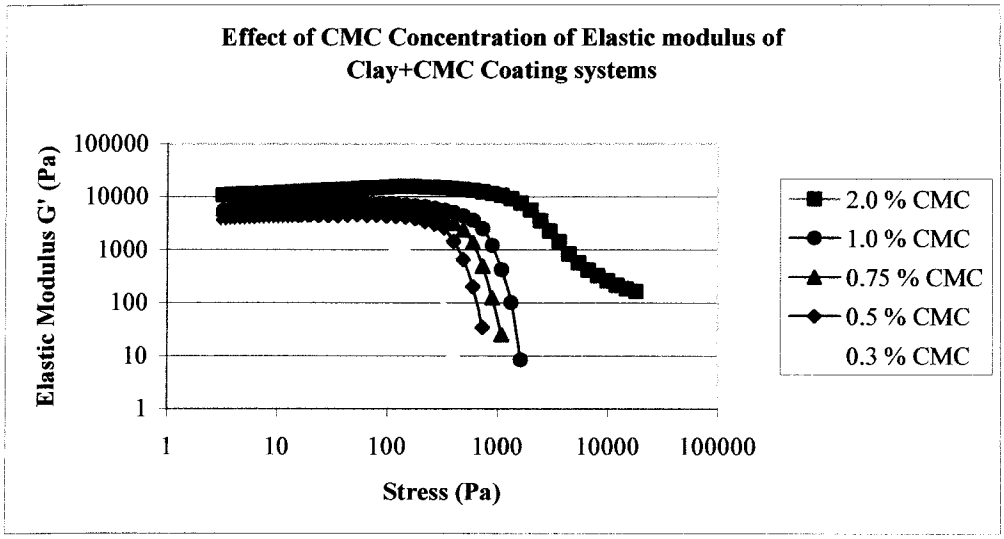

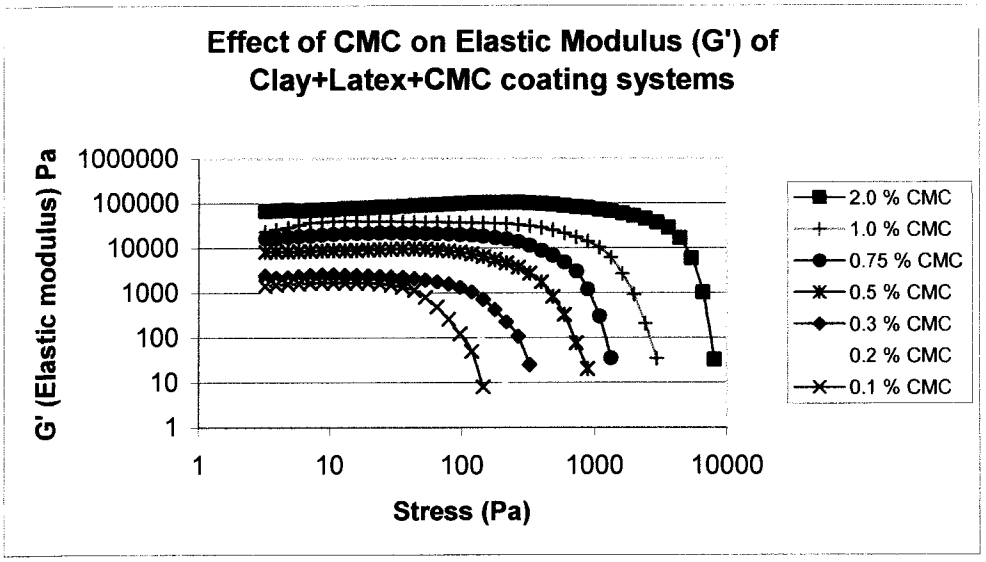

Figure 19. Contribution of coating components on the elasticity of the coatings.

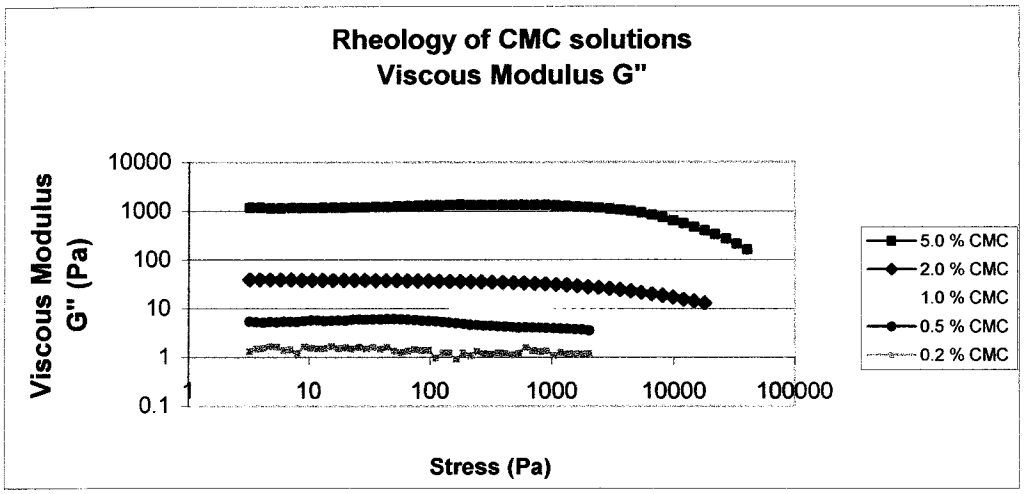

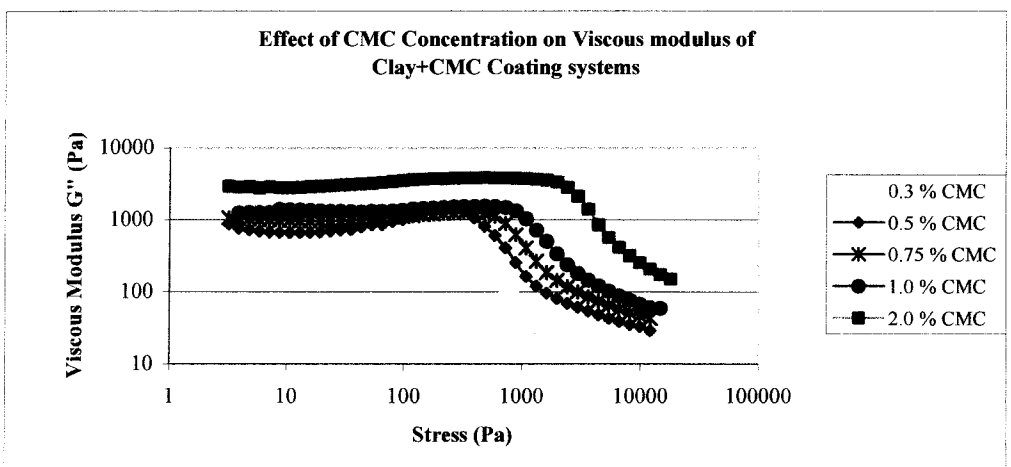

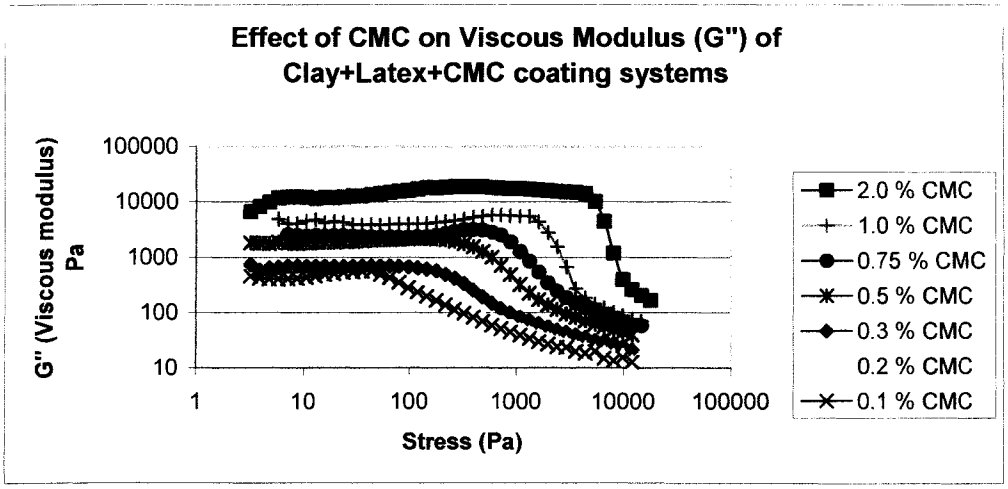

Figure 20. Contribution of coating components on the viscous modulus of the coatings.

Based on the findings of the rheological studies, it was determined that coatings with a broad range of shear thinning, thixotropic and viscoelastic properties could be obtained by adjusting the levels of CMC addition from 0.10-2.0%. Since there was no significant difference in the high shear rheograms of the different GCC pigment coatings, it was decided that the curtain coating application studies would be performed using only one pigment. Surface tension measurements were then performed on these coatings to determine the best level of surfactant addition for maintaining the stability of the curtain at low flow rates. Only one surfactant, Niaproof 4 (Niacet Inc.) was used.

A preliminary study was undertaken to identify the surfactant dosage levels that would provide surface tension values of 40, 35 and 30 dynes/cm. Surface tension measurements were made using a Wilhelmy plate instrument. The sensitivity of the Wilhelmy measurements to viscosity and pigmented dispersions is well known, so due to the high solids (54%) of the coatings, the measurements were not very reproducible. Lacking precision and accuracy, the measurements were nevertheless helpful in deciding on a few appropriate surfactant dosage levels that could be carried forward in the studies. The results of these studies are given in Figure 21.

To improve the accuracy and precision of the data, attempts were made to measure the surface tension at lower coating solids. However, the coating solids could not be reduced too low, as the results would be less representative of the actual formulation. A small study was done to determine the highest acceptable coating solids (solids which will give less than 5% variation from reading to reading). The standard coating formulation was prepared at 54 % with the same surfactant dosage level (0.20 pph) and the surface tension measured at gradually decreasing coating solids.

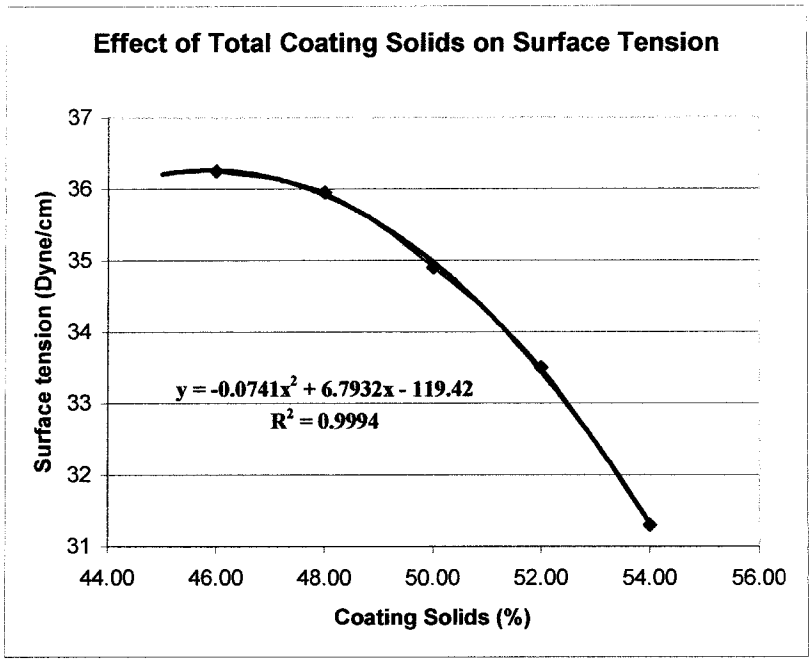

Figure 21. Change in surface tension with coating solids.

The acceptable range of the standard deviation for the surface tension measurements occurred at a maximum coating solids of 45 %. Above this point, large variations occurred. All further surface tension measurements were performed at this solids level.
A surface tension profile was generated to identify the dosages that would give the desired surface tension. A standard coating was prepared at 45% solids and dosed incrementally, with increasing amounts of surfactant. Figure 22 shows the profile to be near linear in the (0.0-1.0 pph) range. Surfactant dosages of 0.02, 0.20 and 0.80 pph gave corresponding surface tension values of 40, 35 and 30 dynes/cm, respectively.

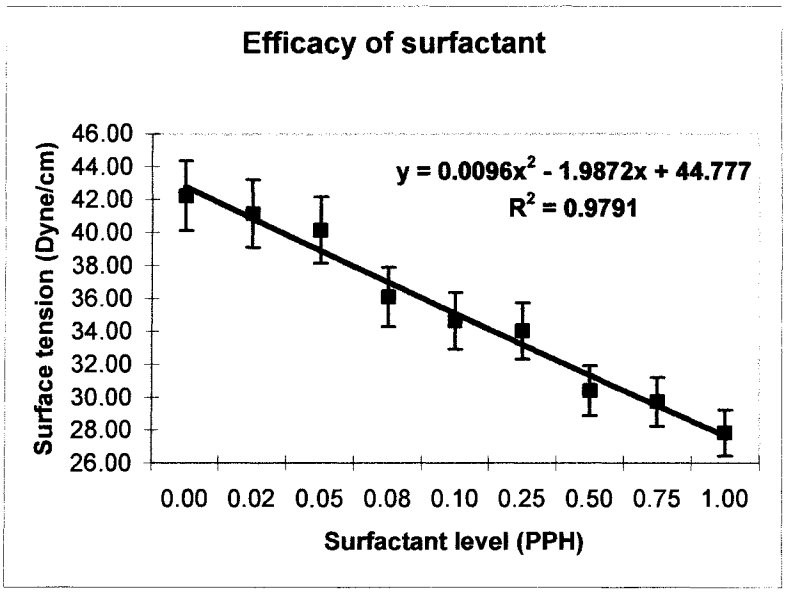

Figure 22. Surface Tension Profile.

Niaproof 4 is a strong anionic surfactant. Anionic surfactants are known to adsorb on to the pigment surfaces; so, the surface pressure or surface tension reduction would depend strongly on the adsorption-desorption isotherm of the surfactant. The adsorption/desorption isotherm of the surfactant would, in turn, strongly depend on the amount of shear encountered during preparation. Therefore, a separate study was performed to determine the effect of mixing on surface tension.

Once again surface tension profiles were generated, but this time the coatings were prepared using three different shear conditions. The standard coating formulation was prepared at 45% solids and an incremental amount of surfactant was added at low shear. Low shear was attained by hand mixing with a spatula. Moderate mixing was obtained with a laboratory mixer equipped with a propeller blade. High shear was obtained using a lab Cowles mixer at 1000 rpm.

The low shear mixing method with the spatula gave lower surface tensions than the high shear mixing method (Figure 23). The coatings prepared under low shear mixing were also found to be much lower in viscosity. This is because at lower shear, the absorption of the anionic surfactants on to the pigment particles is slow, so more surfactant remains in the water phase, lowering both the surface tension and viscosity of the coating. At high shear, the adsorption rate is much faster so considerably less surfactant is in the water phase, resulting in a higher viscosity and surface tension.

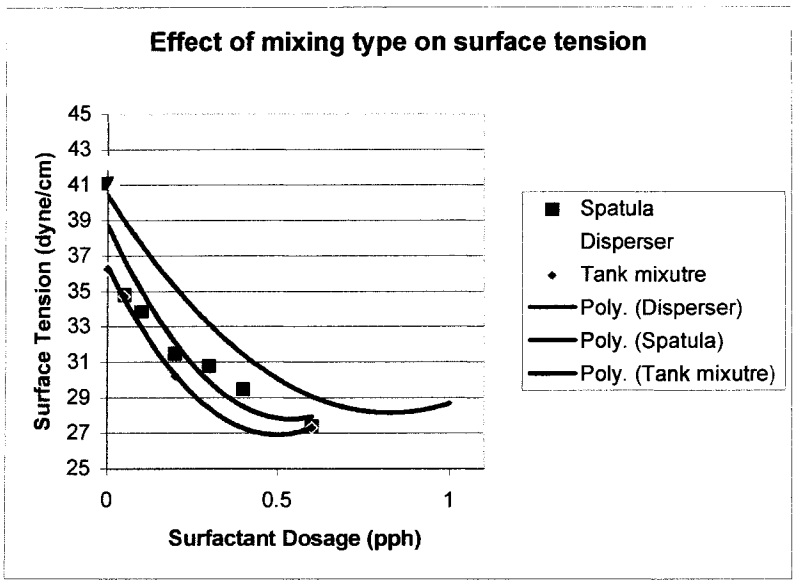

Figure 23. Influence of shear on surface tension.

Having determined the level of surfactant and CMC to be applied, the coating formulations parameters for the first phase statistical DOE experiments for the pilot curtain coater trials were determined. The coatings were prepared and applied on the Mitsubishi curtain coater. A diagram of the Mitsubishi curtain coater is shown in Figure 27.

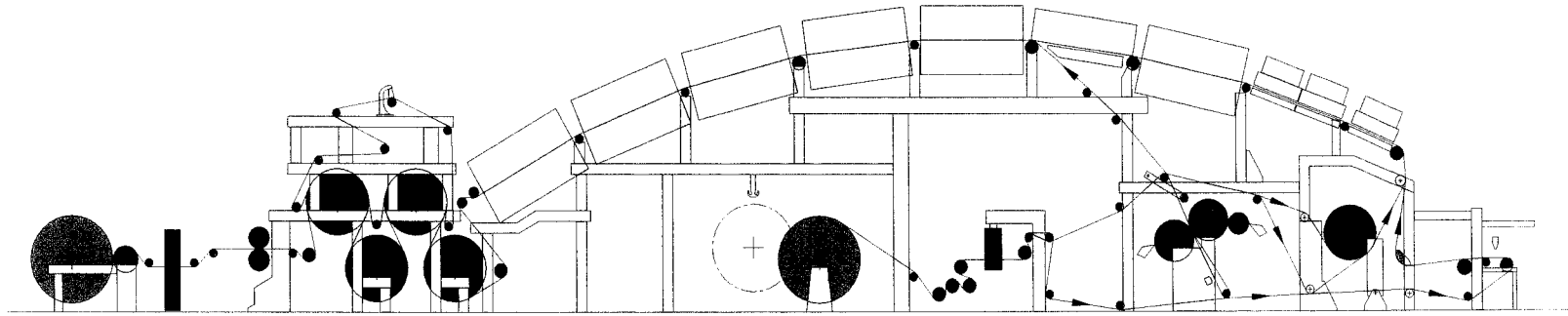

Figure 24. Flow diagram of MHI pilot curtain coater.

FIRST PHASE DOE

A Taguchi Orthogonal Array (OA) was used in the first phase, which allowed for the quick screening of variables in relatively few numbers of trials (Table 3). Taguchi OAs are interesting statistical tools for researchers as they allow for a large number of variables at different levels to be investigated quickly. The model contains only the main effects and does not account for parametric interactions. Therefore, large inherent statistical error, low overall R^2 values, is characteristic of this model, but is useful nonetheless for initial screening of factors. When using this array, the level of variables in the model should be selected in such a way that it reduces wild variations in the response variables. To reduce statistical error, a decent knowledge of the levels of all variables is a pre-requisite. This was accomplished by selecting the levels of our variables from the prescreening experiments performed. Six of the variables, perceived to be important, were assigned 3 levels. The remaining two variables were assigned 2 levels (Table 4).

Table 3. First Phase Statistical Layout

Study Type	Factorial
Initial Design	**Taguchi OA**
Center Points	0
Model	Main effects

Experiments	18
Blocks	None

Factor	Name	Units	Type	Low	High		
A	Nozzle Height	mm	Categorical	1	2	Levels:	2
B	Surface Sizing	gm/m^2	Categorical	1	2	Levels:	2
C	Roughness	PPS	Categorical	1	3	Levels:	3
D	Coating form		Categorical	1	3	Levels:	3
E	Surfactant	pph	Categorical	1	3	Levels:	3
F	Coat weight	gm/m^2	Categorical	1	3	Levels:	3
G	Web speed	mpm	Categorical	1	3	Levels:	3
H	SSS	Kg/min/m	Categorical	1	3	Levels:	3

Table 4. First Phase Variables and Their Levels

Variable	Level of the variable		
	Low (1)	Medium (2)	High (3)
Roughness	3.5 PPS	5.5 PPS	7.7 PPS
Sizing	1 gm/m^2 (C1S)	-	None
Coat weight	6	8	12
Coating Formulation*	I	II	III
Surfactant Dosage	0.02 pph	0.20 pph	0.80 pph
Web Speed	800 mpm	1400 mpm	1800 mpm
Curtain Height	150 mm	-	250 mm
Steam Flow rate	0.20 kg/min/m	0.55 kg/min/m	1.0 kg/min/m

*Coating formulations I, II and III represent different rheologies.

Table 5 shows the coating formulation parameters used for the first phase coating formulations. The levels of all other additives were kept the same. The lubricant, Nopcote C-104, was added at 0.06 pph, resin SPI at 0.5 pph and NaOH at 0.1 pph, to keep coating pH between 9-9.5. Surfactant was added at the predetermined levels of 0.02, 0.20 and 0.8 pph. The low shear viscosities of the coatings are given in Figure 25.

Table 5. First Phase Coating Formulations

Coating #	Clay/Carbonate	CMC	Latex
	pph	pph	pph
I	30/70	0.5	7
II	40/60	0.4	12
III	40/60	0.45	12

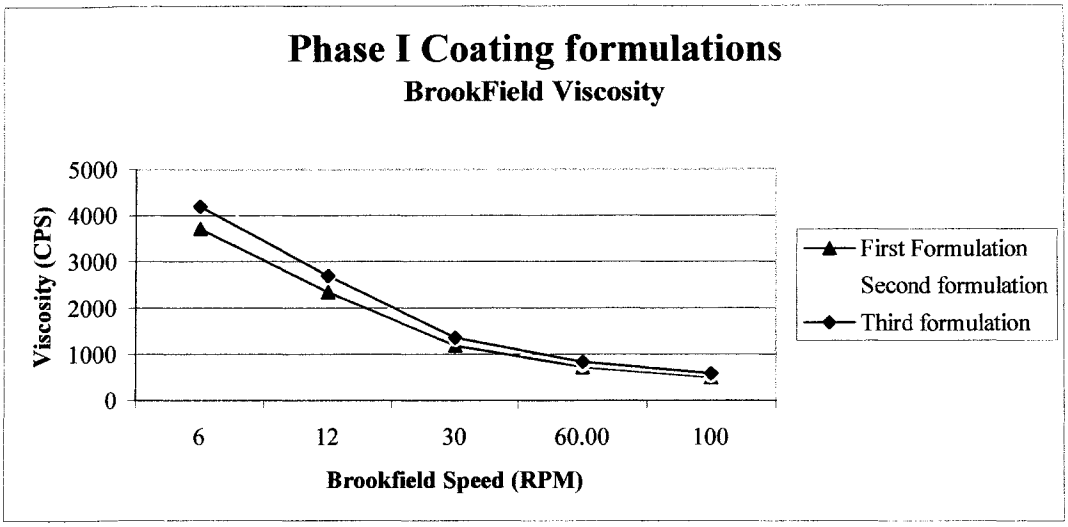

Figure 25. Brookfield viscosities of first phase coatings.

Coatings were prepared in a high shear Cowles mixer in a coating kitchen and then transferred to a constant temperature tank. The temperature of the coatings for the trials was assumed to be constant at 30 °C. Trials were run according to the above-mentioned DOE

The coverage of the coated samples was measured using a burnout method. Samples were soaked in a 10% solution of 50% Isopropanol and 50% ammonium hydroxide for an hour. The samples were then blotted to remove any excess solution and then burned in an oven at 100 °F for one hour. The samples were scanned and analyzed using Adobe Photoshop. Black and white area pixels of the scanned pictures were recorded using a gray threshold and the coverage defined as the ratio of white pixels to total (black +white) pixels.

FIRST PHASE RESULTS AND DISCUSSION

Trial conditions and result of first phase are summarized Table 6 (also see Appendix I). The statistical contribution of each formulation, substrate and process parameter studied to coverage (response variable) is summarized in Table 7. The coverage values were very

high for the 3 coat weights applied. Although coverage improved with coat weight, it was found to be only weakly dependant. This result was expected, as curtain coating is considered to be a true contour coating method. So the results support existing theory and demonstrate the potential benefits of curtain coating.

A higher nozzle height resulted in improved curtain stability, thus favored coverage. No conclusive explanation can be offered at this time but some of the effects of curtain height are well known. Higher curtain height increases curtain velocity and available surface age. Both of these phenomena will result in a higher Weber number, increasing the curtain stability. In addition, a higher inertial force will delay the onset of air-entrapment. It was observed during the trials that at a lower curtain height, the space between the steam substitution system and the curtain nozzle was reduced, resulting in a build up of pressure behind the curtain, increasing the amount of air entrapped in the coating.

As discussed above, Coating I and III are shear thinning (degree of thinning is higher in that order), whereas coating II was Newtonian. The shear thinning behavior favored better coverage, while the Newtonian rheology resulted in poor coverage. Again, no conclusive explanation can be offered at this time, but the results support the reported findings from other curtain coating researchers. Extensional rheological experiments are needed to possibly reach a better conclusion.

The smoother basesheet favored coverage. Again, coverage was very high at all base sheet roughnesses. These results again support the concept of a curtain coater being a true contour coater. Other researches have shown an optimum lower value of basesheet roughness, but as roughness levels are varied in this study, coverage continued to improve with basesheet smoothness.

Sizing with hydrophilic starch improved coverage. Surface sizing with starch improved the wetability of the basesheet. Improving the wetability delays the onset of air-entrapment and resulted in a higher viscous drag on the curtain, increasing the radius of curvature of the pulled film on the impingement zone, reducing total pressure. This resulted in delayed/less air entrapment.

Very low and high surfactant dosages (high and low corresponding surface tensions) resulted in improved coverage. The surface tensions at 0.20 and 0.80 pph surfactant dosage were almost the same and much lower than the surface tension at 0.02 pph dosage. This result contradicts established concepts of curtain stability and is considered in error.

Web speed was the single most dominant process variable. Higher speeds resulted in poor coverage. Air-entrapment and poor curtain stability were clearly visible at high speeds. At high speeds the curtain was fluttering violently and air-entrapment was severe. It is very clear that an efficient boundary layer air removal system is critical at high speeds. It must be noted, though, that the boundary layer air removal system was fixed at predetermined levels; according to the DOE. A stable curtain could have been realized by manipulating the air ejector pressure and steam flow rate of steam substitution system.

The first phase trials did result in a better understanding of the ejector pressures and steam flow rates required to stabilize the curtain at high speeds.

There seems to be an optimum level of steam flow rate, which should be used for each condition. Steam flow rates above or below the optimum level led to unstable and sometimes violent curtain instabilities.

Table 6. First Phase Result Summary

Run #	Roughness	Sizing	Formulation*	Surfactant Level	Coating Weight	Coating Speed	Nozzle Height	Steam Flow rate	Ejector Air Flow rate	Actual Coat weight	Coverage
	PPS (μm)	g/m^2		Parts	g/m^2	mpm	mm	kg/min	m^3/min	g/m^2	%
1	7.20	none	I	0.4	6	800	150	0.20	1.0	6.0	65
2	3.74	1	I	0.4	12	1400	150	0.60	1.8	8.8	75
3	5.57	1	I	0.02	6	1800	150	0.75	2.3	4.3	85
4	3.74	1	I	0.2	8	1800	250	0.20	2.3	6.6	50
5	5.57	1	I	0.2	12	800	250	0.55	1.0	9.1	84
6	7.20	none	I	0.02	8	1400	250	1.00	1.8	6.9	91
7	7.61	1	II	0.2	12	1400	150	0.20	1.8	9.0	90
8	5.57	1	II	0.02	8	800	150	0.20	1.0	6.7	50
9	3.72	none	II	0.02	12	1800	150	1.30	2.3	8.2	87
11	5.57	1	II	0.4	6	1400	250	1.00	1.8	4.4	92
10	7.61	1	II	0.4	8	1800	250	0.75	2.3	5.2	50
12	3.72	none	II	0.2	6	800	250	0.35	1.0	4.1	88
13	3.74	1	III	0.4	8	800	150	0.55	1.0	7.8	85
14	5.54	none	III	0.2	8	1400	150	2.00	1.8	7.8	84
15	7.61	1	III	0.2	6	1800	150	1.30	2.3	5.1	95
16	7.61	1	III	0.02	12	800	250	0.35	1.0	9.5	85
17	3.74	1	III	0.02	6	1400	250	0.20	1.8	4.9	60
18	5.54	none	III	0.4	12	1800	250	0.20	2.3	9.6	50

* (I,II,III) are different coating rheologies

Table 7. First Phase - Overall Statistics

Variable		Coverage	
		Mean Sum of squares	**% Contribution***
Nozzle Height	mm	97.72	**3.11**
Surface Sizing	gm/m^2	7.53	**0.24**
Roughness	PPS	123.00	**3.92**
Coating formulation		365.41	**11.63**
Surfactant	pph	498.09	**15.86**
Coat weight	gm/m^2	19.90	**0.63**
Web speed	mpm	2016.46	**64.20**
Steam Flow	Kg/min/m	12.97	**0.41**

** % Contribution of a variable is contribution it makes in explaining variance in the response variable*

Curtain stability was analyzed by studying videos of the trials and assigning a number between 1-10, higher the better. The videos were analyzed by assessing the straightness of the curtain, the amount of backflow and fluctuations, and the amount of air entrainment and splashing that occurred just around the dynamic wetting line. Three observers were used and the scores averaged to rate the contribution of the input variables to curtain stability. The results are summarized in Tables 8 and 9. The dark colored boxes depict the most important variables. These are the variables that were found to have the strongest effect on air entrapment and curtain stability.

Table 8. Overall Statistical Summary for Air Entrapment

Variable		Air-Entrapment	
		Mean Sum of squares	**% Contribution**
Nozzle Height	mm	0.89	**1.75**
Surface Sizing	gm/m^2	15.34	**30.24**
Roughness	PPS	2.06	**4.05**
Coating Form		8.76	**17.28**
Surfactant	pph	0.89	**1.75**
Coat Weight	gm/m^2	3.35	**6.60**
Web Speed	mpm	17.60	**34.69**
SSS	Kg/min	1.85	**3.64**

Table 9. Summary of Statistical Contribution of Process and Formulation Parameters on High Speed Curtain Stability (colored boxes represent strong dependence)

	N. H	Sizing	Roughness	C. form'n	Surf't	CW	Webspeed	SSS
Straightness	-	↑	↑	↑	↑	↓↑	↓	↑↓
Fluctuation	-	↑	-	↑	↑	↑	↓	↑↓
Back Flow	↑	↑	↓	↓	-	↑	↓	↑
Air Entrainment	-	-	-	↑	↓	↓	↓	↑
Splash	-	-	↓	↑	↓	↓	↓	↑

Surface sizing, web speed and coating formulation have the greatest impact on air-entrapment and curtain stability in that order. Colored boxes represent a stronger effect of the parameter on the particular stability phenomena. These results corroborate with the current understanding of curtain operation as discussed earlier. Surface sizing with starch improves substrate wettability increasing viscous drag. Higher viscous drag results in a higher radius of curvature of the curtain in the impingement zone, reducing total pressure in the zone. Coating formulation affects the stretchability of curtain in viscous drag. Air entrainment is affected by steam substitution, coating formulation and coat weight. Comparing the results for coverage and curtain stability, it is clear that curtain stability and coverage is not governed by the same variables or by the same extent by a variable. The chosen process parameters are interacting strongly.

SECOND PHASE DOE

Phase I resulted in a good understanding of how to utilize the boundary layer air removal system (ejector pressure and steam flow rate) to improve the stability of the curtain, but stabilizing the curtain at high speeds remained a concern. To address this concern, web speed (higher side) was kept as a variable in the next phase of pilot plant trials.

From the results of the first phase study, it was determined that shear thinning rheologies clearly favored curtain coater stability at higher speeds. As a result, it was decided that rheology would be further explored in the next phase of trials. As the degree of shear thinning is also a factor, coating formulations will be formulated to produce coatings of different degrees of shear thinning behavior. Since web speed was found to be the single most important factor. The effect of web speed needs to be examined more closely. As the curtain is very stable at low speeds, only high speeds were considered in the next phase of pilot trials. Since it was determined that the boundary layer air removal system must be fine tuned to the web speed, it was decided that steam flow rates would remain a variable in the next phase.

Although base sheet smoothness had a positive impact on coverage, high coverage was achieved even for high basesheet roughness. As a result, base sheet roughness effects would not be further explored. Because curtain coating coverage was almost insensitive to the coat weight, this parameter was also not considered further. It was also decided that the curtain height would be fixed, as well as the level of surfactant added.

In the second phase, an irregular factorial model, D-optimal, was used (Table 10). This model allowed the two-way interactions between variables to be analyzed, which was critical in understanding the influence of curtain coating stability on coverage. Three variables were assigned 3 levels and one variable was assigned 2 levels. The levels assigned were based on the relative importance of each variable determined from the first phase of pilot studies.

Table 10. Second Phase Statistical Layout

Study Type	Factorial
Initial Design	**D-optimal**
Center Points	0
Design Model	2FI
Response	Name
Y1	Coverage
Y2	Air entrapment

Experiments	26
Blocks	No Blocks

Factor	Name	Units	Type	Low Actual	High Actual		
A	Roughness	PPS	Categorical	-1	1	Levels:	3
B	SSS	Kg/min/m	Categorical	-1	1	Levels:	3
C	Formulation		Categorical	-1	1	Levels:	3
D	Speed	MPM	Categorical	-1	0	Levels:	2

The levels of variables and constant parameters are summarized in Table 11 and 12 for the second phase. The formulations for the second phase coating trials are given in Table 12. Lubricant, Nopcote C-104, was added at 0.06 pph, resin SPI at 0.5 pph and 0.1 pph NaOH to keep coating pH between 9-9.5. Surfactant was added to achieve the desired levels of 0.02, 0.20 and 0.8 pph. The low shear viscosity properties of the coatings are shown in Figure 26.

Table 11. Second Phase Variables and Their Levels

Variable	**Level of the variable**		
	Low (-1)	Medium (0)	High (1)
Roughness	7.2 PPS	6.2 PPS	5.5 PPS
Web Speed	1500 mpm	-	1800 mpm
Coating Formulation*	I	II	III
Steam Flow rate	0.80 kg/min	1.2 kg/min	1.6 kg/min

*Coating formulations I, II and III represent different rheologies

Table 12. Second Phase Fixed Parameters

Sizing	None
Coat weight	6 gms/m^2
Surfactant Dosage	0.20 pph
Curtain Height	250 mm

Table 13. Second Phase Coating Formulations

Coating #	Clay/Carbonate	CMC	Latex
I	40/60	0.55	14
II	40/60	0.55	15
III	40/60	0.5	12

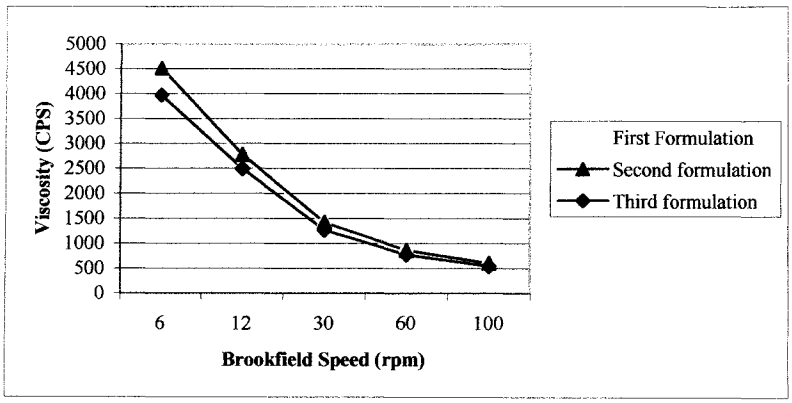

Figure 26. Brookfield viscosities of second phase coatings.

SECOND PHASE RESULTS AND DISCUSSION

The results of the second phase pilot trials are summarized in Tables 13 and 14 (also see appendix II). As shown, the steam flow rate was the only significant main effect. Roughness, in combination with web speed and coating formulation, and steam flow rate in combination with web speed were found to be significant. The roughness/formulation interaction was the single largest effect (39%) followed by the steam substitution flow rate (24%). The next two significant effects are much smaller; roughness-speed (4.7%) and web speed-steam flow rate (6%).

The effect of web speed was surprisingly small but can be explained by the better manipulation of the boundary layer air removal system. The effect of web speed was offset by the dominant contribution of the steam substitution system. In the first phase, the web speed was dominant, whereas the contribution of the steam substitution was insignificant. Web speed – steam flow rate was significant in combination with each

other. This supports the conclusions from the first phase that showed the effect of steam substitution to be dominant for curtain stability. Thus, steam substitution is critical for realizing a stable curtain and it should be tuned with web speed.

Roughness was not found to be significant by itself, but in combination with the coating formulation and web speed it critically impacted the curtain stability. The roughness-web speed interaction can be explained by the effect of roughness on boundary layer air thickness. Roughness also affects the ease of boundary layer air removal, thus the efficiency of the steam substitution system. Its interaction with the coating formulation can be explained with current data or any existing theory.

Table 14. Second Phase Result Summary

Run #	Roughness	Steam Flowrate *	Formulation	WebSpeed	Coverage
	PPS (μm)	Kg/min/m	**	MPM	%
1	5.5	0	III	1800	90
2	6.2	-1	III	1800	73
3	6.2	-1	I	1500	67
4	7.2	0	II	1800	89
5	5.5	0	I	1800	55
6	6.2	0	I	1800	86
7	5.5	0	II	1500	87
8	6.2	0	III	1500	72
9	5.5	-1	III	1500	90
10	7.2	0	III	1800	68
11	6.2	1	II	1500	80
12	7.2	1	II	1800	82
13	7.2	0	I	1500	95
14	5.5	1	I	1500	89
15	6.2	1	I	1800	82
16	7.2	-1	II	1500	73
17	6.2	-1	II	1800	68
18	5.5	-1	I	1800	66
19	7.2	-1	III	1800	70
20	6.2	1	III	1800	86
21	7.2	1	III	1500	84
22	5.5	1	II	1800	84
23	5.5	-1	II	1800	72
24	7.2	1	I	1800	90
25	6.2	0	II	1800	78
26	7.2	-1	I	1800	78

* (-1,0,1) are the levels of steam flow rates.

** (I, II, III) are coating rheologies differing in order of shear thinning

Table 15. Second Phase - Overall Statistics

	Sum of squares	DF	Mean SOS	% Contribution
Roughness (A)	81.74	2	40.87	3.13
SSS (B)	660.80	2	330.40	24.24
Formulation (C)	2.83	2	1.41	0.26
Speed (D)	32.40	1	32.40	3.93
Interaction AB	219.02	4	54.75	3.35
Interaction AC	1024.88	4	256.22	39.37
Interaction AD	5.84	2	2.92	11.36
Interaction BC	164.40	4	41.10	3.20
Interaction BD	209.02	2	104.51	6.43
Interaction CD	115.17	2	57.59	4.73

% Contribution of a variable is contribution it makes in explaining variance in the response variable

CONCLUSIONS

Employing an efficient boundary layer air removal system can alter the operating window of a curtain coater. The boundary layer air removal system should be tuned with web speed. The role of the boundary layer air removal system is especially critical at high speeds. Base sheet roughness, in combination with coating formulation, is the most important variable in curtain coating operation. A smooth base sheet improves coverage. Very high coating coverage is possible at low coat weights with a curtain coater. Shear thinning coating rheology favors curtain coating. The degree of shear thinning is important however, considering the extensional flow field in the process, more rheological studies are needed to establish the single most important rheological parameter to curtain coating. Coat weight improves coverage, but coverage is only a weak function of coat weight. Higher curtain height and Base sheet wettability improves overall curtain operation stability.

ACKNOWLEDGEMENTS

We are indebted to the pilot operators Ikeda-san, Nakashima-san, Izumi-san and research engineer Horie-san. This study was not possible without their hard work and active participation. We would also like to thank Imery's Inc, Engelhard Inc. and DKS, Japan, for their generous support in supplying the materials for these trials.

BIBLIOGRAPHY

1- Triantafillopoulos, Johan G, Iiro L, Petri P., "Operational issues in high speed curtain coating of paper", TAPPI JOURNAL, November 2004, Vol. **3**(11).

2- Sugihara, M., Miura, H., Yamada, K., Miyakura, T., "Control of Dynamic Wetting Line and Entrainment of Boundary Air in High-Speed Curtain Coating", 2002 Coating Conference Proceedings, May.

3- Mendez, B, Tietz, M, and Morita, H. "Curtain coating- a novel coating technique for high-precision coating", 20, Streicherei symposium 2001.

4- Miyamoto K and Katagiri Y, "Curtain coating", Liquid film Coating: Scientific Principles and their Technological Implications, 1997, pp 463-494.

5- Brown D, "A study of the behavior of a thin sheet of moving liquid" Journal of fluid mechanics, vol. **10**, 1961, pp297-305.

6- Citation to Wells.

7- Kistler S F., "The fluid mechanics of the curtain coating and related viscous free surface flows with contact lines", PhD thesis, 1984.

8- Wilson, M.C.T., Summers, J.L., Gaskell, P.H., "Numerical simulations of curtain coating with a moving contact line", Shikhmurzaev,

9- Clarke A, "Recirculating flows in curtain coating", The Mechanics of Thin Films Coating –1995 editors Gaskell, P H, Savage, M D and Summers, J L

10- Carley J, "Flow of melts in "crosshead" – Slit dies; Criteria for die design", Journal of applied physics, vol. 25 , No. 9 ,1954, pp 1118-1123

11- Ruschak K. J. and Weinstein S. J., "Mathematical modeling of fluid dies", The mechanics of thin films coating –1995 editors Gaskell P H, Savage M D, Summers J

12- Lee K and Liu T, "Design and analysis of a dual-cavity coat hanger die", polymer engineering and science, mid-august 1989, vol. 29, No.15

13- Sartor L " Slot coating: fluid mechanics and die design", , PhD thesis, 1990

14- Sinh-Luh Yuan , Polymer engineering and science, mid-April 1995, vol. 35, No. 7

15- Durst F, Lange U and Raszillier "Minimization and control of random effects on film thickness uniformity by optimized design of coating die internals", , the mechanics of thin films coating –1995 editors Gaskell P H, Savage M D, Summers J L

16- Shelley L. Anna, Gareth H.McKinley,Duc. A. Nguyen, Tam Sridhar,Susan J. Muller, Jin Huang and David F.James "An interlaborotary comparison of measurements

from filament-stretching rheometers using common test fluids",. Jounal of Rheology 2001, vol 45,issue-1, pp 83-113

17- ", Thomas Erneux and Stephen H. Davis "Nonlinear Rupture of free films. Physics of Fluids A-Fluid Dynamics 1993, vol.5,no.5, pp 1117-1121.

18- A Vrij, "Possible mechanism for the spontaneous rupture of thin, free liquid films", Discussions of the Faraday Society 1966, no.42 pp 23-33.

19- Eli Ruckenstein and Rakesh K. Jain, Spontaneous rupture of thin liquid films", Faraday Transactions , Part 2, Chemical society of London, 1974 vol.70,#1-4,pp 132-147.

20- C.H. Teng, S.P.Lin and J.N. Chen, "Absolute and convective instability of a viscous liquid curtain in a viscous gas", journal of fluid mechanics –1997, vol 332, pp 105-120

21- S, Yamada K, Miura H and Miyakura T, "Control of dynamic wetting line and entrapment of boundary air in high speed curtain coater", Tappi coating conference 2002.

22- E.B. Dussan V, "On the spreading of liquids on solid surfaces: static and dynamic contact lines". Annual review of fluid mechanics 1979, vol.2, pp 371-399.

23- "The dynamic wettability of paper - Part 2", Tappi Journal 1984, vol.67, issue – 10, pp 96-99.

24- "Wetting and sorption of water by paper under dynamic conditions", Tappi Journal 1982, vol. 65 issue-12, pp 98-101.

25- John A. Roper, Robert Urscheler, Pekka Salminen and Douglas W.Bousfield, "Wetting line in high speed free jet coating"

26- Masato Yamamura, Satoshi Suematsu, Toshihisa Kajiwara, and Kitaro Adachi, "Experimental investigation of air entrainment in a vertical liquid jet flowing down onto a rotating roll", Chemical engineering Science 55(2001), pp 931-942.

27- Y. D. Shikhmurzaev, "Spreading of liquids on dry and pre-wet solid surfaces",

28- T. G. Myers, "Surface Tension Driven Thin Film Flows". the mechanics of thin films coating –1995 editors Gaskell P H, Savage M D, Summers J L

29- R. Byron Bird, Robert C. Armstrong, and Ole Hassager, " The general linear visco-elastic fluid", Dynamics of polymeric liquids, Fluid mechanics 1987, second edition, vol.1.

30- I . Greiffenberg and S. Lohmander M. Rigdahl, "Effects of the air content on the rheological properties of coatings" Advanced coating fundamentals symposium, Tappi proceedings 1999.

31- Fabio B, Bousfield D. S., "Modeling of rheological properties of coating" Journal of rheology, vol. 45, 2001.

32- Kee D.D., Fong M C F C, "Elogantional, Hysteresis and oscillatory flows of complex fluids", Journal of Rheology 2001, vol 45,issue-1

33- Douglass S. Finnicum, Steven J. Weinstein and Kenneth J. Ruschak, "The effect of applied pressure on the shape of a two-dimensional liquid curtain falling under the influence of gravity", Journal of fluid mechanics, 1993 vol.225, pp 647- 665

34- S.P. Lin and Howard Brenner, "Tear Film Rupture" Journal of colloid and interface science, vol. 89, no.1, 1982, pp 226-231.

35- "A flow model of non-Newtonian liquids",

36- Albert Baechi, "BMB curtain coater",

37- Meck D., Kogler W., Becker I., Holtmann B. and Stuffer P, "Non-impact coating in the curtain coater" 20th Streicherei symposium 2001

38- C. H. Teng, S. P. Lin, and J. N. Chen, "Absolute and convective instability of a viscous liquid curtain in a viscous gas", Journal of Fluid Mechanics 1997, vol.332, pp105-120.

39- P.Bourgin, and N. Tahiri, "Generalized Jeffery-hamel flow: Application to high velocity coating", the mechanics of thin films coating –1995 editors Gaskell P H, Savage M D, Summers J L

40- Jack F. Greiller, "Apparatus for production of photographic elements," Patent, United States patent no. 3867901.

41- Keiller R, "Modeling of extensional flow of M1 fluid with Oldroyd equation", Journal of Non-Newtonian Fluid mechanics, 42 (1992) 49-64

42- Benkreira H, "Dynamic Wetting in metering and pre-metered forward roll coating", Chemical engineering science 2002.

43- Cheng D, "A review of the role of rheology in coating process", the mechanics of thin films coating –1995 editors Gaskell P H, Savage M D, Summers J L

44- Liu T, Hong C and Chen K, "Computer aided analysis of a linearly taped coat-hanger die", Polymer engineering and science, mid-Dec 1988, vol. 28, No. 23, pp 1517-1526

APPENDIX -I

First Phase Results

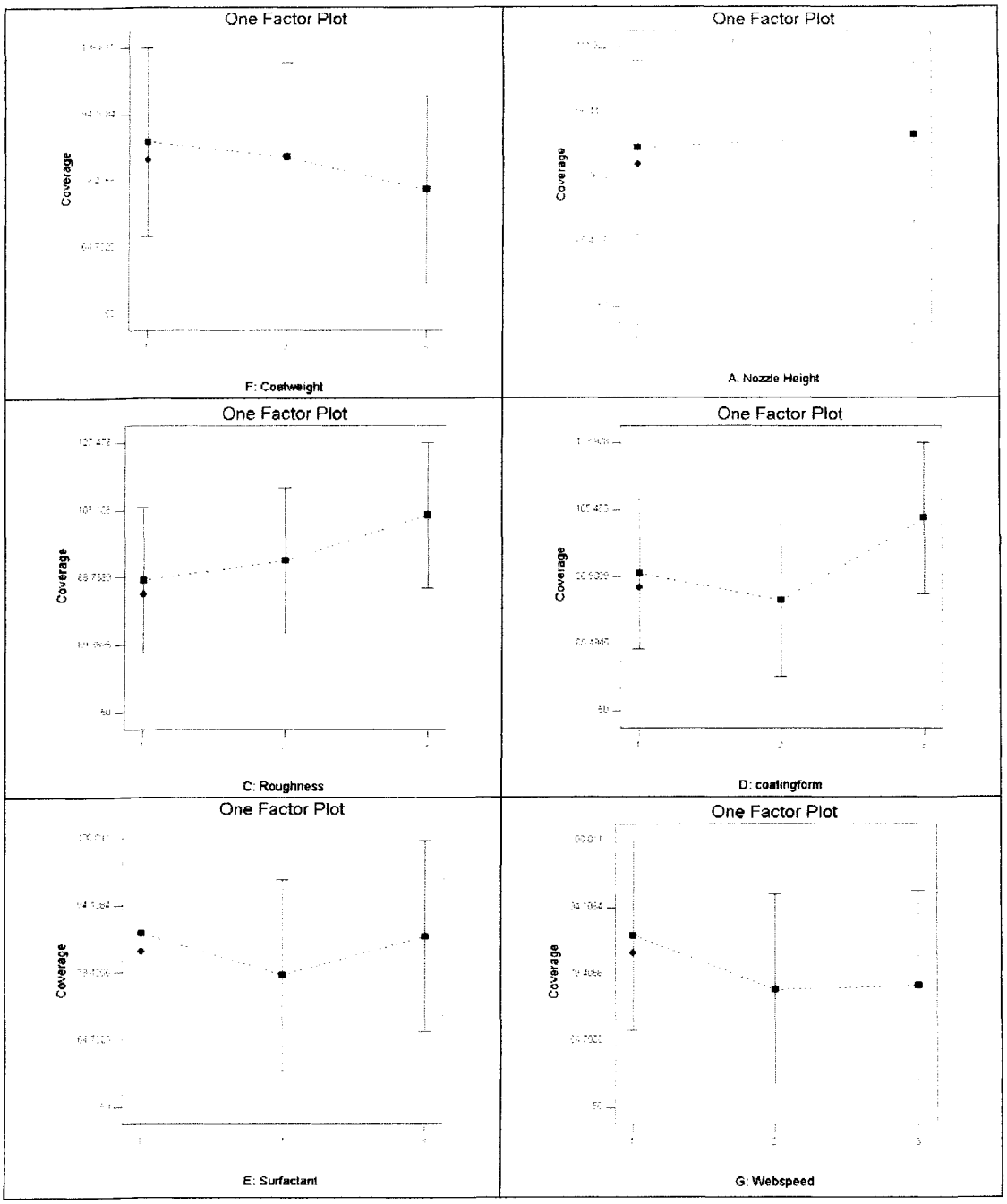

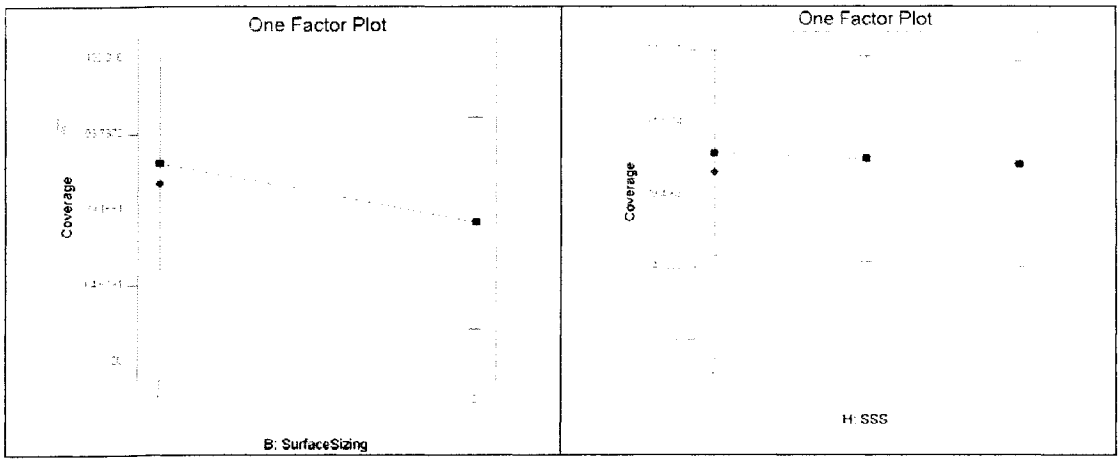

APPENDIX II – Second Phase Results

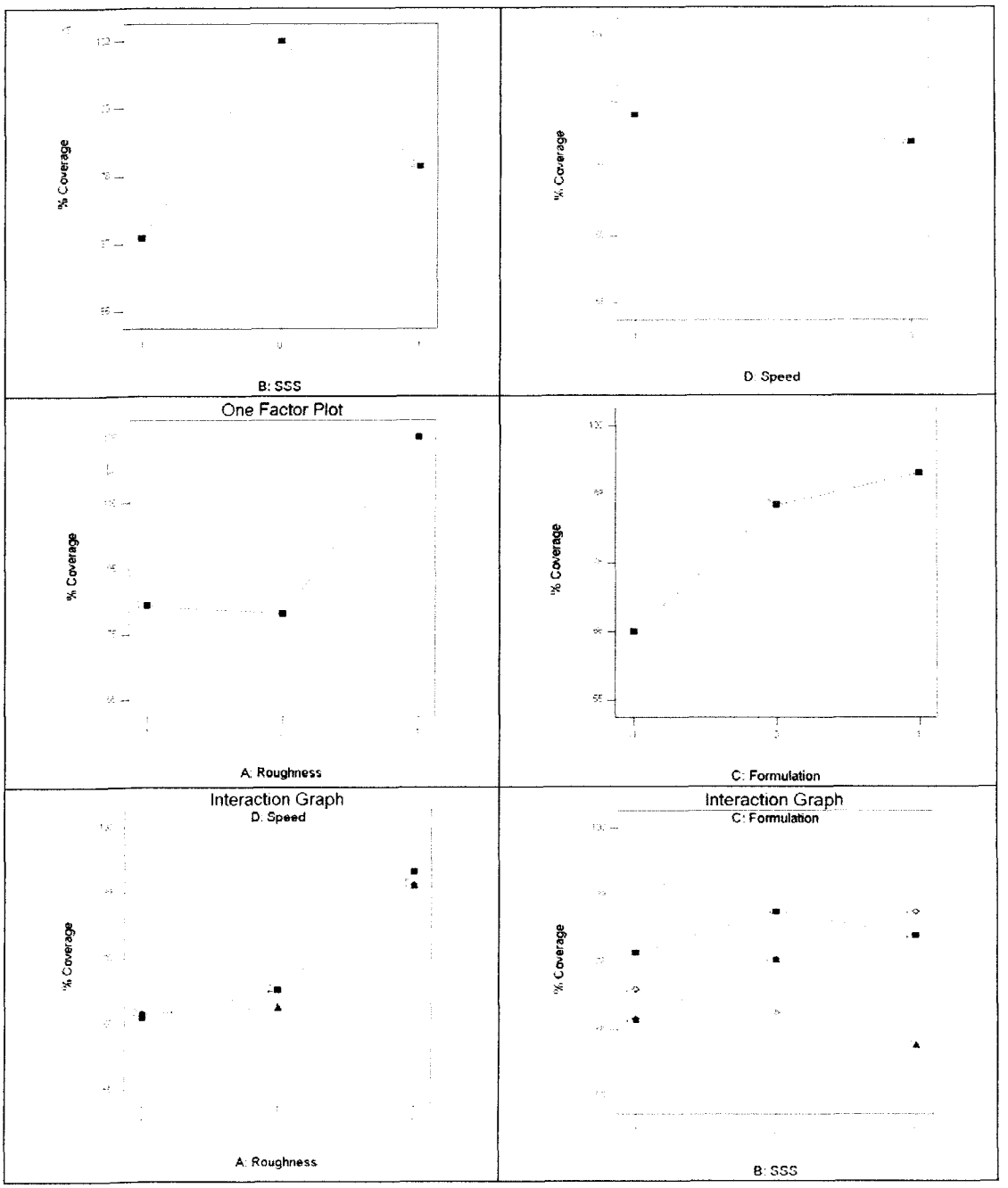

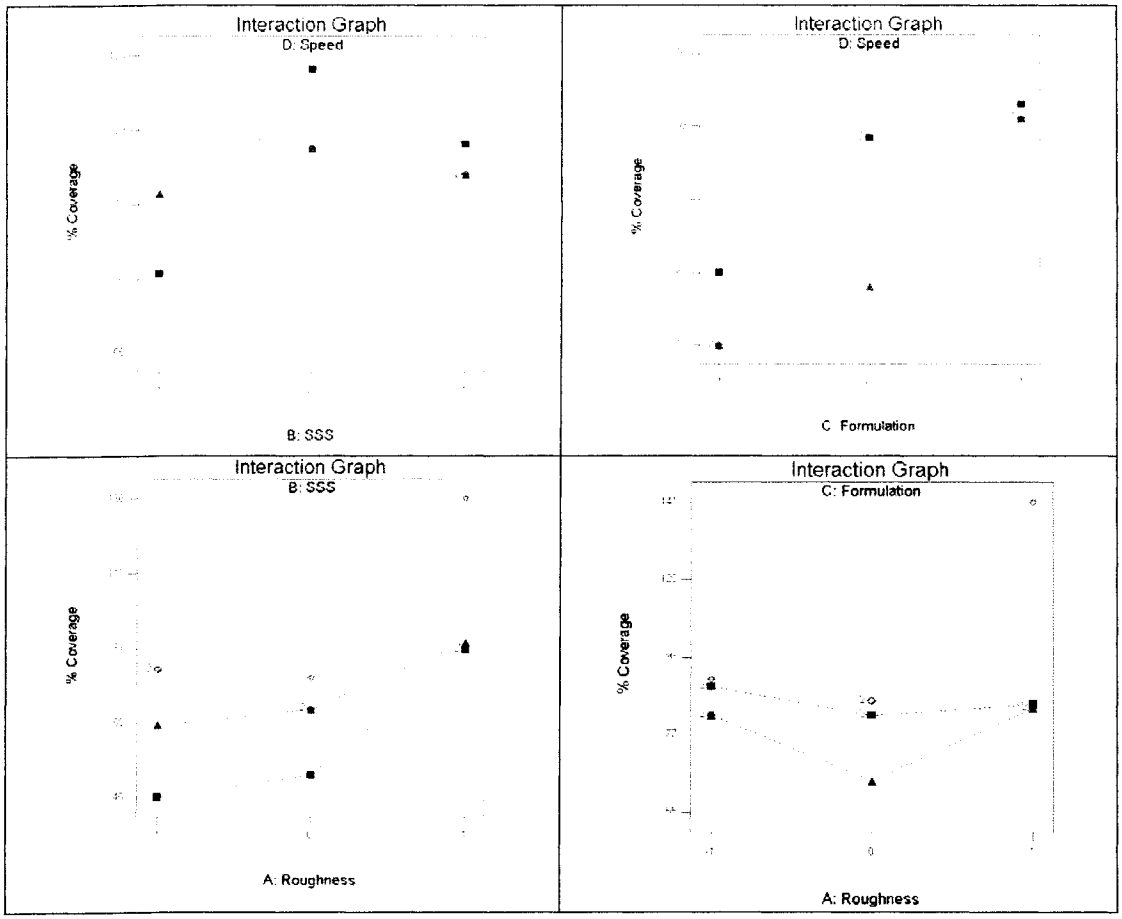

Understanding the Role of Surfactants in the Stabilization of a Coating Curtain

Peeyush Tripathi[a]
Dr. Margaret Joyce[a]
Dr. Do Ik Lee[a]
Dr. Paul D. Fleming[a]
Dr. Masahiro Sugihara[b]

[a]Center for Coating Development
Western Michigan University
[b]Mitsubishi Heavy Industries

ABSTRACT

Curtain coating is a non-contact metering coating process that offers enormous potential as a useful high speed, on machine, coating method for the paper industry. Its ability to coat through non-impact metering provides excellent coverage, and to apply a controlled coating layer of uniform thickness makes curtain coating very attractive as a new coating process. However, to achieve success, curtain stability at commercial speeds must be proven achievable on a consistent basis.

Curtain stability is the most important conditions for the satisfactory curtain coating operation because a uniform coating layer cannot be obtained without it. To obtain a stable curtain a Weber number, $W_e > 2$ should be met throughout the length of the curtain. This criterion can be met at any surface tension, by adjusting flow rate only, but requires a very high flow rate at high surface tension, resulting in high coat weights. Thus, to operate at low flow rates, and expand the operational usefulness of this process, the surface tension of the coating must be reduced.

Today, a large variety of surfactants, which encompass a full spectrum of HLBs, are available for use in this application. However, the suitability of their chemical composition and dosage requirements is not clearly understood. Part of the problem in determining these requirements is that the measurement of static and dynamic surface tension at high coating solids (solids of practical application) is problematic, using presently available instrumentation. In the present study, static and dynamic surface tensions were measured with surfactants in water and coatings (up to 62% solids) using a Wilhelmy plate, maximum bubble and Mach angle measurement method. Dynamic surface tension measurements using maximum bubble pressure and Mach angle methods did not agree well with each other. With the Mach angle method, surface tensions were found to increase in the curtain, as the curtain fell under gravity (increasing surface age), while the maximum bubble pressure method showed the surface tension to decrease with surface age. It was determined that the extent of change in the surface tension values of the coatings depended on the type and dosage of surfactant used. Low HLB soluble surfactants (≈11-13) were found to be better for obtaining and maintaining a stable curtain at high speeds.

INTRODUCTION

Dynamic and Static Surface Tension Theory

The theoretical relationship between surface tension (static and dynamic) and surfactant adsorption is a combination of thermodynamic relations, for ideal solutions, and empirical relationships for practical concentrations. A detailed description of these relations is available in several textbooks, e.g. Ross and Morrison and Adamson (1,2). Based on thermodynamics, for an ideal solution, the variation of the surface tension is related to surfactant adsorption by the Gibbs equation,

$$-\left(\frac{\partial\sigma}{\partial(\ln(C))}\right)_{T,P} = RT\Gamma, \tag{1}$$

where σ is the surface tension, C is the bulk concentration of the surfactant, T is the absolute temperature, R is the universal gas constant and Γ is the surface excess concentration of the surfactant at the interface. At very low concentrations, equation (1) reduces to:

$$\pi = \sigma_s - \sigma = RT\Gamma \tag{2}$$

Here, π is called the film pressure. However, this equation is only applicable when the surfactant behaves as a two dimensional gas in the surface. At such conditions, the film pressure becomes linear in the surfactant concentration. Such behavior is only possible at extremely low surfactant concentrations. For more practical surfactant concentrations, in the range of industrial applications of surfactants, an empirical equation, posed by Von Szyszkowski (3), can be used.

$$\pi = \sigma_s - \sigma = RT\Gamma_\infty \ln\left(1 + C/a\right) \tag{3}$$

Here Γ_∞ is the maximum excess surface concentration and a, is a constant. The constant a-term, is an important characteristic of the surfactant, known as the Langmuir constant. Combining the Gibbs and Szyszkowski equations, an adsorption isotherm (1) is derived for practical surfactant concentrations as follows:

Equation (1) can be rewritten as

$$-\left(\frac{\partial\sigma}{\partial(C)}\right)_{T,P} = \frac{RT\Gamma}{C} \tag{4}$$

Taking the derivative of equation (3),

$$-\left(\frac{\partial\sigma}{\partial(C)}\right)_{T,P} = \frac{RT\Gamma_\infty}{C+a} \tag{5}$$

Combining equations (4) and (5) yields,

$$\frac{\Gamma}{\Gamma_\infty} = \frac{C/a}{1+C/a} \tag{6}$$

The above equation is the Langmuir adsorption isotherm (4), also referred to as, the Langmuir-von Szyszkowski equation. The Langmuir- Szyszkowski equation relates the bulk surfactant concentration, to the surface excess concentration at the interface. It is applicable at practical surfactant concentrations under both static and local equilibrium dynamic conditions. Under dynamic conditions, the concentration gradient driven surfactant diffusion process is responsible for restoring equilibrium at the interface. For such conditions, the diffusion rate of the surfactant, in the given medium and surface age, plays an important role. Surface age is the age of the surface from the time of its disturbance. However, the Langmuir- Szyszkowski equation does not relate to these dynamic variables, because there is no factor to account for diffusion. Under dynamic conditions, surfactant diffusion to and from the interface occurs in an attempt to restore the equilibrium surface excess. The diffusion-controlled adsorption (change in surface excess with surface age) is described by the Ward and Tordai equation (5).

$$\Gamma = 2C_0\left(\frac{Dt}{\pi}\right)^{1/2} - 2\left(\frac{D}{\pi}\right)^{1/2}\int_0^{t^{1/2}} C_s\left(t-\tau\right)d\tau^{1/2} \tag{7}$$

Here D is the diffusion coefficient, C_0 is the bulk concentration, C_s is the subsurface concentration, t is the age of the surface, and τ is the auxiliary variable. The Ward and Tordai equation is the most rigorous description of the diffusion-controlled adsorption process. The first term in the Ward and Tordai equation represents the diffusion from the bulk phase to the subsurface and the second term represents the diffusion from the interface, back to the bulk. Diffusion back to the bulk is appreciable only when the system is at or near the point of equilibrium. For small surface ages, the second term can be neglected.

Physical Variables in Curtain Coating Affecting Surface Tension

The variables of a curtain coater that affect the dynamic surface tension and stability of the curtain are flow rate Q (per unit slot length), slot opening d_0 and curtain height H. Neglecting the curtain swell at the slot exit, d_0, the initial curtain thickness will be the same as the slot opening, Thus, both the initial curtain thickness and slot velocity, U_0, depend on slot opening. To understand how these quantities influence the dynamic surface tension, let us use the following terms to describe and analyze the flow of a curtain. In accordance to Figure 1, let H be the height of the curtain from the slot opening of a curtain die that has an instantaneous curtain velocity of V_H, curtain thickness of d_H, and surface age of, t_H.

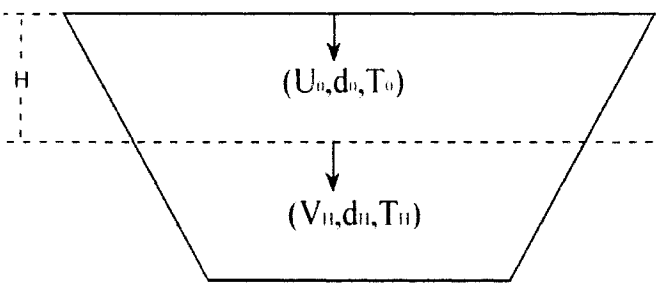

Figure 1. Curtain Coating process.

Using these terms, the conservation of mass says,

$$Q = U_0 \times d_0 = V_H \times d_H, \tag{8}$$

where d_o is the slot opening, neglecting any curtain swell at the slot exit. From the basic equations for free fall of any liquid under gravity, the curtain velocity V_H, at the position H and time t are related as follows:

$$V_H = U_0 + gt \tag{9}$$

$$V_H^2 = U_0^2 + 2gH \tag{10}$$

$$H = U_0 t + \frac{1}{2} g t^2, \tag{11}$$

where g is the acceleration due to gravity.

Brown (6) reported that at the onset of flow, there will be a transition zone between exit of the slot and point of free fall in which the flow field is affected by viscous effects. To correct for these viscous effects, a viscosity correction factor $(H-0.5(\mu/\rho)^{2/3})$, has been suggested (8,9) to be used for replacement of H in the above equation (7). However, for most cases, this viscosity correction can be neglected, as the length of the transition zone is very small for most practical applications i.e., it is about 1mm for 10 mPas and 23 mm for 1000 mPas.

The time of curtain fall from the slot opening to the position, H, is the effective surface age of the curtain at that position. Thus, the surface age of the curtain at position H from the slot opening can be calculated from equation (12) and the Weber number, W_e, at position H can be determined from equation (13).

$$Surface\ Age = t_H = \frac{-u + \sqrt{u^2 + 2gH}}{g} \tag{12}$$

$$W_e = \frac{\rho d_H V_H^2}{2\sigma_H} = \frac{\rho Q V_H}{2\sigma_H} = \frac{\rho Q \sqrt{(U_0^2 + 2gH)}}{2\sigma_H} \tag{13}$$

In equation 13, σ_H is the local surface tension at position H from the slot opening. From equations 8-13, it is clear that increasing the curtain height increases both the surface age and Weber number. A higher surface age also results in lower surface tensions. Our previous research indicates a positive affect of curtain height on curtain stability (10). A graphical representation of the affects of curtain height on curtain properties, derived from equations 8-13 is given in Figure 2.

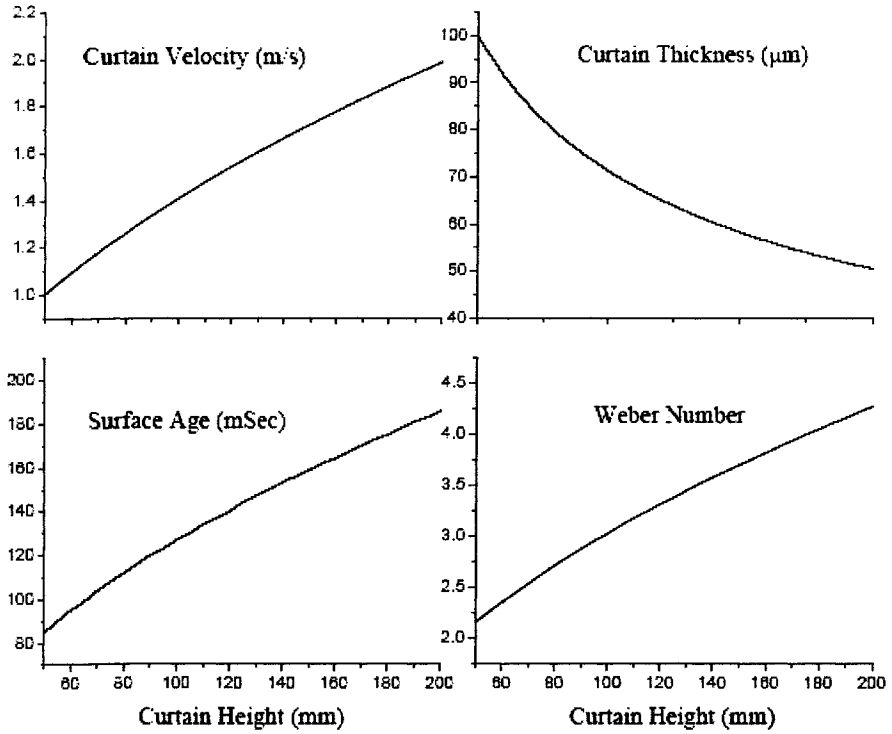

Figure 2 Effect of curtain height on curtain properties; Flow rate 1.0 cm^2/s, Slot opening 600 μm, Viscosity 500 cP, Surface Tension 35 mN/m.

In these calculations, the surface tension is assumed to be constant and the contribution of the slot opening (or initial curtain thickness) on curtain velocity is negligible. Curtain velocity is of the order of 0.2 m/s at the slot exit whereas it is of the order of 1.0 m/s and 2.0 m/s at a curtain heights of 50mm and 200mm, respectively. Since the acceleration due to gravity (g) has a much stronger contribution to the curtain velocity, for all practical purposes the curtain can be considered to be free falling under gravity. The flow rate increases the Weber number, but has a minimum contribution on both the curtain velocity and surface age. For example, for a curtain height of 50 and 200 mm, the surface ages are 84 msec and 184 msec, respectively. To obtain the graphical representations above, a constant surface tension was used, but in reality, the dynamic surface tension is strongly influenced by surface age, surfactant dosage and type of surfactant. As the rate of change in area (or new surface creation) is uniformly increasing, the diffusion rate of the surfactant to the interface will determine if the surface tension increases or decreases with surface age. For this case, the rate of new surface creation per unit slot width w is given by,

$$\frac{1}{w}\frac{dA}{dt} = \frac{dH}{dt} = U_0 + gt = V_H \tag{14}$$

From the Ward and Tordai equation (7), the diffusion rate (D) will be influenced by the medium for a given surfactant. Thus, it will also depend on the coating formulation; coating solids, type of pigments and binders, and viscosity. As dynamic surface tension is critical for achieving curtain stability, its measurement is of critical importance.

Surface Tension Measurements

Surface tension measurements can be performed either dynamically or statically. A description of methods used to measure each and their inherent problems are reviewed below.

Static Surface Tension – Wilhelmy Plate

The Wilhemy plate method[11] is one of the simplest and the oldest methods for measuring the static surface tension of a fluid. In this method, a very lightweight plate, connected to a lever, is lowered on to the surface of a liquid, to the point where it just touches the surface[11]. At this point, the liquid rises and forms a meniscus around the perimeter of the plate. The force exerted by the meniscus on the plate is given by,

$$F = p\sigma\cos(\theta) \tag{15}$$

where σ is the surface tension of the fluid, p the perimeter of the plate edge in contact the with liquid and θ is the contact angle. Although the Wilhemy plate method is a very reliable method for determining the surface tension of low viscosity solutions, it is prone to various errors at higher viscosities. Viscous affects are of particular importance. At high viscosities (>100 mPas), viscous affects become important such that this method is no longer reliable. Since most paper coating viscosities are much higher than 100 mPas, it is not a reliable test method for this purpose. However, it is still useful as an initial screening tool for determining the surfactant efficiency and effectiveness in water.

Dynamic Surface Tension- Maximum Bubble Pressure Method

Another method used to measure the dynamic surface tension of fluids is the maximum bubble pressure drop method (12-14) (Figure3). In this method, air is blown though a capillary into a liquid, forming bubbles at the tip of the capillary.

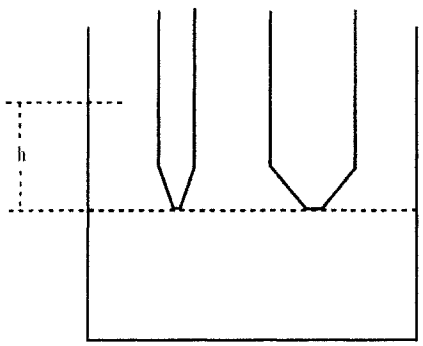

Figure 3.Maximum bubble pressure method.

The pressure inside the bubble increases, until the air pressure and surface pressure of the liquid meniscus are equal, as governed by the Laplace equation. After this maximum pressure is reached, the bubble grows rapidly until it detaches from the capillary, at which time the pressure drops. Pressure is displayed in a saw-tooth form with the maximum pressure is given by the peak of the saw tooth curve. Once the maximum pressure is determined, the surface tension is calculated using the Garret and Ward (12) equation (16).

$$\sigma = \left(\frac{\Delta P - \rho g h}{2}\right) R \tag{16}$$

Surface age is determined by the time between two successive pressure peaks. By adjusting the air pressure, the frequency of bubble formation, inverse of surface age, can be adjusted. The interpretation of surface tension at various bubble frequencies is complex and is marred by inaccuracies. This is because the time between maximum bubble pressure and time of bubble detachment, dead time, is not factored into the surface age, resulting in erroneous data. According to Ward and Garret (12), this dead time is dependant on the measured surface tension and radius of the capillary.

This method is also very sensitive to viscous effects and particulate contamination, thus making it unsuitable for measuring the surface tension of most paper coatings. Coating components like pigments and binder can deposit on the capillary walls, reducing its effective radius.

Dynamic Surface Tension - Mach Angle Method

As a thin liquid film is disturbed, the shape of its free edges is governed by its Mach number, M. A detailed mathematical description of this phenomenon can be found in reference 15. The Mach angle can be determined by measuring the angle formed upon the disruption of a stable liquid curtain (Figure 4). After experimentally determining the Mach angle, the Mach number and surface tension can be calculated from equation 17.

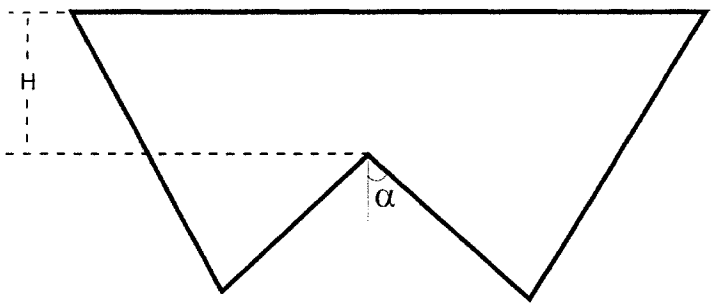

Figure 4.Measurement of Mach angle.

$$\frac{1}{M} = \sin(\alpha) = \left[\frac{2\sigma}{\rho d V^2}\right] \tag{17}$$

$$W_e = \frac{1}{\sin^2(\alpha)} = \frac{\rho d V^2}{2\sigma} \tag{18}$$

Here, α is half the Mach angle, ρ is the liquid density, σ is the local surface tension, d is the local film thickness and V is the local velocity. A freestanding liquid film can be readily created by flow though a die. The Mach angle method is the direct and de facto measurement of dynamic surface tension. Since it is free from viscous effects, it can be used for any liquid as long as it creates a film. The local velocity and thickness can be readily calculated from the basics equations. Precise measurement of flow rate, distance of the curtain disturbance from the slot opening, H, and Mach angle, α, is required.

OBJECTIVES

To understand the dynamics of curtain stability and behavior of surfactants, accurate and reproducible dynamic surface tension measurement are needed. In the current research,

the dynamic and static surface tension for a broad range of surfactants (range of HLBs) is measured in different media (water, coating colors) at different dosage levels and the surface ages of each surfactant are determined. The impact of surfactant chemistry, surfactant dosage, and surface age on curtain stability is proposed.

EXPERIMENTAL

The static surface tensions of nine different surfactants (Table 1) were measured in DI water at room temperature using a Wilhelmy plate tensiometer. Surfactants were added in small increments and aged for 5 minutes at room temperature prior to making the measurement. The titration approach, two similar values consecutively, was employed. Surfactant addition was done at well over the critical micelle concentration, CMC, of the surfactant.

The dynamic surface tension of each surfactant was measured by both maximum bubble pressure (Sensadyne) and Mach angle methods. For the maximum bubble drop measurements, a temperature calibration was performed with hot and cold water and a surface tension calibration performed using distilled water and Methyl di-iodide (50.80 mN/m). The surfactants were then added to distilled water at room temperature and aged for 5 mins. Once aged, the bubble frequency was slowly increased in small increments in the range of 0.5 to 25 bubbles/sec and the data collection started when equilibrium was reached. After completing the measurement, surfactant was added and the procedure repeated.

To determine the Mach angle, a model coating was prepared as given in Table 1. All dynamic measurements were performed using a slide curtain coater (slot opening 0.6mm, slot width 30 cm, slide angle 45° and slope length 5 mm), located at the MeadWestvaco research center in Chillicothe, OH. To prevent inaccuracies, a large master batch of coating was prepared without surfactant. Coatings were prepared by adding slurried pigments and Carboxymethylcellulose to a Cowles disperser. After dispersing the pigments and thickener for 5 minutes, latex and dilution water were added to obtain the desired solids (62%, 58% and 54%). From this master batch 200lbs of coating was transferred to a supply tank for the curtain coater. Predetermined amounts of surfactants, Table 2, were then added directly into the the supply tank, which contained a slow speed mixer. The coating was allowed to mix for 10 min. prior to applying it to the curtain coater die head. The curtain was disturbed using a 2mm steel rod. The placement of the rod was adjusted to four different distances from the exit of the die and measurements were taken at each point. The rod distances used were 50mm, 100mm, 150mm and 200mm. These distances allowed surface ages of 87, 129, 161 and 188 msec., to be obtained respectively. Mach angle pictures were taken using a 2MP digital camera from a fixed distance (Figure 5). In the cases where the curtain failed to break, the wake angle was photographed instead. The Mach angle (or the wake angle) was later measured by analyzing the pictures using Adobe Illustrator.

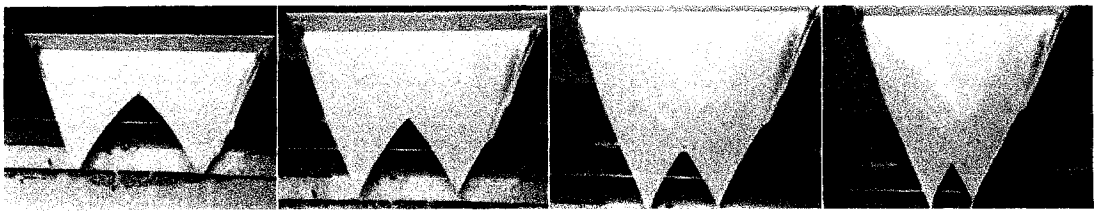

Figure 5. Measurement of Mach angle at 50mm, 100mm, 150mm and 200mm.

To assure a constant flow of coating to the curtain die, a low pulsation mono pump was used. The rpm of the pump was varied and the volumetric flow rate determined for each of the three coating solids, Figure 6.

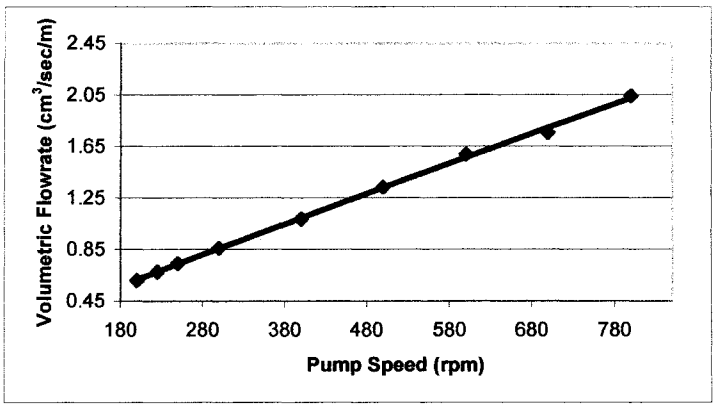

Figure 6. Calibration curve for the supply pump.

Using the equation from the best line fit to Equation 19 of the data, the pump RPM and Flow rate/unit width (cm^2/s) were determined.

$$Q = -1.0832 \times 10^{-7} rpm^2 + 2.4533 \times 10^{-3} rpm + .13042 \quad (19)$$

Three different pump speeds, 300, 400 and 500 rpm, corresponding to 0.86 cm^2/s, 1.10 cm^2/s and 1.33 cm^2/s, respectively, were used. Some surfactants were studied at 250 and 350 pump rpm corresponding to 0.74 cm^2/s and 0.98 cm^2/s. In addition to these measurements, a minimum flow rate study was also performed. For this study the rpm of the pump was reduced gradually until the curtain broke and the rpm at break was recorded.

Table 1. Coating Formulation

	Carbonate	Clay	SBR latex	CMC	Lubricant
Name	Carbitol 90	Ultra white 90	CP 620 NA	Cellogen PR	Nopcote 104
pph	60	40	12	0.45	0.6

Table 2. Surfactants Used in Static and Dynamic Measurements

	Chemistry	Structure	MW	HLB	Charge
Niaproof 4	Alkyl Alcohol sulfate*	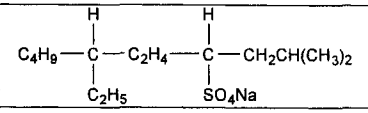	316	14	Anionic
Tergitol Minfoam 1X	Secondary Alcohol Ethoxylate	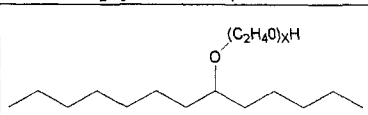	645	12.6	Nonionic
Tergitol 15-S-3	Secondary Alcohol Ethoxylate		336	8.3	Nonionic
Tergitol NP9	NonylPhenol Ethoxylate	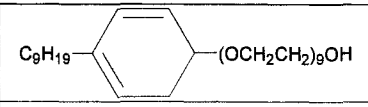	616	12.9	Nonionic
Tergitol TMN6, 90%	Secondary Alcohol Ethoxylate (branched)	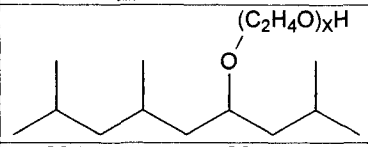	543	11.7	Nonionic
Dowfax 2AO	Alkyl Diphenyl Oxide Disulfonate	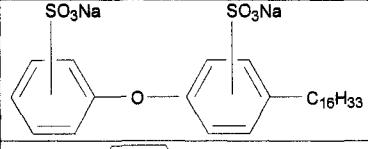	524	NA	Anionic
Dowfax 8390	Alkyl Diphenyl Oxide Disulfonate		643		
Triton X-100	Octylphenol Ethoxylates	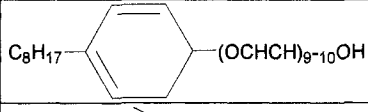	606	13.4	Nonionic
Triton GR-7M	Sulfosuccinate	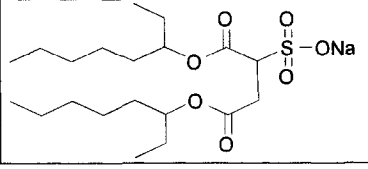	444	NA	Anionic
Triton GR-5M	Sulfosuccinate		338		

RESULTS AND DISCUSSION

Static Surface Tension - Wilhelmy Plate

The influence of surfactant type and concentration on static surface tension are shown in Figures 7 and 8. The nonionic surfactants were more efficient i.e., they reached the CMC (critical micelle concentration) at a very low concentration. They also have a sharp and well defined CMC region. The large decrease in surface tension with surfactant dosage for the nonionic surfactants in comparison to the anionic surfactants indicates that they are more effective in lowering the surface tension of water below 30 dyne/cm than the anionic surfactants. Surface tensions below 31-33 dyne/cm were not obtainable with the anionic surfactants. The Tergitol TMN6 was found to be the most effective and efficient nonionic surfactant. Niaproof 4 was found to be the least efficient of the surfactants tested.

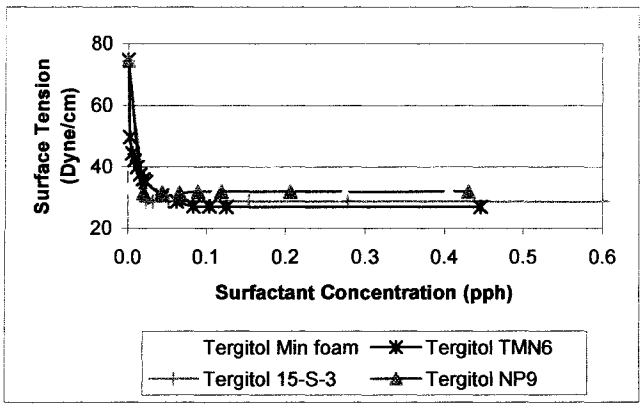

Figure 7. Static surface tension of nonionic surfactants using Wilhelmy plate at room temperature.

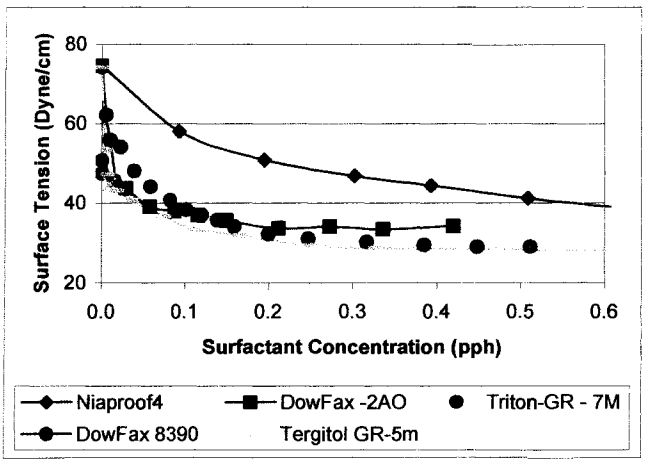

Figure 8. Static surface tension of anionic surfactants using Wilhelmy plate at room temperature.

From the static surface tension values measured, various constants, inherent to the surfactant, were calculated. These values are given in Table 3. The maximum surface excess, Γ_∞, and Langmuir constant (*a*) were obtained by iterative curve fitting the data to the Von Szyszkowski- Langmuir equation. The area per molecule was calculated directly, at the surfactant's CMC.

Table 3. Results of Static Surface Tension Measurement

Surfactant	Maximum Surface Excess	Lamgmuir Constant		Area per molecule	Minimum Surface Tension	CMC
	Γ_∞ x10^6 (Mols/m^2)	a x10^6 (Mol/dm^3)	R^2	$Å^2$	mN/m	ppm
Niaprooof 4	4.27	890	0.99	53	34	NA
Tergitol Minfoam 1X	NA	NA	NA	NA	29	34
Tergitol NP9	NA	NA	NA	NA	30	NA
Tergitol TMN6, 90%	1.07	2.55	0.966	64	26	580
DowFax 2AO	1.91	0.99	0.98	77	34	NA
DowFax 8390	7.39	510	0.97	47	44	NA
Triton X-100	NA	NA	NA	NA	31	130
Triton GR-7M	0.09	4.5	0.99	80	NA	2300
Triton GR-5M	1.499	2.17	0.99	64	26	2300

Dynamic surface tension - Maximum Bubble Pressure Method

The maximum bubble drop measurements showed the surface tension of all the surfactants to decrease with surface age, although by varying degree. Surfactant behavior showed a marked dependence on HLB. The low HLB surfactants had much lower surface tensions and their variation with surface age was also much lower than the high HLB surfactants. This is due to the differences in the solubility of surfactants in water. The low HLB surfactants have a lower solubility in water. As a result, they have a higher surface excess and a broader sub layer. In Figure 9, the dynamic surface tensions of selected anionic and nonionic surfactants at 0.10 % concentrations are compared.

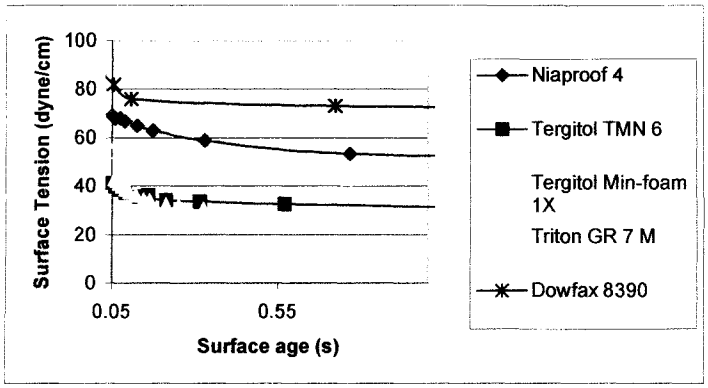

Figure 9. Dynamic surface tension of selected ionic and nonionic surfactants at 0.10pph using maximum bubble pressure method.

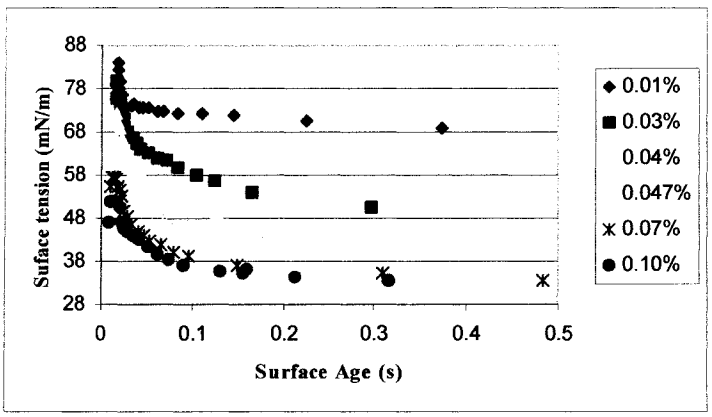

Figure 10. Dynamic surface tension of nonionic surfactant (Tergitol TMN6) at various concentrations using maximum bubble pressure method.

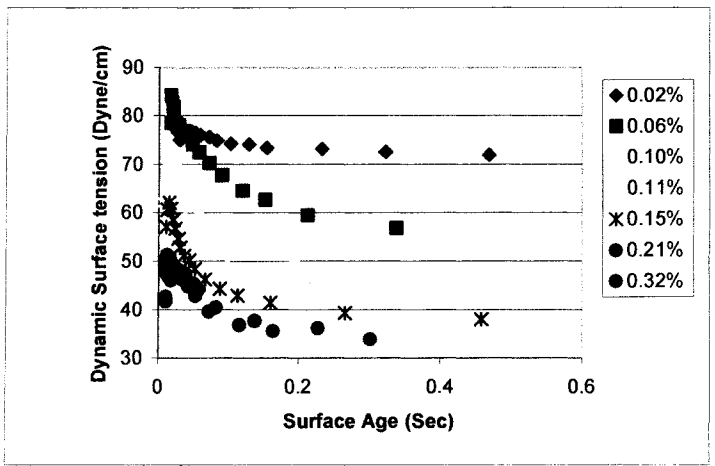

Figure 11. Dynamic surface tension of ionic surfactant (Triton GR 5M) at various concentrations using maximum bubble pressure method.

A decrease in surface tension with surface age was found for all the surfactants tested. The results show the dependence of dynamic surface tension at any surface age on bulk concentration. For simplicity the results for only the Tergitol TMN6 and ionic Tergitol GR 5M surfactants are shown (Figures 10 and 11).

The dynamic surface tension measurements revealed a critical surfactant concentration, above which surface tension is dependant only on surface age and not on concentration. Again, low HLB surfactants are more efficient than high HLB surfactants i.e. they reach this critical concentration much faster than higher HLB surfactants. Table 4, shows the dynamic critical concentrations of found for the surfactants.

Table 4. Dynamic Critical Concentrations of Surfactants

Niaproof 4	Triton GR 7M	Triton GR 5M	Tergitol TMN 6	Tergitol Minfoam 1X	Dowfax 8390	Dowfax 8390 2AO
Anionic	Anionic	Anionic	Nonionic	Nonionic	Anionic	Anionic
pph	pph	pph	pph	pph	pph	pph
0.30	0.20	0.20	0.10	0.15	0.26	0.22

Dynamic surface tension - Mach angle Method

Niaproof 4

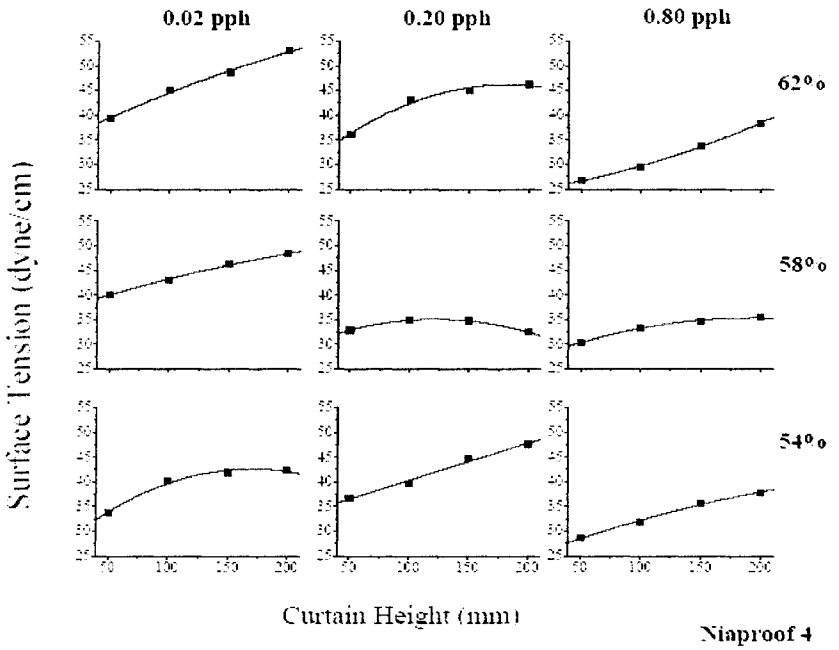

Figure 12. Dynamic surface tension of curtain at 50mm, 100mm, 150mm and 200mm curtain heights and coating solids of 62%, 58% and 54%. Surfactant, Niaproof 4 is dosed at 0.02 pph, 0.20 pph and 0.80 pph.

Surface tension increases with curtain height at all concentrations and coatings solids. Surface tension reduces with surfactant concentration, but the extent of reduction is higher at higher curtain heights (surface age). At lower curtain heights, the difference in surface tensions is very little across surfactant concentrations and coatings solids. Surface tension increases for about the same extent in all coating solids, about 15 dn/cm. The increase in surface tension with curtain height is higher at lower surfactant concentration, whereas it is lower with higher concentrations. This suggests that dynamic surface tension is dependant on initial surfactant surface excess and as the curtain surface area increases, surface excess decreases, increasing surface tension. Niproof 4 is highly soluble and not a very effective surfactant, as suggested by static surface tension measurements. As a very soluble surfactant, its initial surface excess is relatively low, resulting in rather high surface tension increases. Coatings also have a strong effect. The increase in surface tension with curtain height is lower at lower coatings solids.

Tergitol Minfoam 1X

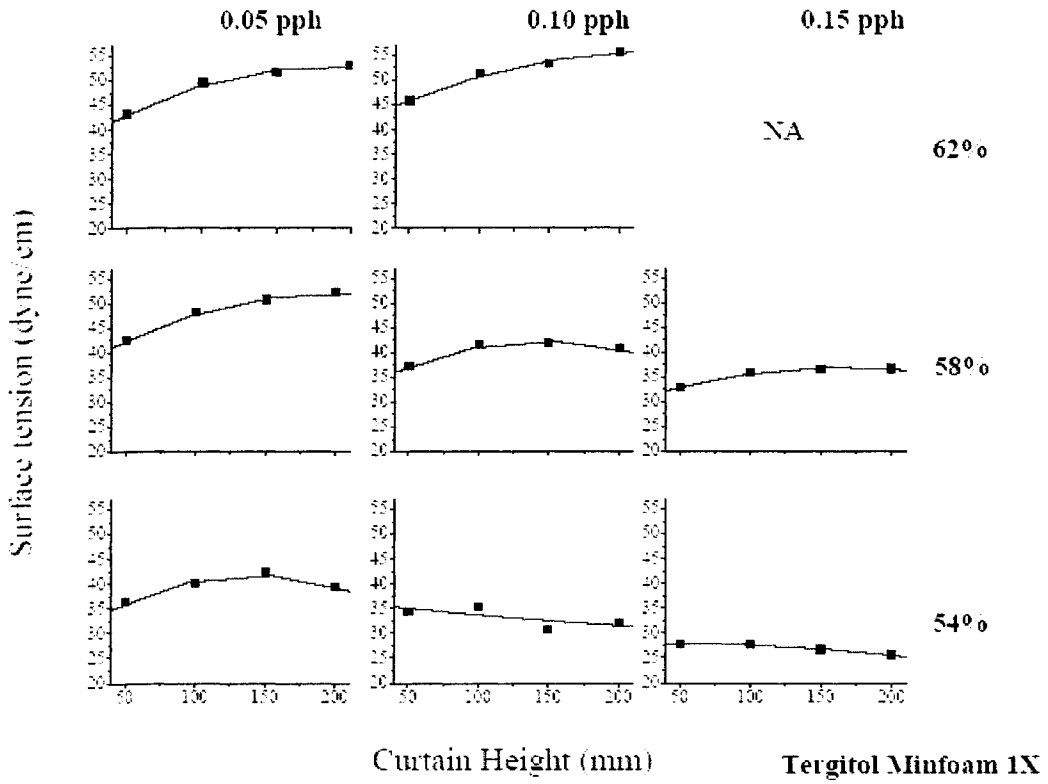

Figure 13. Dynamic surface tension of curtain at 50mm, 100mm, 150mm and 200mm curtain heights and coating solids of 62%, 58% and 54%. Surfactant, Tergitol Minfoam 1X, is dosed at 0.05 pph, 0.10 pph and 0.15 pph.

Tergitol Minfoam 1X is a very effective low HLB surfactant. It has large surface excess at the air interface. The surface tension drops with surfactant concentration across curtain heights, but increases with curtain height. The extent of surface tension increase is lowers with lower coatings solids. This is expected as coating medium has more water with reducing coatings solids, low HLB surfactant like Tergitol Minfoam 1X will preferably migrate to the air interface, increasing surface excess. At 54 % solids there is no increasing in surface tension with curtain height at all surfactant concentration. This results in increasing Weber number with curtain height and is reflected by very stable curtain and low minimum flow rates.

Tergitol 15-S-3

Tergitol 15-S-3 has a low HLB of 8, so is sparingly soluble in water. It is widely used as defoamer. Because of its very Low HLB, Tergitol 15-S-3 phase separates in aqueous media and is not an effective surfactant.

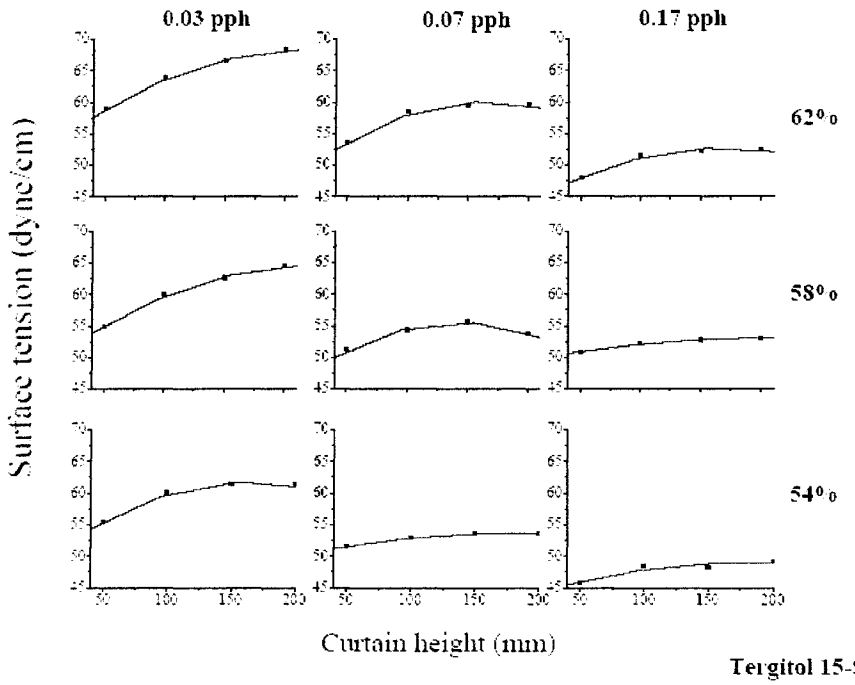

Figure 14. Dynamic surface tension of curtain at 50mm, 100mm, 150mm and 200mm curtain heights and coating solids of 62%, 58% and 54%. Surfactant, Tergitol 15-S-3, is dosed at 0.03 pph, 0.07 pph and 0.17 pph.

Surface tension drops with concentration across coating solids, but increases with curtain height. Surface tension is relatively higher than other more soluble surfactants. Again the extent of surface tension increases is higher for higher coating solids and is very low at

lower solids. This suggests more efficient phase separation at more aqueous media, resulting is higher surface excess at lower coatings solids. At its highest concentrations, there is no or little change in surface tension at curtain heights, indicating little or no change in surface excess as curtain expands under gravity. Because of its low HLB, this surfactant seems to have reached its maximum surface excess within the die itself, the coating-steel interface. As the surface tension does not increase with curtain height, the Weber number increases, improving curtain stability. The curtain with Tergitol 15-S-3 surfactant, because of phase separation, produces "burps", making it unsuitable the curtain coating.

Tergitol NP9

Tergitol NP9 is a low HLB, water soluble and effective surfactant as suggested by static surface tension measurements in water.

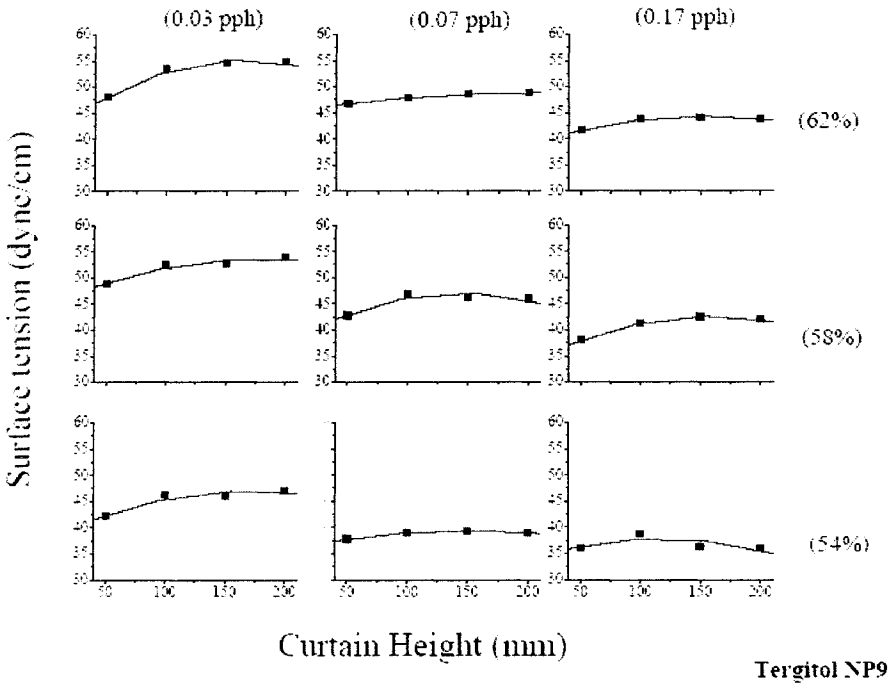

Figure 15. Dynamic surface tension of curtain at 50mm, 100mm, 150mm and 200mm curtain heights and coating solids of 62%, 58% and 54%. Surfactant, Tergitol NP9, is dosed at 0.03 pph, 0.07 pph and 0.17 pph.

There is little or no surface tension change with curtain height but it drops with concentration. Again, surfactant efficiency improves with lower coatings solids as with other low HLB surfactants. Surface tension is especially stable at higher surfactant

concentration. As Tergitol NP9 has a low HLB, its surface excess at the Coating-steel interface is not very different from its surface excess for coating-air interface. In addition, because of the low HLB it has a broad sublayer. The combination of a high surface excess and a broad sublayer, the surface tension remains stable across curtain heights and coatings solids. In addition, Tergitol NP9 is fairly soluble in water, so there are no phase separation issues as with Tergitol 15-S-3. It is reflected in stable curtain and low minimum flow rates.

Dowfax 8390

Dowfax 8390 is an very efficient anionic surfactant with high HLB.

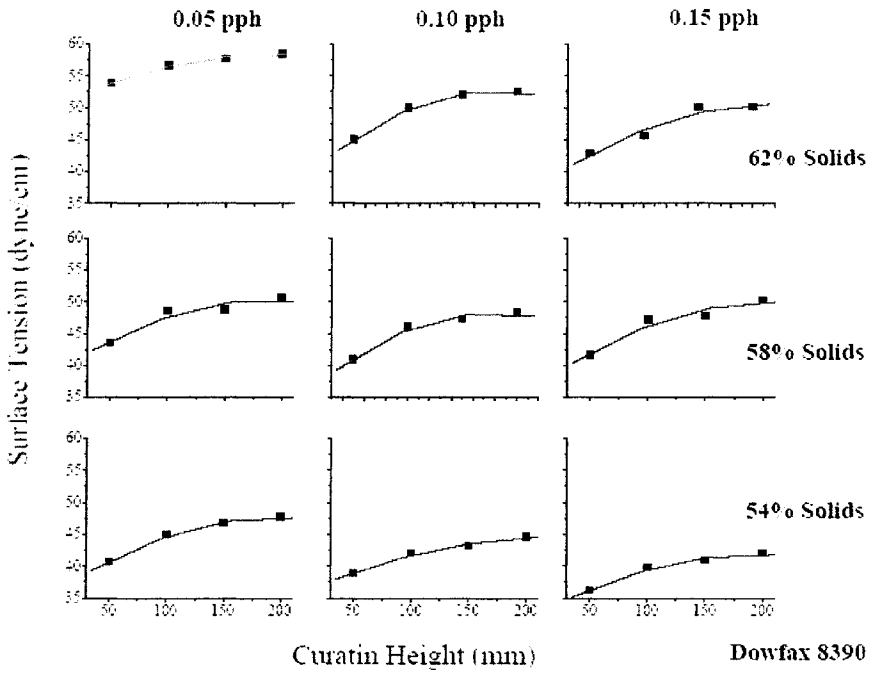

Figure 16. Dynamic surface tension of curtain at 50mm, 100mm, 150mm and 200mm curtain heights and coating solids of 62%, 58% and 54%. Surfactant, Dowfax 8390, is dosed at 0.05 pph, 0.10 pph and 0.15 pph.

Surface tension increases with curtain height at all concentration by about 7-8 dyn/cm. Surfactant efficiency improves lower coatings solids. The extent of surface tension increase is higher than for low HLB surfactants. In addition, the almost a symmetric increase in the surface tension, as with other anionic surfactants, with curtain height and surfactant concentration suggests that the drop in surfactant surface excess from the initial is at a constant rate. As Dowfax 8390 is very soluble in water, it has low surface

excess and a very narrow sub-layer. As curtain surface area increases under gravity, surface excess decreases, increasing the surface tension.

Tergitol TMN 6

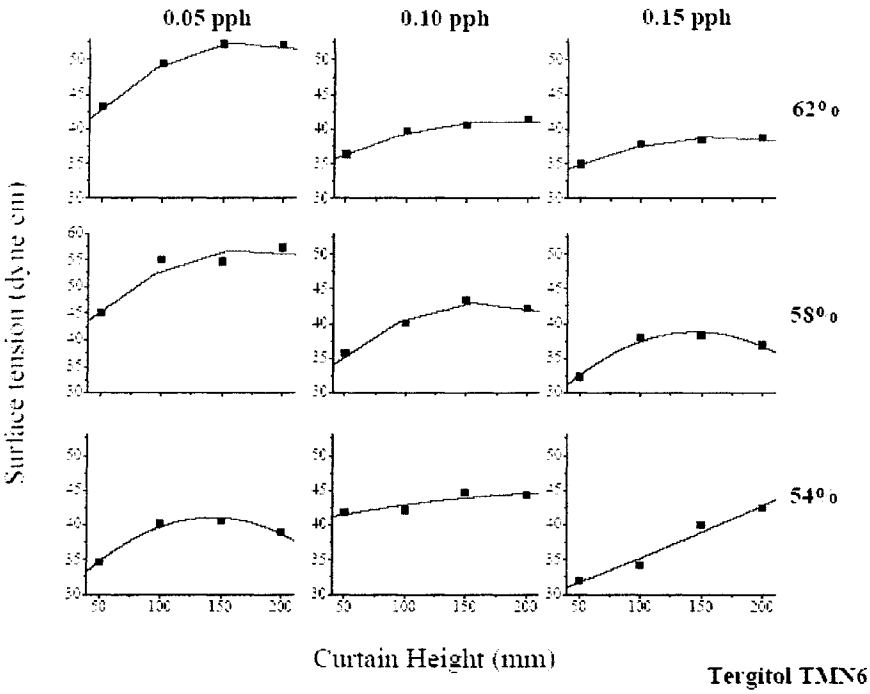

Figure 17. Dynamic surface tension of curtain at 50mm, 100mm, 150mm and 200mm curtain heights and coating solids of 62%, 58% and 54%. Surfactant, Tergitol TMN6, is dosed at 0.05 pph, 0.15 pph and 0.15 pph.

Tergitol TMN is a low HLB, soluble surfactant. It behaves like other low HLB surfactants.

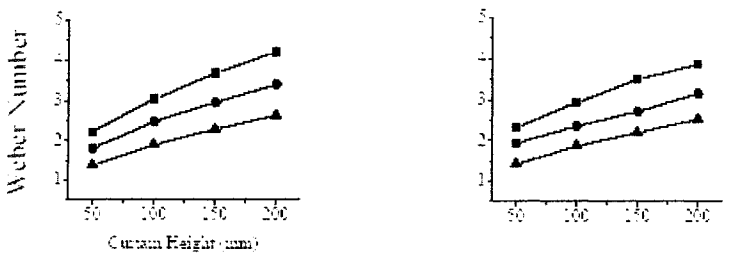

Tergitol NP9 Dowfax 8390

Figure 18. Comparision of Weber numbers for nonionic and ionic surfactants at the same flow rate ▲ 0.86 cm²/s, ● 1.10 cm²/s, ■ 1.33 cm²/s.

Curtain Instabilities

The type and dosage of surfactant affects curtain stability. Figure 19 shows non-uniform thinning for the curtain as it falls under gravity. The first row is at low flow rate (0.70 cm2/s) and very high anionic surfactant. The second row is the chessboard (patchy) curtain with low HLB surfactant.

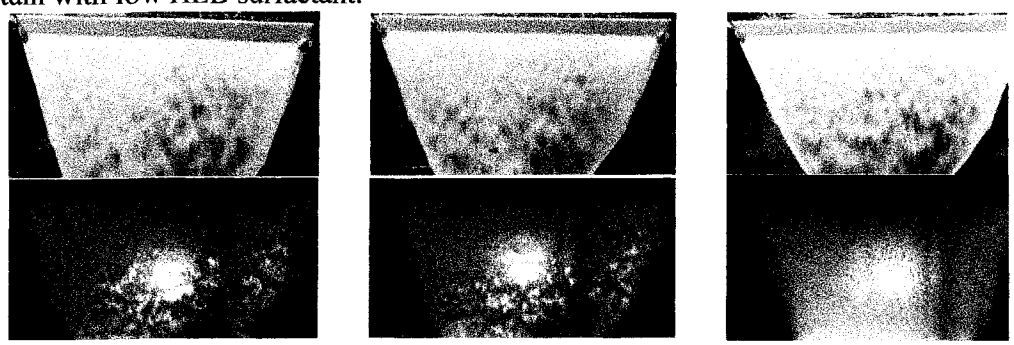

Figure 19. Uneven thinning of the curtain.

Tergitol 15-S-3 is a very low HLB surfactant (8), insoluble in water. In a well-dispersed aqueous coating, it forms tiny droplets. These droplets coalese, forming a bigger drop. As these droplets expand on curtain falling under gravity, the curtain is intermittently broken, forming a "burp" fig 20. A burp will lead to local coat weight changes or skips on coated paper, thus is undesirable. Insoluble surfactants may not be used in curtain coating.

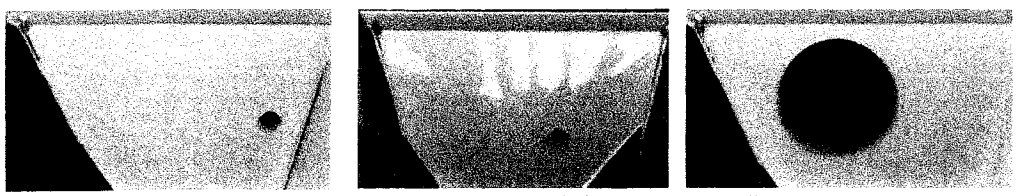

Figure 20. Curtain instabilities "Burps."

Minimum Flow Rates (MFR)

The minimum flow rate that produces a stable curtain is an indirect measure of surfactant efficacy. The Weber Number is a better criterion of curtain stability. A minimum flow rate merely suggests the flow rate required to achieve a Weber number for the given surface tension. There is no evidence in the literature that type of surfactant affects the Weber number criteria itself. Figure 21shows minimum curtain flow rates at various coatings solids and surfactant dosages.

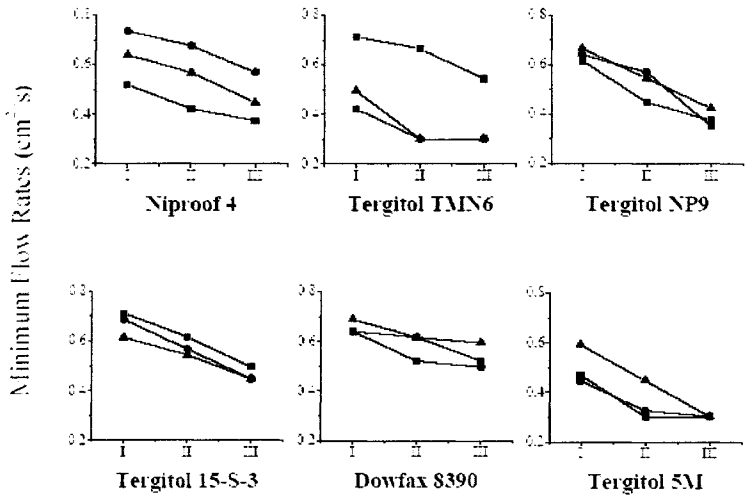

Figure 21. Minimum flowrates at various surfactant dosages and coating solids —●— 52% —▲— 58% —■— 54% .

Anionic surfactants (high HLB) have higher MFR than low HLB surfactants. In figure 21, above 0.30 cm^2/s was the minimum flow rate achievable and the curtain did not break. The MFR can be misleading, as it may be affected by factors other than surfactant efficacy. The flow profile of the curtain can dramatically change with any deviation of coating viscosity and flow rate from the design viscosity and flowrate Liu et at (19), Figure 22.

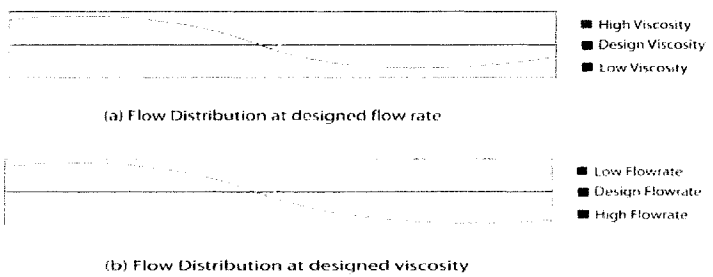

Figure 22. Change of flow distribution in slot die by deviation of designed flow rate and viscosity.

In addition, figure 23 shows the same phenomena observed. Figure on left is coating with high viscosity, higher than the design viscosity of the die, resulting in higher flow rate from the entrance side. Figure in the right is the coating with low viscosity, resulting in higher flowrate from the opposite side. As flow profiles differ, it will affect how the curtain breaks, due to the lack of flowrate (MFR). The above coatings may result in different MFRs, even if surfactant efficacy is the same in all cases.

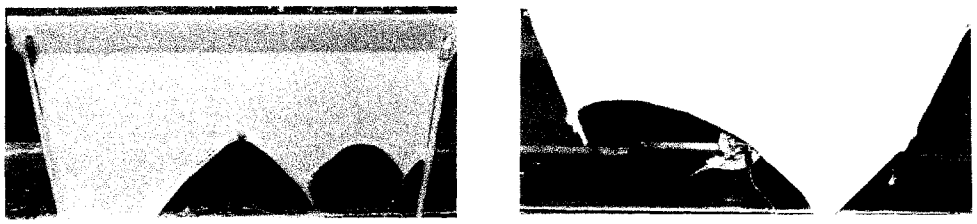

Figure 23. Change in flow rate profile with viscosity (a) 450 cP (b) 260 cP.

CONCLUSIONS

Understanding the role of surfactants in curtain stability is critical to realizing the full potential of curtain coating. Dynamic surface tensions of paper coatings, pigmented and with high viscosity, is hard to measure and difficult to related to dynamic surface tension measurement in water. The Mach angle method is a viable method of surface tension measurement. De-facto surface tension measurement and complete duplication of the process makes the Mach angle method particular effective for curtain coating. Surfactants are very effective in lowering dynamic the surface tension of coating. Surface tension increases with surface age in curtain coating for all surfactants with varying degree. There is a large increase in surface tension of anionic surfactants. Low HLB, 11-13, surfactants are more effective in curtain coating than anionic or very low HLB surfactants. Very low HLB surfactants may produce "burps" in the curtain. Coating solids also affect dynamic surface tension with lower coating solids promoting curtain stability with low HLB surfactants. Minimum flow rate may be a misleading parameter and should be compared across surfactants only when the curtain die is designed for those flow rates and the coating viscosity is within the range of design viscosity.

BIBLIOGRAPHY

1. Ross S. and Morrision, I, D., *Colloidal Systems and Interfaces*, Wiley. 1988.

2. Adamson, A.W. and Gast, A. P., *Physical Chemistry of Surfaces*, Wiley, 1997.

3. B. von Szyszkowski, *Z. Phys. Chem.* **64**, 385, (1908)

4. I. Langmuir, *J. Am. Chem. Soc.*, **40**, 1361, (1918).

5. Ward A. F. H and Tordai L., "Time dependency of boundary tensions of solutions. I- The role of diffusion in time effects", *Journal of physical chemistry*, vol. **14**, 453-461

6. Brown D, "A study of the behavior of a thin sheet of moving liquid" *Journal of fluid mechanics*, vol. **10**, 1961, pp297-305.

7. Schweizer P M,, "Curtain Coating- stability a critical operating parameter", *Paper Technology*, March 2004

8. Whitaker, S., "Effect of surface active agents on the stability of falling liquids films", *Industrial engineering chemical fundamentals*, 1964, Vol**3**, 131-142.

9. Whitaker, S, and Jones L.O., "Stability of falling liquids films: effect of interface and interfacial mass transport", *AIChE J.*, 1966, Vo **12**, 524-531.

10. Peeyush Tripathi, Margaret Joyce, Do Ik Lee, Paul D. Fleming and Masahiro Sugihara, "A Study for the Statistical Optimization of a Curtain Coater", in preparation.

11. L. Wilhelmy, *Ann. Phys.* **119**, 177 (1863).

12. Garrett, P.R.; Ward, D.R., "A reexamination of the measurement of dynamic surface tension with maximum bubble pressure method", *Journal of Colloidal Interface Sciences*, **132**, 475-490 (1989).

13. Bendure, R. L, "Dynamic surface tension determination with maximum bubble pressure method", *Journal of Colloid Interface Science*, 1971, Vol. **35**, 238-248.

14. Mysels, K, "Some limitations in the interpretation of the time dependence of surface tension measured by maximum bubble pressure method". *Langmuir* 1989, Vol. 5, 442-447

15. Emily Meyer, Waves on thin sheets: Examining G.I. Taylor's paper on the dynamics of waves on thin sheets of fluids, MIT Publication, April 2000 downloadable from http://www.deas.harvard.edu/brenner/taylor/handouts/thinsheet/thinsheet.htm.

16. Legrand N, Brunet P, Flesselles M, Limat L, "Perturbations of liquid curtain near break-up", Laboratoire de physique et mecanique des milieux heterogenes

17. Tricot Y M, Surfactants: Static and Dynamic surface tension, *Liquid film Coating: Scientific Principles and their Technological Implications*, 1997

18. Sshunk, P, R and Scriven L. E., "Surfactant effects in coating process".

19. Liu T, Hong C and Chen K, "Computer aided analysis of a linearly taped coat-hanger die", Polymer engineering and science, mid-Dec 1988, vol. 28, No. 23, pp 1517-1526

Comparison of the Surface and Print Quality of Curtain and Blade Coated Papers

Peeyush Tripathi[a]
Dr. Margaret Joyce[a]
Dr. Do Ik Lee[a]
Dr. Paul D. Fleming[a]
Dr. Masahiro Sugihara[b]
[a]Center for Coating Development
Western Michigan University
[b]Mitsubishi Heavy Industries

ABSTRACT

Curtain coating is non-contact metered coating process, which offers great potential for improved coverage at lower coat weights for the coated paper industry. Absence of shear and hydrostatic force leads to differences in coating-basesheet interactions and process dynamics currently experienced with other conventional coating processes. These differences may lead to surface characteristics of curtain coated papers that are very different from conventional coating methods. Due to these differences, printing attributes of curtain coated papers are crucial to their acceptance in the marketplace. Due to the absence of shear, pigment alignment is not as strong, as in other conventional coating processes. In addition, as there is little hydrostatic pressure, binder migration is minimal, so more binder is present at the surface. The increase in binder at the surface improves the interaction of the coating layer with the ink resulting in a thicker layer of ink transfer to the base sheet in offset printing.

In this study, the calendering response, printability and surface of curtain coated papers were compared with blade coated papers at equal coat weights and surface roughness. An uncoated, commercial, light weight basesheet was curtain coated at Mitsubishi Heavy Industry's state of the art coating research center in Hiroshima, Japan and blade coated on a cylindrical laboratory coater, CLC 6000, at 4.8 and 5.8 gsm (C1S). The samples were supercalendered to equal gloss values, and then printed with black ink, using a HAMADA sheetfed offset duplicator press. The calendering response, print density and print mottle were measured. Surface attributes were compared by SEM and AFM measurements.

The calendering response of curtain coated paper was found to be typical of for contour coated surfaces. The print densities of the curtain and blade coated papers were found to be comparable; although the print densities of the curtain coated papers were slightly higher. The print mottle of the curtain coated papers was much higher. A possible explanation of observations is; higher micro roughness of curtain coated papers results in higher immobilized layer of ink in offset printing, which in turn results in higher but non uniform ink transfer. AFM measurements revealed the curtain coated papers to have higher amounts of binders on the surface and the pigment alignment to be almost random. The higher amount of binder on the surface was contributed to the porous structure of coating lattice, which facilitated binder migration to the surface during drying.

INTRODUCTION

Curtain coating [1-6] is a non-contact pre-metered coating operation offering great potential for the coated paper industry (see Figure 1). Absence of shear and hydrostatic force leads to very different coating-basesheet interactions and process dynamics than seen in other conventional coating processes.

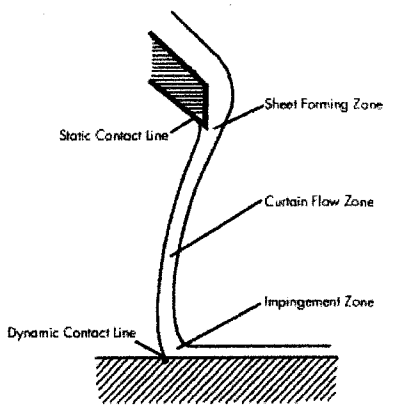

Figure 1. Curtain coating operation.

These differences may lead to surface characteristics that are very different from the conventional coating process, which may, in turn, lead to substantial differences in their printing properties. Due to the absence of shear during metering, pigment alignment is not as strong as in other conventional coating processes [7]. In addition, as there is little hydrostatic pressure, coating and binder penetration into the base sheet is minimal, so more binder is expected to be present at the surface. An enhanced amount of binder at the surface would influence the interaction of the coating with the fountain solution and ink during the offset printing process. This may result in differences in the amount and uniformity of ink transfer during printing.

Pigment Alignment

The pigment alignment [7] on a coated surface profoundly influences its optical and printing properties; opacity being one of the most important for lightweight coated papers. Pigment alignment is strongly influenced by the shear experienced during application and metering (Figure 2).

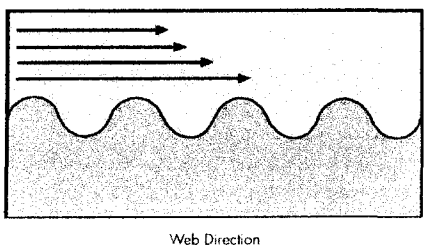

Figure 2. Development of shear at the impingement zone.

Curtain coating is a low shear operation. Coating flow in the die is of low shear and low Reynolds number; flow in the film formation zone is extensional. As a result, there will be little particle alignment in the film formation zone as the curtain is stretched. [8] As the curtain impinges on the moving substrate, it is dragged forward. This sudden drag creates some shear, which is greatest in the immediate vicinity of the impingement zone. The maximum shear in the curtain coating process is available in this zone and is strongly dependant on curtain and substrate velocity difference. Therefore, maximum particle alignment takes place in this region. The amount of shear can be controlled by the ratio of the curtain velocity to web speed [9]. This is illustrated in Figure 3.

Shape of the Curtain Coated Surface

Curtain coating can be understood as a lamination process where a wet film is laminated on to the surface of a substrate [2-5]. As the curtain wets the basesheet (Figure 3a), there are several scenarios that may develop depending on the roughness scale of the basesheet (see Figure 3). If the roughness is of low amplitude and low frequency, the curtain will follow the contour of the paper (Figure 3b). If the roughness is of high amplitude and high frequency, it will coat on the peaks of the surface and upon drying, the shrinkage of the coating will cause the coating to retract to the corners, leaving a crater defect (Figure 4c). Incomplete contour following is illustrated in Figure 3d.

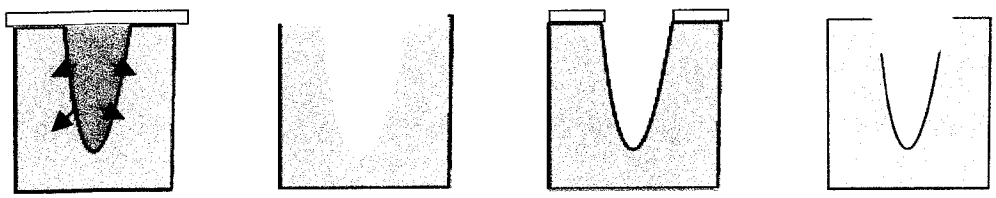

(a) **(b)** **(c)** **(d)**

Figure 3. Various scenarios on curtain wetting of substrate (a) initial wetting (b) contour (c) classic crater (d) incomplete contour following.

Binder Migration

Binder migration affects gloss, smoothness, mottle and print quality. The amount of binder present at the surface, affects the interaction of the coating with fountain solution and ink [10]. Coating processes affect migration as they apply varying amounts of hydrostatic pressure during application and metering. Curtain coaters impart little or no hydrostatic pressure, so binder migration is minimal.

Binder migration under drying conditions presents a different scenario. During drying, binder follows the path of water vapors and is affected by factors like coating lattice compaction (or lack of it), drying rate and orientation of particles. As there is no hydrostatic force to facilitate compaction of coating layer in the curtain coating process, the resultant coating lattice is porous. In addition, as there is absence of strong shear, high aspect ratio pigments (like clays) are almost randomly orientated. A porous coating layer

and random orientation of pigments facilitates binder migration to the surface in curtain coating.

Calendering Response

Calendering is an important operation to improve the smoothness and gloss of paper [11]. The calendering response determines the properties of the paper surface and is influenced by the coating formulation, coating process and the type of calendering itself. Figure 4 shows the differences in basesheet densification and surface smoothness profiles of super and hot-soft nip calendered papers. Due to the higher pressures and roll hardness of supercalenders, supercalendered papers are densified more than with hot-soft nip calendars, as the surface profiles are flattened. Hot-soft nip calenders utilize heat to enable less pressure to be used to improve the surface profiles. The soft roll is deformable resulting in a more even pressure profile in the nip and less sheet densification of the higher caliper areas of the sheet. Due to these differences, the calendering conditions required to obtained a desired smoothness is closely related to the calendering response of the coating layer[11].

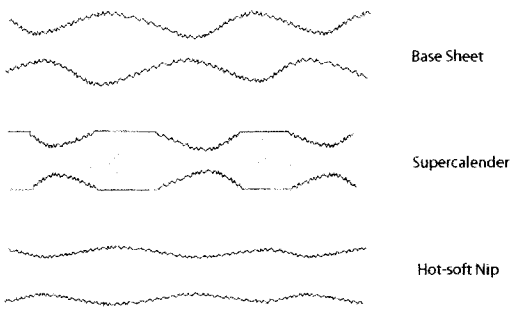

Figure 4. Calendering response of super and hot-soft nip calendaring.

The coating process also affects the calendering response as it strongly influences the physical (surface type) and chemical (binder migration) properties of the surface. T_g of the coating formulation and bulk of the paper are the coating color and base sheet contribution, respectively. Curtain coating is a true contour coating method.

OBJECTIVE

In this study, differences in print quality, pigment alignment, and binder distribution of curtain coated papers were compared to blade coated papers after printing on a one color sheetfed offset duplicator press.

EXPERIMENTAL

An uncoated light weight commercial base sheet (42 gsm) was curtain (Mitsubishi, Hiroshima Japan) and blade coated (CLC 6000, Western Michigan University) at 4.6 and 5.7 gsm (C1S). The coating applied was a typical offset formulation (see Table 1). The coated samples were then supercalendered at 1500 PLI (4 passes). The calendering response was measured with a Parker Print Surf (PPS) roughness instrument. The

samples were then printed with black ink on a one color HAMADA sheetfed offset duplicator press. Print density was measured using an X-Rite densitometer. Mottle was measured by image analysis using Verity IA software. To understand and explain the differences in print quality, AFM and SEM measurements [12-14] were performed to observe the alignment of the pigment and distribution of binder in the coating layer.

Table 1. Coating Formulation

	Carbonate	Clay	SBR latex	CMC	Lubricant
Name	Carbitol 90	Ultra white 90	CP 620 NA	Cellogen PR	Nopcote 104
pph	60	40	12	0.45	0.6

RESULTS AND DISCUSSION

Comparison of Surfaces

Figure 5 shows the z direction cut of curtain coated paper. The figure confirms the scenarios for curtain coating as discussed in figure 3. At low amplitude and frequency roughness variation of paper, the curtain follows the contour of the paper (a). High amplitude and frequency roughness scale, the curtain may coat on lower and upper part (b) or form a classical crater (c). As discussed in previous session, curtain may also partially wet the surface, which on calendaring will show up as surface crack (d).

(a) **(b)** **(c)** **(d)**

Figure 5. Z-direction cut of curtain coated paper and the surface.

Calendering Response

Figure 6 shows the response of curtain and blade coated papers to calendering. The comparison is typical of contour and surface coated papers. The curtain coated, calendered paper remains slightly rougher regardless of the number nips experienced. For both papers there was a significant drop in roughness after the second pass through the nip. Little or no improvement in smoothness was obtained after the 3rd pass.

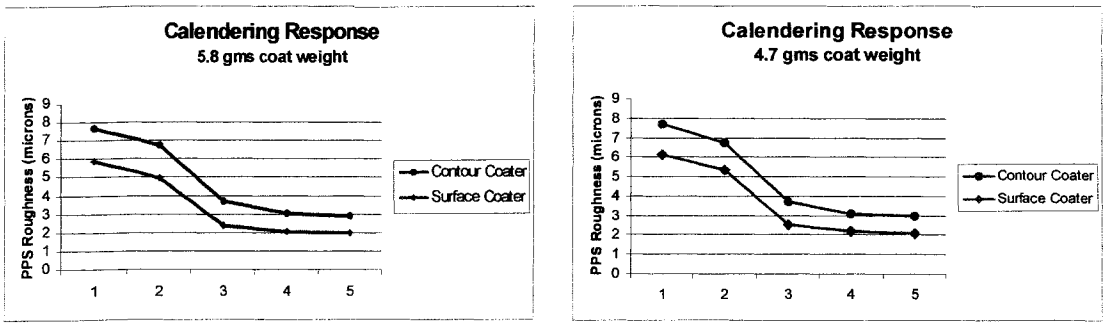

(a) (b)

Figure 6. Calendering response of curtain and blade (surface) coated papers.

Surface of Curtain and Blade Coated Paper

Figure 7 shows selected AFM pictures of curtain and blade coated papers. Uncoalesced SBR latex particles are visible as classical grape clusters in a uniform phase whereas pigments are seen as larger particles of varying shape and size.

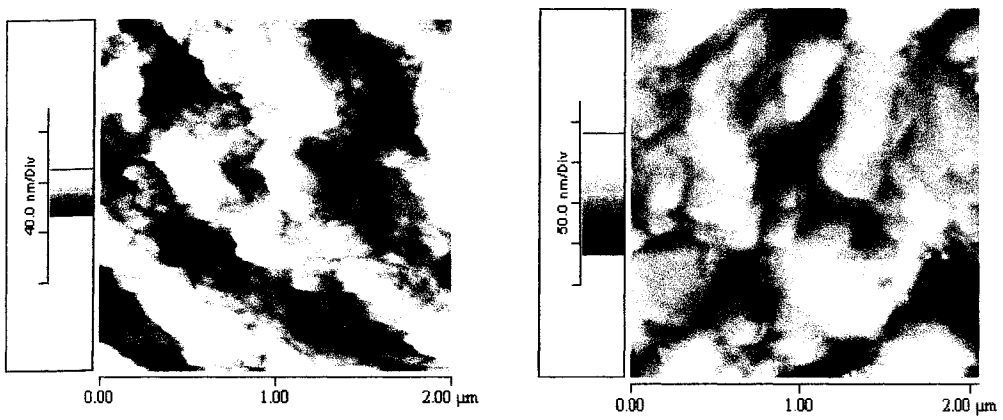

(a) (b)

Figure 7. Atomic force micrograph (AFM) of curtain (a) and blade (b) coated papers showing SBR latex.

It is clear from Figure 7 that much more latex is on the surface of curtain coated paper than for the blade coated paper. There is no binder on the surface of the blade coated samples. The only visible SBR latex on the blade coated papers is present in the microcontours of the basepaper that do not come in contact with the blade. The binder distribution on the curtain coated paper is uniform throughout the surface. Figure 8 shows the alignment of the coating pigments in the curtain and blade coated papers. In the blade coated paper, not only are the high aspect ratio clay particles aligned (flat) prominently, but also overall, the surface is much more compact. For the curtain coated paper, the clay particles are observed to be almost random and the coating structure is noticeably more open. The orientated (flat) high aspect ratio pigments hinder binder migration during drying.

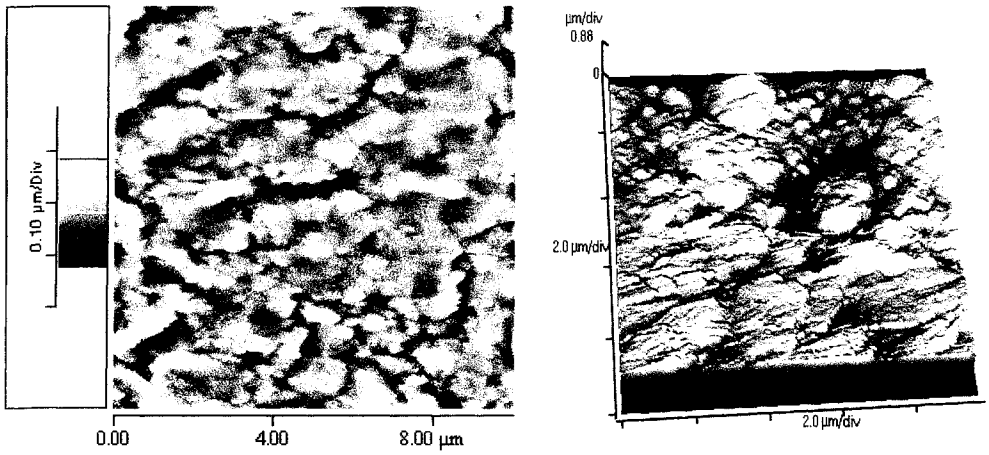

(a) (b)

Figure 8. Atomic force micrograph curtain (a) and blade (b) coated papers showing alignment of clay particles.

The results show that curtain coating forms a much more open coating lattice, due to the random alignment of pigment in the absence of significant shear and hydrostatic pressure. The open structure of the coating lattice facilitates binder migration during drying, resulting in a much higher concentration of SBR latex on the surface of the curtain coated papers than the blade coated papers.

Figure 9 shows SEM pictures of calendered and uncalendered curtain and blade coated papers at 700X and 7000X magnifications. A large number of surface pores are visible on the curtain coated coating layer (a) and (b). This suggests that the coating lattice is very open and there is no compaction of the coating layer as is common in blade and rod coated papers. There is some loss of openness of the structure on calendering but the structure remains very porous, nonetheless (c) and (d). The blade coated coating layer (e) and (f), on the other hand, is almost completely closed with only few surface pores visible on the surface. Thus, the blade coated surface is "closed".

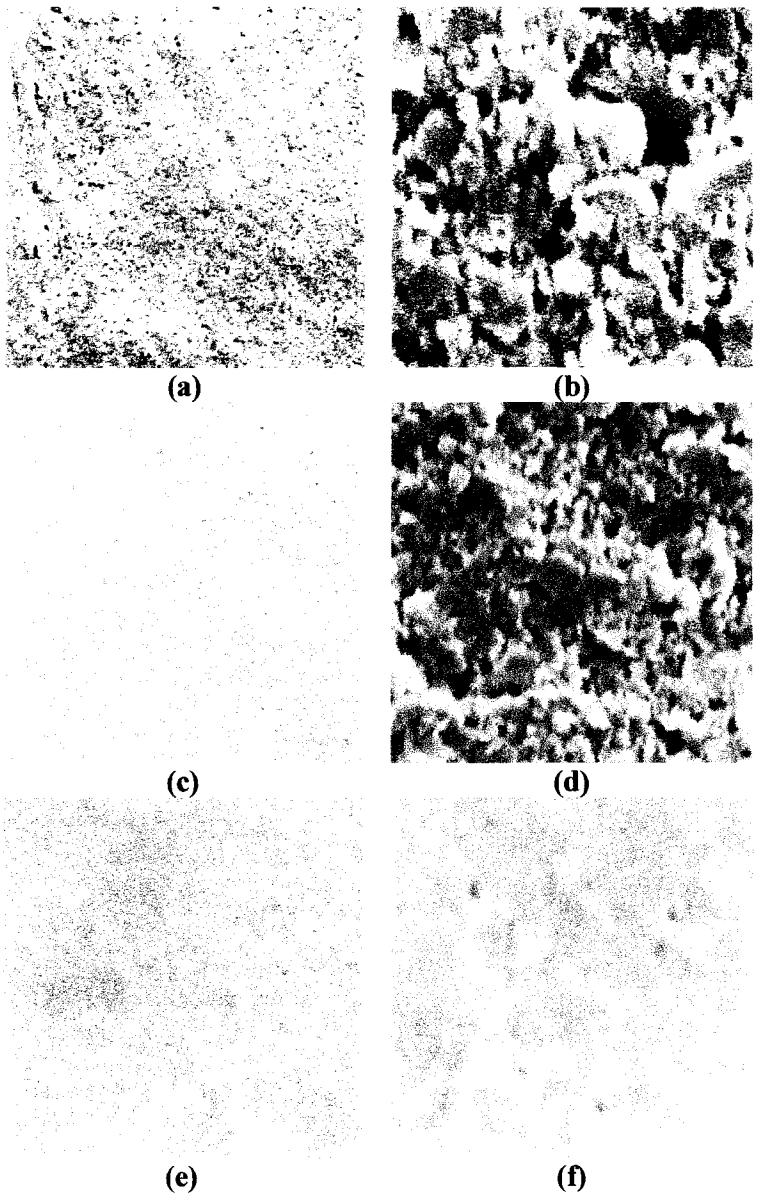

Figure 9. Scanning electron micrograph (SEM) at 700X and 7000X magnification of Curtain coated-uncalendered (a) and (b), Curtain coated – calendered (c) and (d) and Blade coated calendered (e) and (f) respectively.

This interpretation is consistent with the AFM surface topography shown in Figure 10.

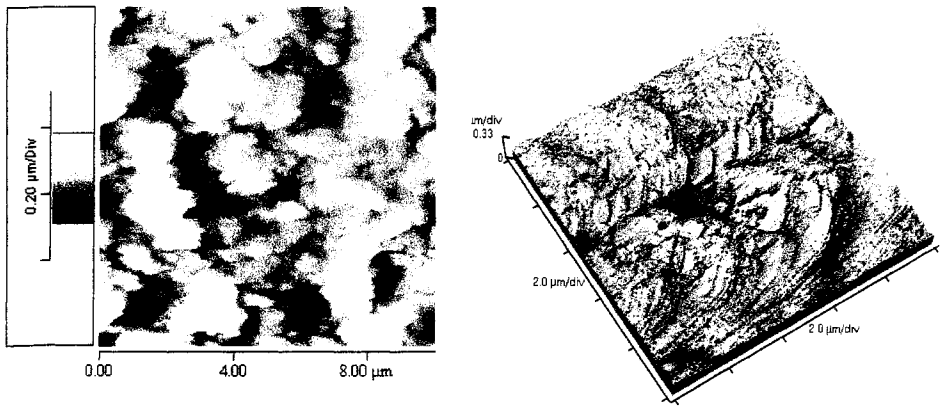

(a) *(b)*

Figure 10. AFM showing porous layer for curtain coated and a nonporous "closed" layer of blade coated paper.

Those differences in surface topography are also reflected in air permeability (PPS porosity) and opacity (Figure11). The permeability, a measure of openness of the surface to fluid flow, of the curtain coated layer is an order of magnitude higher than that of the blade coated layer for the same coat weight. In addition, opacity, which is strongly influenced by factors such as void fraction and pigment alignment, is 3-4 points higher for curtain than blade coated layer. This difference in opacity can not be accounted to one of the individual factors, void fraction or pigment alignment, but it is believed that lower opacity of blade coated layer is due to higher alignment of clay pigments.

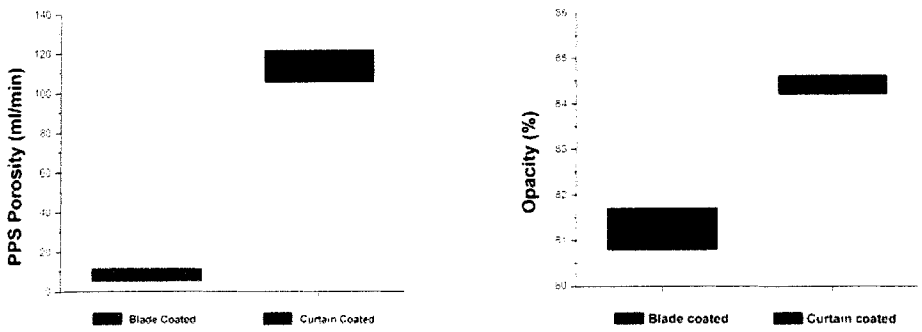

(a) (b)

Figure 11. Statistical comparison of porosity and opacity of blade and curtain coated paper (5.8 gm/m2, C1S, Calendered 4 passes, 1500 PLI).

Figure 12 shows Root Mean Square (RMS) roughness of blade and curtain coated papers obtained from the AFM measurements a 10µ×10µ sample area. Again for same coat weight mean RMS roughness for curtain coated layer is 58 nm whereas it is 30 nm for blade coated layer. This is consistent with the PPS roughness values, although smaller by two orders of magnitude.

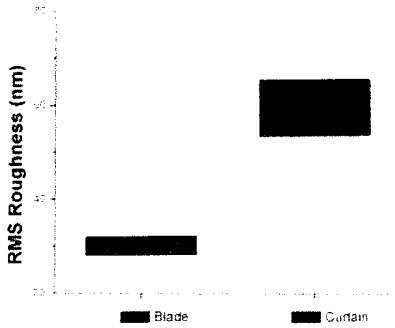

Figure 12. Root Mean Square (RMS) roughness of blade and curtain coated papers from AFM measurements in a 10μx10μ sample area (in nanometers).

Comparison of Print Quality

The print density of the curtain coated paper was comparable to that of the blade coated paper, with the print density of the curtain coated paper being slightly higher. The mean print densities were 1.2 and 1.39 for blade coated and curtain coated papers, respectively. The print mottle for the curtain coated paper was significantly higher, as seen in Figure 13. For the curtain coated papers, there was little or no effect of coat weight on print quality. Nevertheless, for the blade coated papers, print quality improved with coat weight.

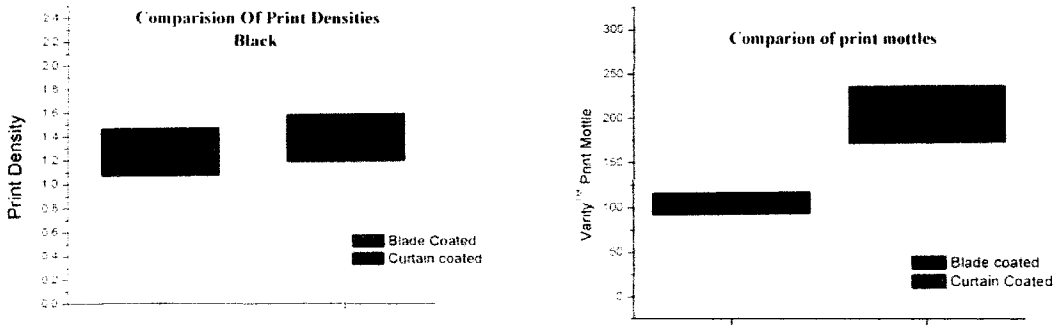

Figure 13. Comparison of printability of curtain and blade coated papers.

Smith [15] presented an explanation of the effect of basesheet –ink interactions on offset printability. High print densities are indicative of a higher thickness immobilized ink layer resulting from an open coating lattice and stronger base sheet and ink interaction. Due to the greater migration of the binder to the surface as a result of the more open coating lattice, the curtain coated papers received a thicker immobilized ink layer resulting in higher print densities.

Print mottle is a measure of ink uniformity. Contour coated papers usually have higher print mottle [16] due to the incomplete contact of the paper with the ink film on the blanket

resulting in uneven ink transfer. This was confirmed by our results. The curtain coated papers were significantly more mottled than the blade coated papers.

CONCLUSIONS

A curtain coater is a true contour coating operation. As a result, the surface properties vary significantly from blade coated (surface coated) papers. The scale of base sheet roughness dictates whether the wet film will follow the contour of the base paper or skim the surface, resulting in the formation of craters. The coating lattice of the curtain coated paper was determined to be much more open and the pigment alignment more random. The open coating lattice and random pigment alignment enabled more binder migration to occur during drying. The greater migration of binder during drying increased the concentration of the binder at the surface, resulting in higher print densities. However, the higher roughness of the paper resulted in a less uniform transfer of the ink, resulting in more print mottle. The near absence of shear during the curtain coating processes reduced the alignment of the pigment particles.

BIBLIOGRAPHY

1. Triantafillopoulos, Johan G, Iiro L, Petri P., "Operational issues in high speed curtain coating of paper", *TAPPI JOURNAL,* November 2004, Vol. **3**(11).

2. Sugihara, M., Miura, H., Yamada, K., Miyakura, T., "Control of Dynamic Wetting Line and Entrainment of Boundary Air in High-Speed Curtain Coating", *2002 Coating Conference Proceedings*, May.

3. Mendez, B, Tietz, M, and Morita, H. "Curtain coating- a novel coating technique for high-precision coating", 20, *Streicherei symposium 2001.*

4. Miyamoto K and Katagiri Y, "Curtain coating", *Liquid film Coating: Scientific Principles and their Technological Implications*, 1997, pp 463-494.

5. Peeyush Tripathi, Margaret Joyce, Do Ik Lee, Paul D. Fleming and Masahiro Sugihara, "A Study for the Statistical Optimization of a Curtain Coater", in preparation.

6. Peeyush Tripathi, Margaret Joyce, Do Ik Lee, Paul D. Fleming and Masahiro Sugihara, "Understanding the Role of Surfactants in the Stabilization of a Coating Curtain", in preparation.

7. Vaha-Nissi M, Lahti J, Rintanen J, Savolainen A, Rissa K, Characterization of barrier clay coatings using AFM and SEMTAPPI, 2000 coating conference proceedings.

8. G. Binnig, H. Rohrer, C. Gerber and E. Heibel, "Tunnelling through a controllable vacuum gap", *Appl. Phys. Lett.*, 40(2) (1982) 178-180.

9. G. Binnig and H. Rohrer, *Physica* B **127**,37 (1984).

10. G. Binnig, C. F. Quate and C. Gerber, "Atomic force microscope", *Phys. Rev.Lett.*,**56**(9) (1986) 930-933.

11. Dave S, TAPPI coating conference, 2002, San Diago

12. Karlos Niskanen, Paper physics

New Curtain Coating Technology Offers Benefits for Barrier Coated Grades

Peeyush Tripathi
Dr. Margaret Joyce
Dr. Paul D. Fleming

Center for Coating Development
Western Michigan University

ABSTRACT

Curtaining coating has been extensively used by the photographic paper industry for a number of decades and is an emerging coating technology with great potential for the specialty coated paper industry. A curtain coaters is a non-contact metering coating method, which provides excellent coverage and a uniform coating layer. The uniform thickness of the coating layer makes curtain coating particularly attractive to specialty paper markets. This paper explores the possibility of using a curtain coater for barrier-coated grades of paper and board.

Barrier grades of paper and board are produced by applying a functional coating to the surface of the substrate. The coating imparts resistance to flow/penetration with certain types of permeates. The theoretical coating layer thickness needed to deter or prevent the flow of permeate through the basesheet, for a given application, can be readily calculated. However, due to limitations of the coating process used and various imperfections in the coating layer, the papermaker will always have to apply more coating than the calculated amount for safe measure. The required thickness of the coating layer needed to meet the shelf-life requirements of the packaged material depends on the number and type of imperfections present in the coating layer, i.e., pinholes and microcracks. To compensate for these imperfections, as much as 40-60% excess coating may be applied than needed if the imperfections did not exist. As barrier coatings are some of the most expensive coating formulations, the potential for savings by eliminating coating imperfections can be substantial.

Curtain coating is a pre-metered type of coating operation, which enables the application of a uniform pinhole free coating layer. The liquid curtain is formed before it comes in contact with substrate, so the integrity of the coating layer and coverage is virtually guaranteed. Also, coverage is almost independent of coat weights and base sheet roughness. In addition, the thickness of the coating layer can be precisely controlled by adjusting the flow rate of the curtain and speed of the moving web. The application of a defect free coating layer enables barrier properties to be obtained with significantly lower coat weight.

This paper discusses the dynamics of permeant flow through a barrier coating layer and the effect of coating coverage (or lack of it) on the barrier properties. Based on the discussion, we believe that curtain coater is a superior and economically suitable coater for barrier specialty papers.

INTRODUCTION

Barrier paper is produced by coating paper with various types of coatings to impart resistance to permeation/penetration of certain types of permeates through it (1-3). Vast arrays of barrier coated papers are produced today from pizza boxes to burger wrappers to corrugated boards. Environmental issues, cost pressures and dwindling profitability is forcing mills to rethink their coating strategy. Coating technology is one the critical areas that lead to radical changes in barrier coating paradigm (4-5). Current coating processes have some inherent disadvantages e.g. pinholes, low coverages especially at low coat weights, base sheet penetration and saturation and non uniform coating layer (6-8). This pushes coat weight demand higher. As barrier coatings are some of the most expensive paper coating, any improvement would result in substantial savings.

The theoretical coating layer thickness requirement for barrier applications can be readily calculated from the permissible permeate flow rate, shelf life of the product and permeate diffusion in the barrier layer. Actual coat weight is always higher to achieve the same permeate flow rate. The actual required thickness of the coated layer depends on the number of imperfections present in the coating layer due to the coating process (6-7). To make up for these process variables, coat weight is generally 40-60% higher than the required.

Curtain coating is a pre-metered type of coating operation, as the coating layer is formed before it comes in contact with the substrate. Curtain coating can be considered as an improved lamination process where a liquid "sheet" and a substrate are merged together.As a uniform pinhole free liquid curtain is formed before it comes in contact with the substrate, the integrity of the coating lattice and coverage is virtually guaranteed. In addition, the thickness of the coating layer can be precisely controlled by adjusting the flow rate and substrate speed. As the coating layer is free of any imperfections and pinholes, a lower coat weight is required to produce a desired permeate flow rate. As barrier coatings are some of the most expensive coatings in the specialty coated grades, the potential saving can be substantial.

This paper analyzes the possibility of using the curtain coating process for the barrier coating applications. Curtain coating seems to be most suited for the barrier application as it delivers uniform, pinhole free coating layer with high coverage at low coat weights. Understanding the role of topography of coated layer on the permeation through it is central to understanding the effect of coating process on barrier properties. The brief discussion on concentration driven flow through the layer is now presented.

Mass Transport Through a Layer

The mass transport of a permeate through a coating layer of thickness L is described by the Darcy's (10) equation,

$$Q = AP\left(\frac{\Delta p}{L}\right)t$$

Here Q is the mass of permeate transferred, A is area, P is the permeability coefficient, (Δp/L) is the partial pressure (or concentration) gradient across the length of the layer, and t is time (Figure 1).

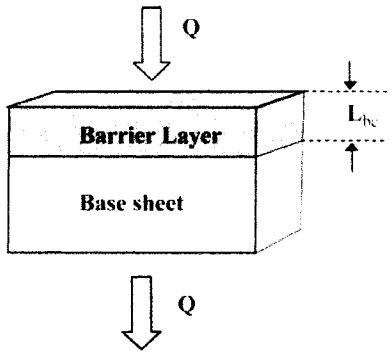

Figure 1. Flow through uniform barrier layer.

In use of the above equation in the barrier application (Q/t) can be treated as the permissible flow rate of permeate. Thus, Q depends on the tolerable permeation which in turn depends on type of the product, for example, meat, fish, cookies, or vegetables. The pressure gradient (Δp/L) is proportional to the concentration gradient of permeate across the barrier layer. For gaseous permeates, it is taken as the difference of partial pressures across the barrier layer. For the most cases in barrier application (O_2, CO_2, smell etc.), it is taken to be the highest differential across the barrier layer e.g. permeant is assumed to be saturated one side and absent on the other side. The partial pressure (or concentration) gradient can be altered by changing the thickness L of the barrier layer. Thus, we observe that for the barrier coating applications, barrier layer thickness and permeability coefficient are the only true variables. Permeability coefficient P can be related to the diffusion coefficient D and solubility S of the permeant in the layer as

$$P = DS$$

The diffusion coefficient relates to the physical characteristics of the layer and the permeate, whereas solubility is related to chemical characteristics of the barrier layer and the permeate. Physical characteristic of the layer, like density, pore size and lattice imperfections in the layer, affect the diffusion rate. These characteristics will, in turn, depend on the binder system of the coating, aspect ratio, and size distribution of

pigments, drying condition and any post coating operation like calendaring. The solubility of the permeate in the layer is related to chemistry of the layer and the permeate. This includes any chemical reaction, for example hydration, and interactions of surface tension origin. Thus, by closely controlling physical and chemical properties of the surface, permeate flow at the surface can be controlled.

Pinholes in the barrier layer or the uncovered areas on the base sheet are the unavoidable features of the coated paper and board. They are introduced by various mechanisms such as insufficient coat weight, over metering in the coating process, and the type of coating process itself. The problem is especially acute when operating the coating process at the lower end of its coat weight window.

Overall permeation through a barrier coated paper is given by,

$$Q = Q_{Barrier} + Q_{hole}$$

$$Q = t\Delta p\left(\frac{AP_{Barier}}{L_{barrier}} + \frac{A'P_{Basesheet}}{L_{basesheet}}\right)$$

As the $P_{basesheet} >> P_{barrier}$, permeation through a pinhole or uncovered base sheet will have a disproportionate contribution to the over all permeation rates. To reduce the probability of pinholes in the coated layer, the two-bump strategy is already in place in paper industry. In the two-bump approach, the total coat weight is applied in two coatings, thus reducing the possibility of pinholes in two layers to coincide, thus eliminating the pinhole. Due to this dynamic, two-bump coating provides a more effective barrier than when coating is applied in one pass.

As permeation is a concentration driven diffusion process, the path of the diffusion through a pinhole is not straight across the thickness of the layer, but is in a solid hyperbolic space (Figure 2). This is known as the edge effect. The edge effect is a very significant phenomenon in barrier coated paper and board.

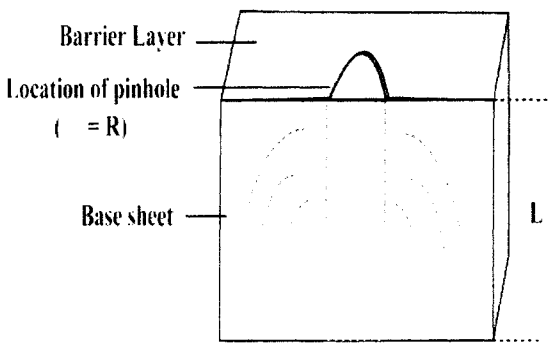

Figure 2. The edge effect.

Due to the edge effect, the permeation takes place through a much larger area than the area of the pinhole. For a pinhole of radius R, an equivalent radius R_E can be calculated as (11),

$$R_E = \sqrt{2RL + R^2}$$

Where L is the thickness of the base sheet. Based on this equation, as L>>R, the effect of the pinhole on failure of the barrier layer is much greater for a thicker base sheet. Thus, a single pinhole can saturate a large area of the base sheet with permeate. This effect is observed in heavily wax-coated corrugated boards. If moisture is the permeate, the board can get saturated locally due to a single pinhole, resulting in loss of strength properties in that localized area, leading to catastrophic failure of the board.

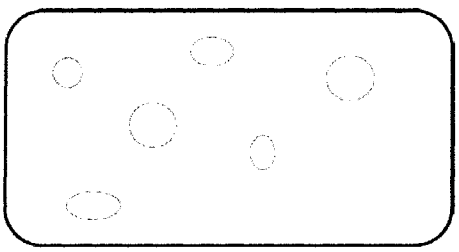

Figure 3. Pinhole size distribution.

On a coated paper and board, for a mean pinhole radius of R and standard deviation σ (Fig. 3), the permeation decrease factor ρ can defined as (12)

$$\rho = f\left[\left(\frac{2L}{R}+1\right)+\frac{2}{r}\sqrt{\frac{2}{\pi}}\left(\frac{L}{R}+1\right)\sigma+\left(\frac{1}{R}\right)^2\sigma^2\right]$$

Here, f is the fraction of area covered by pinholes. As can be seen from the above equation, a lower pinhole area and base sheet thickness and larger pinhole radius favors the decrease factor. The barrier improvement factor (BIF) is defined as the reciprocal of permeation decrease factor ρ.

$$BIF = \frac{1}{\rho}$$

In the case of fluid permeation like water or oils, pinholes can give rise to capillarity. Capillary transport is much faster, almost instantaneous, than the concentration driven diffusion and is governed by the Lucas Washburn equation (13,14)

$$\frac{dL}{dt} = \frac{\gamma.r.\cos(\theta)}{4\mu.L}$$

Here, dL/dt is rate of penetration, L is the length of liquid penetration, γ is the surface tension of the fluid, μ is the fluid viscosity, and θ is the contact angle of the liquid with

the substrate. Capillary transport is especially critical for short life span products such as convenient food wrapping papers.

Current Coating Methods

Blade, roll and air-knife coaters are used extensively for the barrier coating applications. Blade coaters are surface coaters, giving an extremely uneven surface profile, Fig.4 Surface coaters will have to fill all the valleys on the paper surface before any effective barrier layer can be achieved. Even after filling the valleys, the effective barrier layer thickness is much smaller.

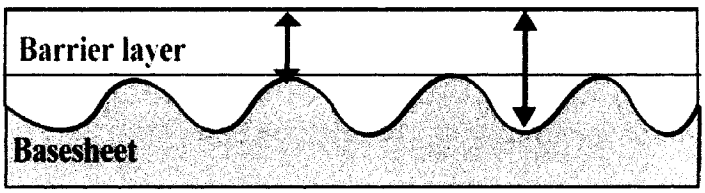

Figure 4. Thickness profile of surface coaters.

This increases the coat weight demand substantially. Rod coaters are hybrid coaters (surface-contour). Both blade and rod coaters operate under larger hydrostatic pressure leading to penetration of coating into the base sheet. From the above discussion, it is clear that any coating material which does not contribute to the effective thickness of the barrier layer can be considered a loss. Blade and rod coaters have very low coverage at the lower end of their coat weight window. This renders them useless for lower end barrier applications. Air-knife is a contour coater, but due to low viscosity demand on coating color, penetration of coating color into the base sheet can be substantial. This further increases the coat weight demand.

Summary of Current Coating Processes

To achieve effective barrier properties, the barrier layer should be of uniform thickness, free from pinholes, and provide complete coverage. Pinholes, or insufficiently covered base sheet areas, will have a large impact on the barrier properties. A non-uniform coating thickness layer, pinholes, and incomplete coverage, increases the coat weight demand to achieve the desired permeate transmission rate. Current coating technologies result in the application of a non-uniform coating thickness profile that results in poor coverage at low coat weights. A coating method that provides a uniform layer thickness and good coverage is highly desirable for a barrier coating.

CURTAIN COATING

Curtain coating is a low-impact true contour coater. Curtain coating can be considered as a lamination process of a liquid film and a substrate. As the free liquid film is formed before it comes in contact with the substrate, film is pinhole free. This leads to virtually 100% coverage at any coat weight. Previous results [9,13] have indicated that the coverage

is almost independent of coat weight. In addition, as a curtain coater is a true contour coater, the coating layer thickness is uniform (Fig.6 and 7) and can be easily controlled by manipulating flow rate and web speed.

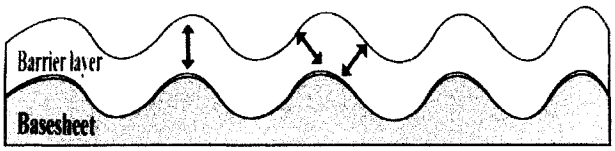

Figure 5. Thickness profile of contour coaters.

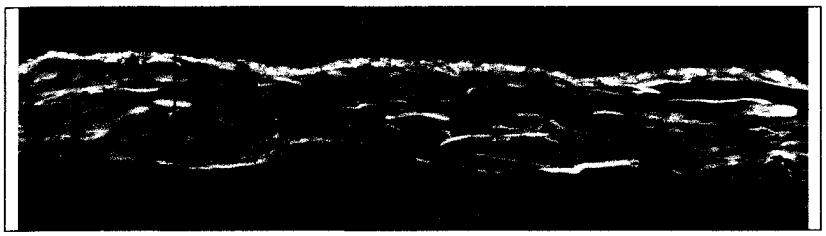

Figure 6. Z-direction cut of curtain coating paper showing coating layer.

Curtain coating is a low impact coating process with little hydrostatic pressure. This leads to little or no coating penetration into the base sheet. A uniform coating thickness and no penetration of coating color into the base sheet will lead to substantial reduction in coat weight demand for the same barrier performance. In addition, excellent coverage at low coat weight makes curtain coating especially attractive for short life span products.

CONCLUSIONS

The most effective barrier performance is achieved when the barrier layer is uniform in thickness, free of pinholes and coating coverage is complete. Curtain coating is a low impact true contour coater, making it an attractive coating process for barrier applications. Uniform coating layer, easy and effective control over layer thickness, low impact and excellent coverage make curtain coating a good fit for barrier applications.

BIBLIOGRAPHY

1. G. Mortwnsen and J. Sorensen, "Reduction of Photo-oxidative Quality Changes in Cheeses by Proper Packaging", International Association of Packaging Research Institutes (IAPRI)-WORLDPAK Conference. East Lansing, Michigan, June 23-28, 2002.

2. Bob Hartog, Carolien Bosch, Pim Knol, Ferry Stekelenburg, and Sandra Tap, "Efficacy of Hygienic Coatings for Applications in Food Industries", 2002 International Hygienic Coating Conference, Brussels, Belgium, July 8-9, paper 13.

3. Michelman I R, Barrier coatings for paper: uses, composition and hot melts, "The PLACE", TAPPI, Sept 2000

4. Klass C., "Emerging Barrier Coating Market Trends", Barrier Coating Symposium, Western Michigan University Kalamazoo, MI, Oct. 8-9, 2002.

5. C. Klass, "Emerging Barrier Coating Market Trends", Barrier Coating Symposium, Western Michigan University Kalamazoo, MI, Oct. 12-13, 2004.

6. Vaha-Nissi M, Lahti J, Rintanen J, Savolainen A, Rissa K, Characterization of barrier clay coatings using AFM and SEM, TAPPI, 2000 coating conference proceedings.

7. Smith R H, Edwards R, Heat seal induced pinholing in double coated boards, TAPPI, 1997 polymers, laminations and coating conference proceedings.

8. Vaha-Nissi M, Savolainen A, Filled dispersion barrier coatings, Tappi, 1999 coating conference proceedings.

9. Rodolph O, "Practical aspects of DF curtain coating applications", Curtain coating symposium proceedings, Gorham International, Oct 6-8, 2004.

10. H. Darcy, "Les Fontaines Publiques de la Ville de Dijon", 1856, Dalmont, Paris.

11. Lucas, R., 1918, Kolloid – Z., 23, p. 15.

12. E. W. Washburn, Phys. Rev. Ser. 2, 17, 273 (1921).

13. Tripathi P, Joyce M, Fleming P D, Sugihara M, "Statistical optimization of curtain coater at high speeds", Submitted for publication